UNIVERSITY OF OKLAHOMA

GRADUATE COLLEGE

A NEW STRATEGY FOR PHOTO-TRIGGERED RELEASE OF DRUGS BY VISIBLE/NEAR IR LIGHT: PHOTO-UNCLICK CHEMISTRY

A DISSERTATION

SUBMITTED TO THE GRADUATE FACULTY

in partial fulfillment of the requirement for the

Degree of

DOCTOR OF PHILOSOPHY

By

MOSES K. BIO
Norman, Oklahoma
2012

A NEW STRATEGY FOR PHOTO-TRIGGERED RELEASE OF DRUGS BY VISIBLE/NEAR IR LIGHT: PHOTO-UNCLICK CHEMISTRY

A DISSERTATION APPROVED FOR THE
DEPARTMENT OF CHEMISTRY AND BIOCHEMISTRY

BY

_____
Dr. Daniel Glatzhofer, Chair

_____
Dr. Youngjae You

_____
Dr. Ann West

_____
Dr. Wai Tak Yip

_____
Dr. Lloyd Bumm

Acknowledgments

I would like to express my sincere gratitude to: 1) my advisor, Dr. Youngjae You, for his direction, criticism and encouragement which has seen me through the project, 2) the chair of my graduate committee Dr. Daniel Glatzhofer, for his extraordinary direction and advice, my committee members: Dr. Ann West, Dr. Wai Tak Yip, Dr. Lloyd Bumm, for their understanding and encouragement throughout the program.

I would also like to thank the members of the medicinal chemistry laboratory, both past and present especially Dr. Rajesh Murthy whom I worked with in the first screening for a potential linker, Dr. Praveen Kumar Pogula, Gregory Nkepang, Pallavi Rajaputra, Samuel Gorman Awuah and Dr. Abugafar Hossion for their enormous contributions to the project.

The journals entitled “click and photo-unclick chemistry of aminoacrylate for visible light-triggered drug release” (reference # 93) and “low energy light-triggered oxidative cleavage of olefins” (reference # 88) were reproduced in this dissertation with permission from the Royal Society of Chemistry and Elsevier, respectively.

Finally, I would like to thank my family and friends for their support and encouragement. This project was funded in part by DOD (CDMRP breast cancer program, W81XWH-09-1-0071) and South Dakota Board of Regents (Competitive Research Grant).

Table of Contents

Page

List of Abbreviations

$^1O_2$:	Singlet oxygen
^{1}PS:	Singlet state photosensitizer
$^3O_2$:	Molecular oxygen
^{3}PS:	Triplet state photosensitizer
CA4:	Combretastatin A4
CA4-L-PS:	Combretastatin A4 (CA4)-linker- dithiaporphyrin (PS)
$CDCl_3$:	Deuterated chloroform
CMP:	Core-modified porphyrin (Dithiaporphyrin)
DABCO:	1,4-Diazabicyclo[2.2.2]octane
DCC:	*N,N′*-Dicyclohexylcarbodiimide
DCM:	Dichloromethane
DMAP:	4-Dimethylaminopyridine
DMF:	Dimethylformamide
DMSO:	Dimethyl sulfoxide
DNA:	Deoxyribonucleic acid
FRET:	Fluorescence resonance energy transfer
GC-MS:	Gas chromatograph-Mass spectrometry
HCl:	Hydrochloric acid
HMPA:	Hexamethylphosphoramide
HPLC:	High pressure liquid chromatography

IP:	Intraperitoneal
ISC:	Inter-system crossing
MCF-7:	Michigan cancer foundation-7(human breast adenocarcinoma cell line)
MTT:	3-(4,5-Dimethylthiazol-2-yl)-2,5-diphenyltetrazolium bromide
NMR:	Nuclear magnetic resonance
NIR:	Near infrared
PAMAM:	Polyamidoamine
PDT:	Photodynamic therapy
PEG:	Polyethylene glycol
PGA:	Polylactide-co-glycolide
PLA:	Polylactic acid
PLGA:	Polylactide-co-glycolide
PS:	Photosensitizer
PS-L-Rh:	Dithiaporphyrin (PS)-linker-and rhodamine B (RhB)
RT:	Room temperature
TFA:	Trifluoroacetic acid
THF:	Tetrahydrofuran
TLC:	Thin layer chromatography
TPP-OH:	5,10,15-triphenyl-20-(4-hydroxyphenyl)-21*H*,23*H*-porphyrin
UV:	Ultra-violet

List of Tables

List of Figures

List of reaction schemes

Appendix

Figure Page

List of ^{1}H-NMR spectra

Page

Abstract

Spatio-temporally controlled release of therapeutic or diagnostic agents by the use of light has gained much attention in recent times. Controlled release of bioactive molecules and drugs is a critical issue for many biological applications. In cell biology, caged compounds (photo-releasable compounds) have been used to study the molecular processes in biological systems. In drug delivery, controlled release of active form of drugs from inactive forms (prodrugs and nano-drug delivery carriers) is critical to achieve local expression of pharmacological action of the drug, especially toxic drugs such as anti-cancer drugs. Current strategies use UV light or short-visible light to release the active compounds. However, UV or short visible light can be used only at a cellular level. Its application at a tissue/animal level (*in vivo*) has been hampered by its limited tissue penetration. The other concern is the cellular damage by UV light itself.

To address the above limitations, our strategy was to develop a releasing mechanism based on the unique reaction of singlet oxygen generated by a combination of photosensitizer and low light energy. To achieve this our first goal was to identify chemical bonds which can be cleaved by tissue penetrable low energy light. We therefore systemically examined various substituted olefins to find the optimal linker for our strategy. This screening led to vinyl dithioether and vinyl diether as potential singlet oxygen mediated cleavable linkers. Both vinyl dithioether and vinyl

diether were cleaved more than 80% by singlet oxygen within 15 min by the irradiation with 690 nm diode laser (200 mW/cm^2) with a photosensitizer (core-modified porphyrin). Between the two, vinyl diether was our first choice because its photo-oxidation did not generate any side product. However, the synthetic methods for vinyl diether were limited to symmetric molecules, lengthy step and low yield. Due to such limitations of vinyl diether, the second screening was performed to identify better linker for our strategy. Among the screened linker candidates, aminoacrylate showed excellent characters: facile synthesis by a click chemistry, fast cleavage, and release of intact parent compound, stability in aqueous medium. We first introduced the concept of “photo-unclick chemistry” of aminoacrylate, where the aminoacrylate linker is synthesized by a click chemistry (amine-yne reaction) and intact drugs are released by irradiation.

A prodrug of drug-linker-photosensitizer CA4-L-PS was prepared to prove the photo-unclick chemistry in cells. The results obtained were consistent with our expectation. While the prodrug CA4-L-PS was 20 times less toxic than parent drug CA-4 without irradiation (IC_{50}: 8 vs. 200 nM). Photo-toxicity of CA4-L-PS was close to dark-toxicity of CA-4 (IC_{50}: 6 vs. 8 nM), presumably due to the released CA-4. In addition, I also confirmed that the linker in the conjugate system could be cleaved at low intensity light (1 mW/cm^2). It is a critical result to support the feasibility of photo-unclick chemistry at the systemic level because limited light intensity is the key

problem. We further investigated the cleavage of the linker at systemic level (mouse) with a model compound PS-L-Rh, whose cleavage can be readily monitored by increase of Rh fluorescence. Light-dose dependent increase of Rh fluorescence was observed by IVIS bioluminescence imaging system in a nude mouse. The photo-unclick chemistry showed promising results. We envision that it could provide a novel releasing mechanism for spatio-temporally controlled release of biological active molecules from various drug delivery systems such as prodrug and nano-drug delivery vehicles.

Chapter 1. Introduction and Background

The primary objective of drug delivery is the ability to control the drug dosing in terms of quantity, location and the time in order to maximize therapeutic effects and to minimize side effects by eliminating the potential for both under and overdosing. To achieve this objective especially in cancer treatment, various delivery systems have been developed such as dendritic macromolecules,[1] liposomes,[2] polymers,[3] metal nanoparticles[4] and viruses.[5] These carriers are decorated with targeting vectors for more specific delivery. To express activity, parent drugs should be released from the delivery vehicles. Thus, an effective release strategy is one of key issues to achieve spatial-temporally controlled delivery of drugs.

Several strategies have been explored for spatio-temporally controlled release of biologically active molecules using either internal or external stimuli such as pH,[6, 7] enzyme,[8, 9] ultrasound,[10-13] magnetism,[14] and heat.[15] Most of these release mechanisms are passive, dependent on endogenous physicological factors and thus difficult to actively control release. Passive release mechanisms have also been found to be too slow to obtain optimal therapeutic effects. These challenges in current release strategies led to new approaches toward light-activated release mechanism that seek to improve drug release rate and maximize therapeutic effects.

Recently, light triggered release has gained much attention[16-19] because light as external signal is a very appealing tool for the spatio-temporal release. Light has been explored for the release of therapeutic agents from delivery systems or as activation agents that produce cytotoxic species. Photochemical mechanism mediated by light has been applied in delivery purposes.[20-22] There are also reports of caged compounds and photo-cleavable linker that decompose under photo-irradiation. Photocaging has served an important tool for spatio-temporal control of biological processes[23-25] and release of therapeutic agents from nanoscale materials.[26, 27] However, their applications have been limited mostly at the cellular level due to the use of high energy UV light causing cell damage and limited tissue penetration (< 1mm).[28] To apply this exciting tool in clinic, new strategies should be invented where active compounds can be released by tissue penetrable low energy light (preferably, > 650 nm).[29,30] Unfortunately, the energy of longer wavelength lights is too low to directly initiate cleavage of covalent bond.

We address these issues by taking advantage of the unique reaction of singlet oxygen that can be generated by the combination of photosensitizer and low energy light. We envisioned that the olefinic bond cleavage reaction by singlet oxygen could be employed in controlling drug release. We hypothesized that spontaneous cleavage of dioxetane following 2+2 cycloaddition reaction of singlet oxygen with olefins could be used for

releasing free drugs by the irradiation with low energy light. If therapeutic molecules can be released upon the irradiation of low energy light, it could provide two critical advantages. First, the release of free drug can be actively controlled by external light noninvasively (i.e., in a remote controlled manner). We can control the release dose by the irradiation dose. Second, the low energy light (~650-800 nm) allows its application at the tissue level due to its high transparency.[30]

1.1. Principles of photodynamic therapy (PDT)

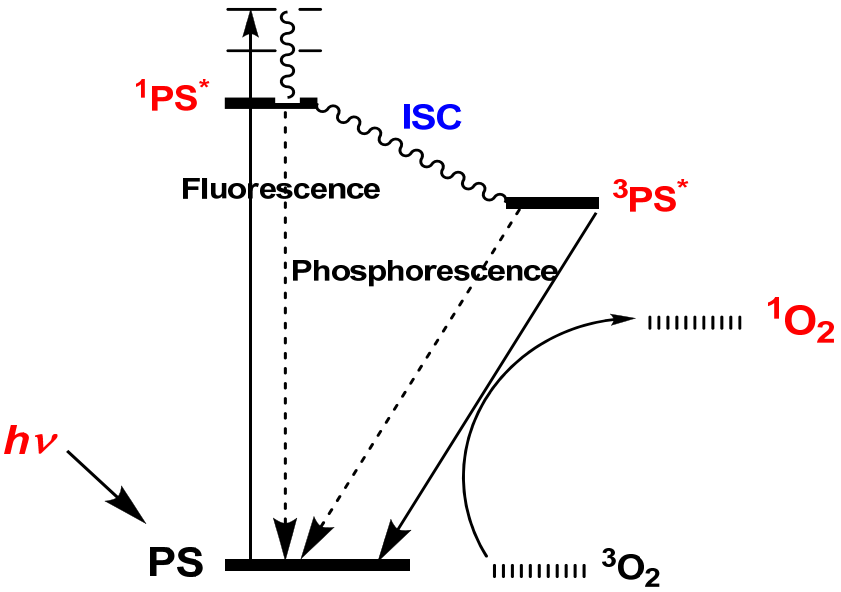

Figure 1. Modified Jablonski diagram.

PDT employs three components: a photosensitizer (a drug for PDT), low energy light (visible and near IR, 690-800 nm) and oxygen (Fig. 1).[31-

[34].The principle involves absorption of low energy light by a photosensitizer, which then reaches triplet state from ground state. This activated photosensitizer then converts surrounding non toxic molecular oxygen to singlet oxygen.[35] The singlet state of molecular oxygen is highly reactive and can oxidize biomolecules such as lipids, proteins and nucleic acids. It is this oxidation that results in cell death.[36, 37] *In vivo* antitumor effect of PDT is a result of a combination of the following three mechanisms: direct damage on cancer cells, damage to vasculature in tumor tissue (antiangiogenic effect) and immunological response.[31] PDT is an attractive modality due to its unique features such as selective, mild and rapid-acting to treat various cancers.[38-40] Selectivity is achieved in two dimensions: firstly, there is some degree of localization of a photosensitizer in tumors and secondly, the focused irradiation with low energy light on/around the tumor. This results in the damage of only the irradiated area. The inherent low toxicity of PDT can be attributed to the fact that each component of PDT is less toxic unless the three components are combined at the same time. This makes PDT a mild treatment causing less side effects compared to chemotherapy and radiation.[41]. To enhance the response of PDT the treatment can be performed on multiple regions simultaneously and can also be repeated. The use of Photofrin (photosensitizer) for the treatment of esophageal cancer, endobronchial cancer and high-grade dysplasia in Barrett's esophagus has

been approved.[38, 42] Though PDT looks promising there are several aspects that need improvement to achieve higher efficacy and selectivity.

Light delivery to larger and deeper residing tumors is one of the major challenges of PDT. Low energy light has a therapeutic depth of about 1 cm, which makes light delivery to tumors of internal organs very difficult. To address the challenge of light delivery inside the tumor mass or into the internal organs interstitial thin optical fiber has been developed. [43-45].Another issue PDT is the hypoxic nature of solid tumors.[46-48] Spectroscopic detection technologies have been investigated to enable oxygen or generated singlet oxygen to be monitored.[45, 49] Since the concentration of oxygen in tumor is limited procedures such as fractional or slow irradiation have been employed to allow supply of oxygen during treatment.[31, 50].Of all the problems of PDT the most prominent is achieving selectivity of photosensitizer towards cancer cells. The lack of ability of singlet oxygen to distinguish cancer cells from normal surrounding cells makes selectivity of PDT to be considered two dimensional. This consequently leads to damage of normal tissue around the irradiated area. Hence there is a need to develop new photosensitizers with three dimensional selectivity towards cancer cells.[51-54]

1.2. Singlet oxygen and typical reactions of singlet oxygen

Singlet oxygen is a useful reagent in organic synthesis and plays an important role in biological systems[55, 56] and therapeutic applications.[31, 57]

Singlet oxygen can be generated thermally by the decomposition of phosphate ozonides (or endoperoxides) or photochemically by the sensitization of a photosensitizer like rose bengal, methylene blue, or porphyrin.[58] Typically, singlet oxygen reacts with olefins (C=C bonds) leading to ene, 1,2-cycloaddition, and 1,4-cycloaddition reactions. 1,2-Cycloaddition reaction generates dioxetane as an intermediate which decomposes to two carbonyl compounds (Fig. 2).[56, 59-63]

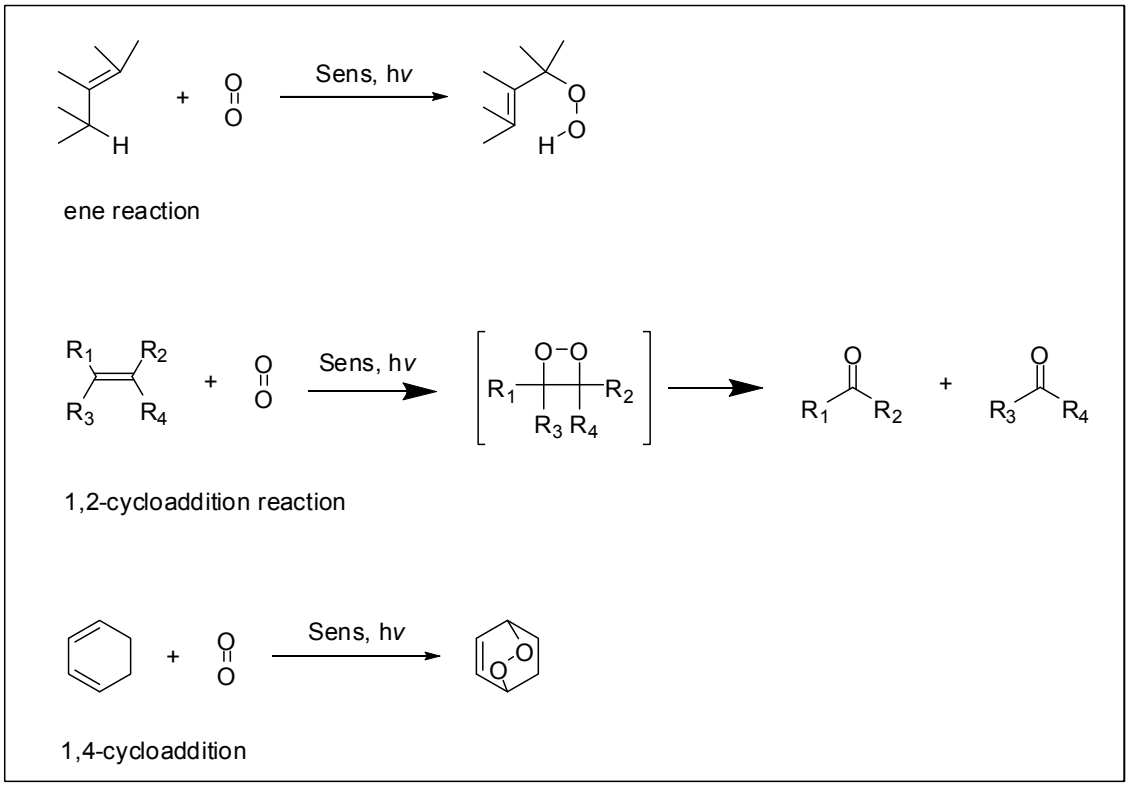

Figure 2. Typical reactions of singlet oxygen.

1.3. Current drug delivery systems

1.3.1. Liposome drug delivery

Liposome is composed of amphiphilic phopholipids and cholesterol that forms a bilayer with an encapsulated aqueous interior usually of size between 80 and 100 nm. Hydrophilic drugs are encapsulated in the aqueous interior while hydrophobic drugs are within the bilayer. Different methods have been used for the encapsulation such as gradient method for vincristine[64] and ammonium sulfate method for doxorubicin.[65] Interaction between liposome and plasma proteins is prevented by incorporation of hydrophilic polymer (polyethylene glycol, PEG) to reduce recognition by reticuloendothelial system[66] and improve circulation lifetime. However, the major challenges of liposomal drug delivery are : difficulty for controlling the release of drugs from liposomes, extravasation from the blood and binding to cell surface receptors.[67]

1.3.2. Polymer drug delivery

The use of synthetic polymers as agents for targeted drug delivery has been widely explored. Most commonly used synthetic polymers are the aliphatic polyesters specifically hydrophobic polylactic acid (PLA), more hydrophilic polyglycolic acid (PGA), and copolymers polylactide-co-glycolide (PLGA). A unique property of polymer as drug delivery includes controllable release profile ranging from days (PGA) to months (PLA) by modification of

the ratio of PLA to PGA.[68] Hydrophobic entrapment and conjugation to the polymer are some of the techniques for encapsulation of the drug. Sustained and controlled drug release from internalized or localized PLGA nanoparticles can be very useful as it provides ability to control the rate, duration and amount of intracellular drug concentration. The rate and extent of duration of release are critical determinants of efficacy. Some polypeptides still have limitations in their drug delivery potential such as limited sites for conjugation with drug and ineffective sustained release.

1.3.3. Dendrimer drug delivery

Dendrimers are monodisperse macromolecules with repeated branching structures emanating from a central core.[69] Drug molecules can be entrapped in the labyrinthine core created by the branches.[70, 71] A typical example of dendrimers used for drug delivery and imaging application is polyamidoamine (PAMAM) which is made of repetitive addition of branching units to an amine core such as ethylenediamine. PAMAM core is used as a drug reservoir and has been applied for delivery of small molecules.[70, 72] Dendrimers have served as multifunctional agents due to the high number of functional groups on the termini. Beside its use as drug delivery tool, dendrimer has been explored for targeting, typically by conjugation to folic acid for targeting tumors,[73] prostate-antigen-specific antibodies for targeting the prostate[74] and peptides for targeting vascular endothelium[75] and

intestinal epithelium.[76] Although dendrimeric drug delivery improves selectivity and stability of therapeutic agents, there are still some difficulties such as reticuloendothelial system uptake, drug leakage, immunogenicity, hemolytic toxicity and hydrophobicity.

1.4. Overall objective and hypothesis

Current drug delivery systems (polymer, liposome and dendrimer) have a common objective of improvement of drug delivery by addressing the major challenges of drug delivery for reducing the toxicity of drug, improving their release profile and increasing absorption. Although significant advances have been made, controlling the release profile and reducing toxicity still remain major challenges. Hence new strategies for addressing these limitations of drug delivery need to be developed. My objective was to develop a new bio-orthogonal strategy using visible/near IR light for controlling/triggering drug release for drug delivery systems. One way for releasing drug is by cleaving a covalent bond between the delivery system and attached drug. While high energy UV can initiate the bond cleavage, low energy visible/near IR cannot directly cleave a covalent bond. To circumvent this problem, we take advantage of principles of PDT and the [2+2] reaction of single oxygen. The hypothesis was that drug can be released by visible/near IR light if drug is conjugated to the delivery systems via singlet

oxygen cleavable linker and PS is at the proximity to the linker. As a simple model system, we designed visible/near IR activatable prodrug (Fig. 3).

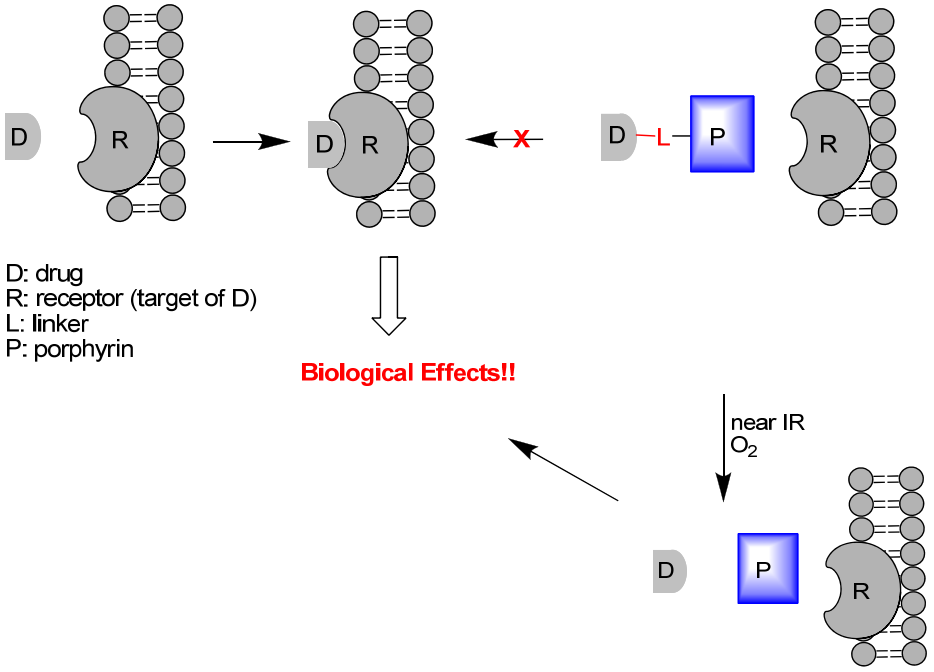

Figure 3. Singlet oxygen cleavable prodrug.

Chapter 2. Screening for Potential Linkers

2.1. Introduction

There are several references to the kinetic study of reactions of singlet oxygen with olefins, but it was difficult to use these data because either the reaction conditions were not described in detail such as intensity and/or wavelength of the light at target samples or the reactions were performed under saturated oxygen conditions.[77-80] To be applicable in a drug delivery system, an olefinic linker should produce a high yield of the photo-oxidation products within a short period of time under physiological conditions. No side reactions and/or products should be observed. In addition, a linker should be chemically stable in the ground state. Since intensity and wavelength of light are important for drug delivery applications, we (Dr. Rajesh Murthy and I) systemically examined various olefins to find the optimal linker for the strategy and to estimate rates of reaction.

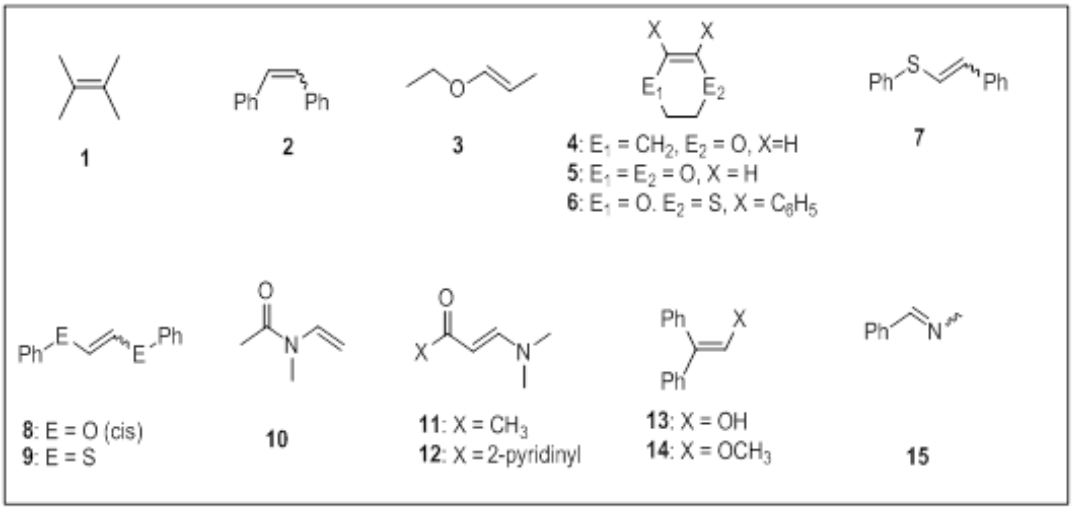

Figure 4. Olefins screened for photo-oxidation.

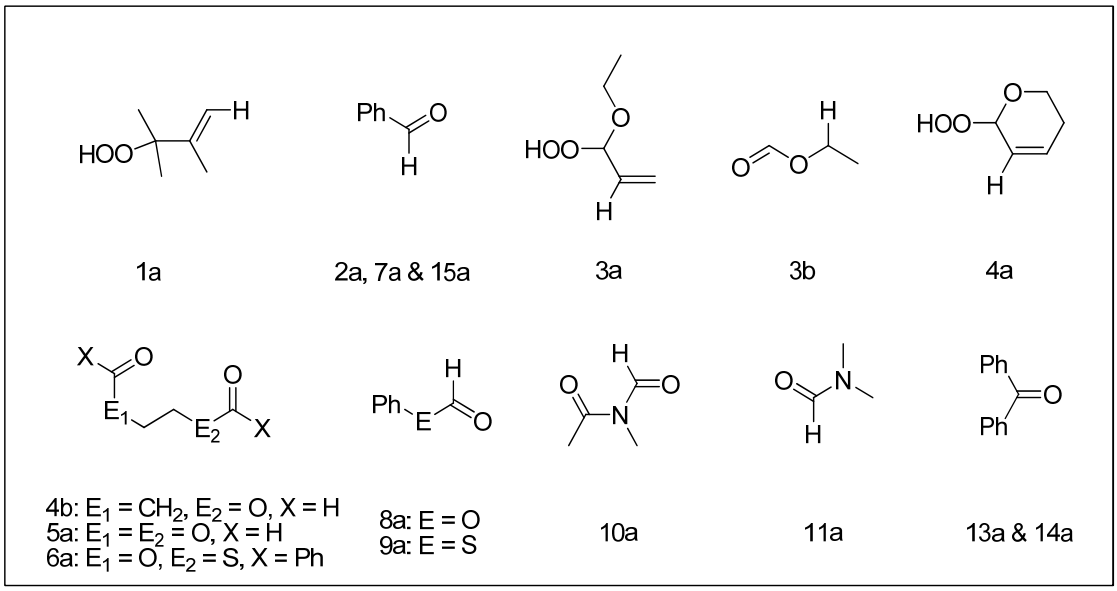

Figure 5. Photo-oxidation products of olefins 1-15 with hydrogen used for the quantification by ^{1}H NMR.

2.2. Experimental section

2.2.1. Synthesis

2.2.1.1. Synthesis of 35 and 36. Compound **8** was prepared based on reported method[81] but the details of reaction conditions were not described therein. To a solution of 1,2-diphenoxy ethane (2.14 g, 10 mmol) in benzene (30 mL) was added *tert*-butoxy chloride (2.26 mL, 20 mmol) dropwise. The solution was stirred at room temperature and irradiated using a wavelength of 400-800 nm for 15 min. The reaction mixture was reduced under vacuum and the crude product was purified on a silica gel column using hexane:ethyl acetate (99:1). An inseparable mixture of 1-chloro-1,2-diphenoxy ethane (**35**,

0.96 g, 38%) and 1,2-dichlorodiphenoxy ethane (**36**, 0.60 g, 21%) was obtained. This mixture was then used for the next step.

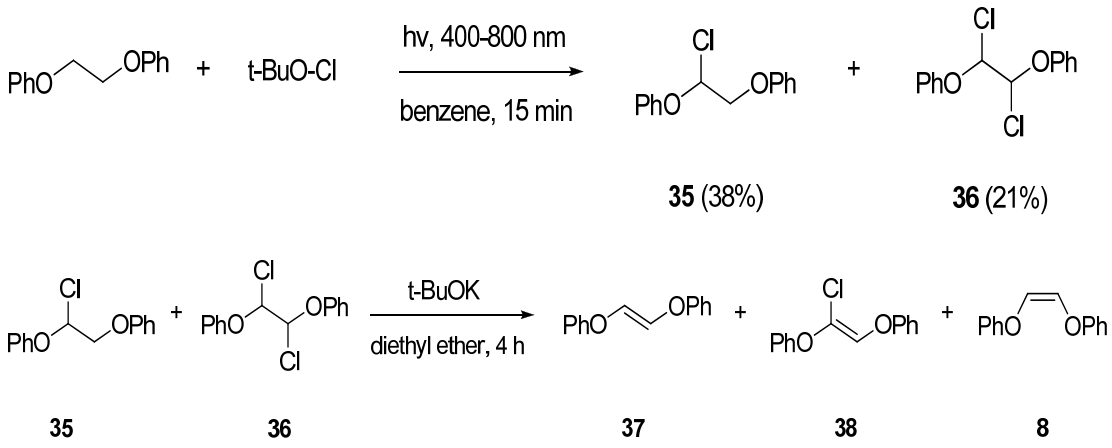

Scheme 1. Synthetic scheme for the preparation of **8**.

2.2.1.2. Synthesis of 8. To a stirred solution of potassium *tert*-butoxide (677 mg, 6.3 mmol) in anhydrous ether at 0 °C was added a solution of the mixture of **35** and **36** (500 mg) in anhydrous ether dropwise. The reaction mixture was then stirred at room temperature for 4 h. The progress of the reaction was monitored by TLC. The starting material had completely disappeared with two close moving product spots. The reaction was stopped at this stage. The reaction mixture was diluted with ether and washed with water. The organic layer was separated and dried under vacuum. The crude product was purified on a silica gel column using hexane:ethyl acetate (99:1). The second fraction couldn't be completely separated. A part of the second fraction was however obtained 3 mg as a pure compound **8** showing identical ^{1}H NMR data in a reference. Based on ^{1}H NMR spectra the first fraction was

a mixture of products **37**, **38** and **8** identified by their vinylic proton peaks as *trans*-diphenoxy ethylene (6.91 ppm), 1-chloro-1,2-diphenoxy ethylene (6.60 ppm) and *cis*-diphenoxy ethylene (6.18 ppm), respectively.

2.2.2. General photo-oxidation procedure

Olefins **1**-**15** except **8** were purchased from Sigma-Aldrich Co. or Acros Organics, and used without purification. In a NMR tube, an olefin (0.0048 mmol) and of 5,10,15-triphenyl-20-(4-hydroxyphenyl)-21H,23Hporphyrin (TPP-OH) (3 mg, 0.0048 mmol) was dissolved in $CDCl_3$ (0.5 mL) and the reaction mixture was irradiated for 1 h using a filtered mercury xenon lamp (300 W). The filtered light intensity used was 200 mW/cm^2 at the target NMR tube and the whole sample solution was irradiated. Wavelength of the light was 400 – 800 nm after passing through two glass filters (FSQ-GG400 and FSQ-KG1, Newport Corporation) and a water filter to remove heat. The NMR tube was closed with a cap during the experiment to avoid solvent evaporation. The photo-oxidized mixture was analyzed by ^1H NMR or HPLC. To maintain the significance for biological applications, we used low intensity light (200 mW/cm^2) of wavelength of 400-800 nm. At the standard condition, a reaction solution was irradiated for 1 h. The olefins were first irradiated without TPP-OH to observe their stability in the absence of singlet oxygen generation.

2.3. Results and discussion

2.3.1. Synthesis and photo-oxidation

Table 1. Photo-oxidation of various alkenes by singlet oxygen

Olefin	Products (yields)[a]	Olefin	Products (yields)[a]
1	1a (99%)	9[b]	9a (14%)
2	2a (11 %)	10	10a (30%)
3	3a (23 %) & 3b (18%)	11	11a (64%)
4	4a (34%) & 4b (65%)	12[c]	-
5	5a (77%)	13	13a (18%)
6	6a (99%)	14	14a (1%)
7	7a (22%)	15	15a (16%)
8[b]	8a (80%)		

[a] Yields by NMR integration from photo mixture, except substrates 6, 13 and 14 by HPLC. [b] Substrates irradiated only for 15 min. [c] Olefin peaks completely consumed but no aldehyde peak was observed on ^{1}H NMR.

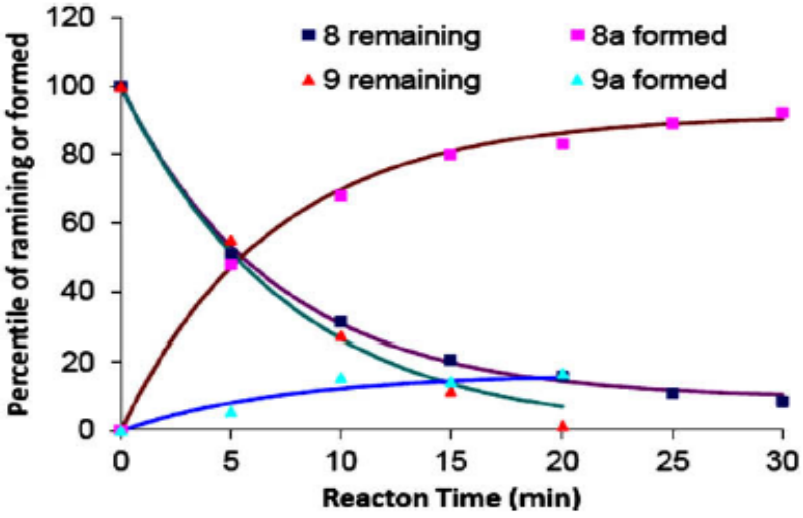

Figure 6. Comparison of kinetics of photo-oxidation of **8** and **9**.

The reactivity of the substrates with atmospheric oxygen was very negligible (< 1%). Another important study which was irradiation of the substrate without photosensitizer showed negligible reactivity except benzophenone oxime **13** which showed oxidation with about 7% conversion. This may be expected as there are reports of the slow conversion of benzophenone oxime to a mixture of benzophenone and nitric acid in the presence of oxygen and moisture.

The photo-oxidation of 2,3-dimethyl-2-butene **1** resulted in the formation of 3-hydroperoxy-2,3-dimethyl-1-butene **1a** in 99% by ene reaction[59, 82]. The higher reactivity of **1** with singlet oxygen as compared to other substrates can be attributed to its electron-rich double bond. It has been shown by Kearns[59] that substrate **1** has a lower $\pi_{C=C}$ ionization potential and hence has an increased reactivity towards singlet oxygen.

Substrate **2** was studied to observe 1,2-cycloaddition reaction with singlet oxygen yielding the dicarbonyl compounds as oxidative cleavage products. It also seemed interesting to study the effect of aryl groups as substituent's on the olefin. As previously reported by Rio and Berthelot[83] the singlet oxygen reaction with aryl-substitued olefins doesn't tend to be an accelerated process, due to its inability to act as an electron donating group when compared to hetero atoms or alkyl groups. Thus, benzaldehyde **2a** was formed as the only photo product in a low yield.

We then planned to study alkenes activated by hetero atoms. Substrates **3-6**, belong to the family of vinyl ethers and diethers, whose reactions with singlet oxygen have been extensively studied by Schaap and co-workers. Substrate **3** afforded the ene reaction product **3a** due to the presence of three hydrogens at the allylic position. The hydroperoxide **3a** was formed in competition with the dicarbonyl compounds as oxidative cleavage products via the 1,2-cycloaddition reaction. For the dicarbonyl compounds, we detected only ethyl formate **3b** in the reaction mixture by ^{1}H NMR. The other product, acetaldehyde, seemed to evaporate due to its low boiling point, 21 °C. Dihydropyran **4** also exhibited a similar reactivity to the substrate **3**, except that the 1,2-cycloaddition reaction product **4b** was formed twice as higher as the ene reaction product **4a**. It has been reported that for dihydropyran the solvent polarity plays an important role in determining the yield of 1,2-cycloaddition and ene reaction products.[78, 84] It has been shown

that when dichlormethane is used as a solvent for the photo-oxygenation reaction the dicarbonyl compounds are 2.7 times more favored than the hydroperoxide.[84] However, for substrate **3** the same explanation doesn't hold true although the same solvent ($CDCl_3$) was used for **3** and **4**. Slower formation of the dioxetane intermediate from *trans* isomer of **3** can act as a plausible explanation for the lower yield of **3b** as compared to **3a**. Both substrates **5** and **6** on photo-oxidation gave high yields of the product esters **5a** and **6a**, respectively. The strong electron donating effects of disubstituted hetero atoms O & S enhanced the reactivity with singlet oxygen.

Substrate **7** is sulfur activated olefin and exhibited a comparatively lower reactivity than vinyl ethers **3** & **4**. This could possibly be explained by the lower electron density on the π bond in substrate **7**, since substrates **3** & **4** are activated by the electron donating effect of alkyl groups. Substrates **8** & **9** were chosen to compare the reactivities of dioxygen substituted olefins vs. dithio substituted olefins. Substrate **9** was synthesized by the method reported by Sales et al.[81] Initially when we irradiated **8** & **9** the reaction mixtures showed complete conversion of the starting materials. Hence a time dependent study was conducted to analyze the reactivities of **8** & **9** in greater detail. Both the substrates **8** & **9** were irradiated for every 5 minutes and analyzed by ^{1}H NMR each time. Analysis of reaction mixture showed that the formation of product **8a** was directly proportional to the decrease of substrate **8**. However, the conversion of substrate **9** didn't show a corresponding

increase of product **9a** (Fig. 6). Thus product **9a** was formed in much lesser yield although the starting material was consumed to a much greater extent. This could be possibly explained by the formation of dithiooxalate and disulfide as side products which cannot be detected by ^{1}H NMR. Hence substrate **8** seemed to be a better linker for our drug delivery system with respect to its reaction kinetics and absence of side reactions.

Further continuing with our series of hetero atom activated olefins, we photo-oxidized substrates **10-12**. *N*-Methyl-*N*-vinyl acetamide **10** showed a reasonable reactivity with singlet oxygen as compared to vinyl ethers. This is probably due to the keto-amine resonance which can decrease the electron density of the π bond, thereby retarding the 1,2-cycloaddition reaction. Substrate **11** showed a higher reactivity with singlet oxygen possibly due to the availability of the lone pair electrons of nitrogen for enriching the double bond. Substrate **12** on irradiation showed complete disappearance of the starting material without any formation of the aldehyde product. However some unrecognizable products were obtained in the reaction mixture spectrum. It is possible that substrate **12** may have decomposed. Substrates **13-15** are examples of the reactivity of a π bond between carbon and nitrogen other than the olefins. Wamser and Herring[85] have previously studied the photo-oxygenation of oximes and have shown that methyl substituted oxime **14** has a greater rate of reaction than the unsubstituted oxime **13** due to greater electron density on the π bond. However, in our

case substrate **13** was more reactive than **14**. Wamser and Herring used saturated oxygen conditions for their photolysis with methanol as the solvent, whereas we studied our olefins under atmospheric conditions using $CDCl_3$ as a solvent. Thus the availability of oxygen for the reaction is due to the dissolved oxygen in the solvent and oxygen from air. Imine **15** on photo-oxidation yielded 16% of benzaldehyde. There is not much information available in the literature about the photo-oxidation of imines with singlet oxygen. Expectedly, **15** showed a similar reactivity to **13.**

2.4. Conclusion

The screening of various substituted olefins resulted in the choice of vinyl diether **8** and vinyl dithioether **9** olefins for the singlet oxygen-liable linkers. Both can be cleaved more than 80% by the irradiation of 200 mW/cm^2 light of 400-800 nm within 15 min without oxygen saturation. However, vinyl diether **8** was chosen because the cleavage reaction does not generate any side products. The potential of low energy light-induced C=C bond cleavage looks promising.

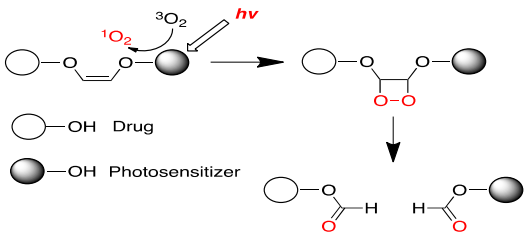

Figure 7. [2+2] Oxidation of vinyl diether by singlet oxygen and subsequent cleavage of dioxetane for the release of drug.

Chapter 3 Aminoacrylate Linker for Visible Light-triggered Drug Release

3.1. Introduction

Our initial screening of various olefins resulted in the choice of vinyl diether **8** and vinyl dithioether **9** olefins as singlet oxygen mediated cleavable linkers. I and my colleagues in my lab (Dr. Praveen Pogula and Mr. Gregory Nkepang) tried to develop prodrugs [D-linker-PS (D=drug, PS: photosensitizer)] using vinyl diether. However, we encountered several problems. First, the synthetic methods for vinyl diether were very limited and the available reaction conditions were limited with low yield and non-stereospecfic.[81, 86, 87] Second, intact parent drug was not released after the photo-cleavage. Instead, formylated product was released (**Fig. 7**), which might attenuate the activity of the drug (e.g., Drug- CHO).

Due to these limitations of the vinyl diether linker, I started searching for new linkers and turned our attention to β-enamino ketone. In the previous screening, these linkers showed relatively fast photo-oxidation by singlet oxygen (**11** & **12**, 64 & ~ 100% in 1 h, Table 1).[88]

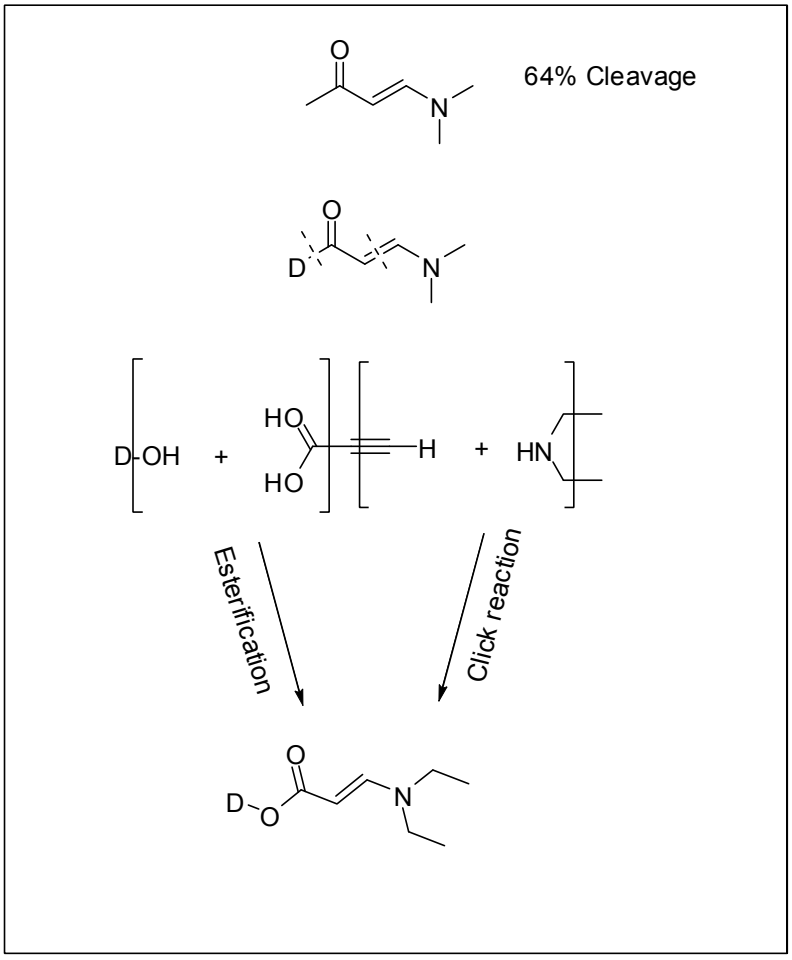

Figure 8. β-Amino ester and strategy for its synthesis.

Inspired by the oxidation rate of β-enamino ketone, I designed analogues of β-enamino ester (compounds **17** and **18**, **Fig. 8**) as new linker candidates that could readily be prepared through high yield reactions [esterification and amine-yne reaction (a click chemistry)].[89, 90] The esterification of 4-phenylphenol with propynoic acid was performed by the Steglich Esterification with DCC and DMAP at 0 ^{o}C (to RT) to give biphenyl propiolate **16**.[91] The thiol-yne type reaction of **16** with diethylamine or

piperidine gave **17** and **18** in 89% and 80% yields respectively at RT in 10-15 min.

To examine the scope of the preparation and photo-oxidation, I then prepared analogues by replacing the nitrogen with sulfur or oxygen [thio-acrylate **19**, **20** and oxy-acrylate **21**, **22**, and] or the oxygen with nitrogen or sulfur [amino-acrylthioate **23**and aminoacrylamide **24**] (**Fig. 9**).

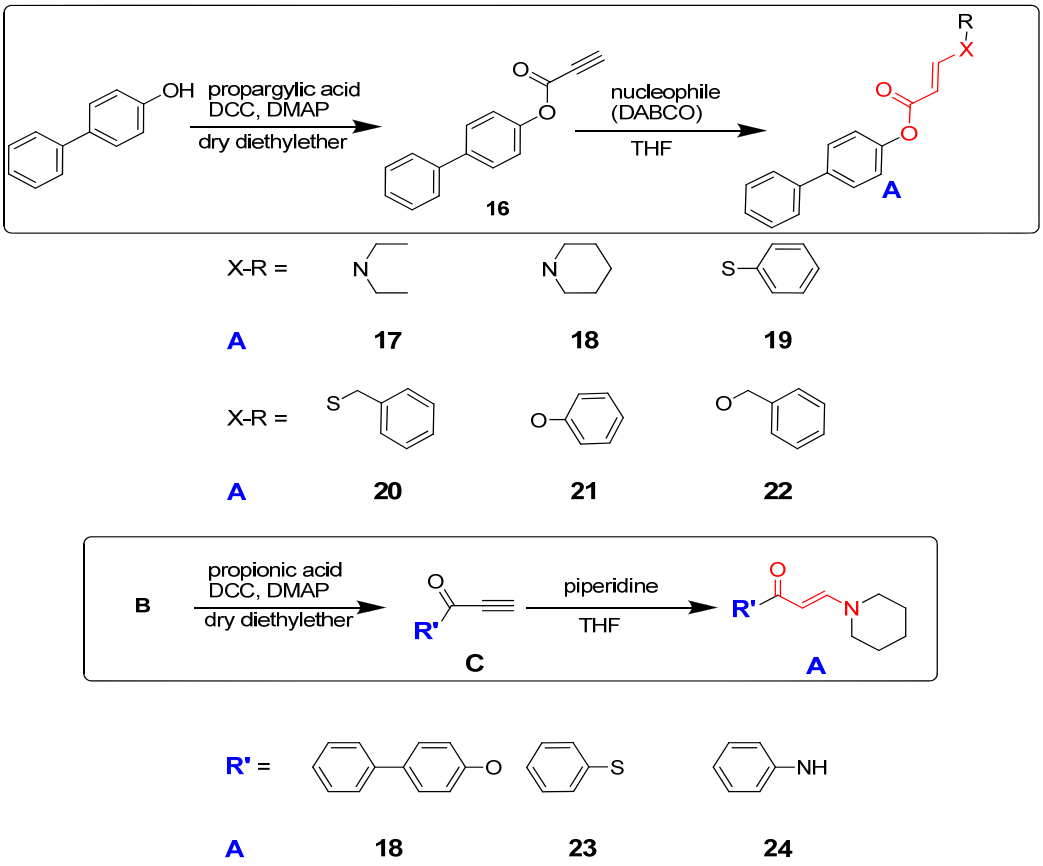

Figure 9. Reaction sequence and prepared substrates for heteroatomacrylate, aminoacylthioate and aminoacrylamide (**B**: 4-phenylphenol, thiophenol, or aniline).

Since the aminoacrylates **17** and **18** showed fast reaction with singlet oxygen (62 and 72%) at comparable rate with the control (vinyl dithioether), I further designed model systems **25**-**28** with a spacer to accommodate two parts of alcohol (e.g., 4-phenylphenol and phenol). All were prepared using high yield click reaction **(**84-90%). Compounds **26** and **27** showed faster reaction than **25**, presumably due to weaker electron withdrawing effect of the ester bond to enamino group in **26** and **27**. Using the spacers of **27** and **28**, I tried to prepare prototypes (compounds **14** and **15**) having both the linker and a photosensitizer (**PS**) in one molecule. Prototypes **29** and **30** were successfully prepared. Indeed, both showed much faster oxidation reaction (89% in 10 min for **29**; and 79% in 15 min for **30**) even faster than the control (87% in 25 min).

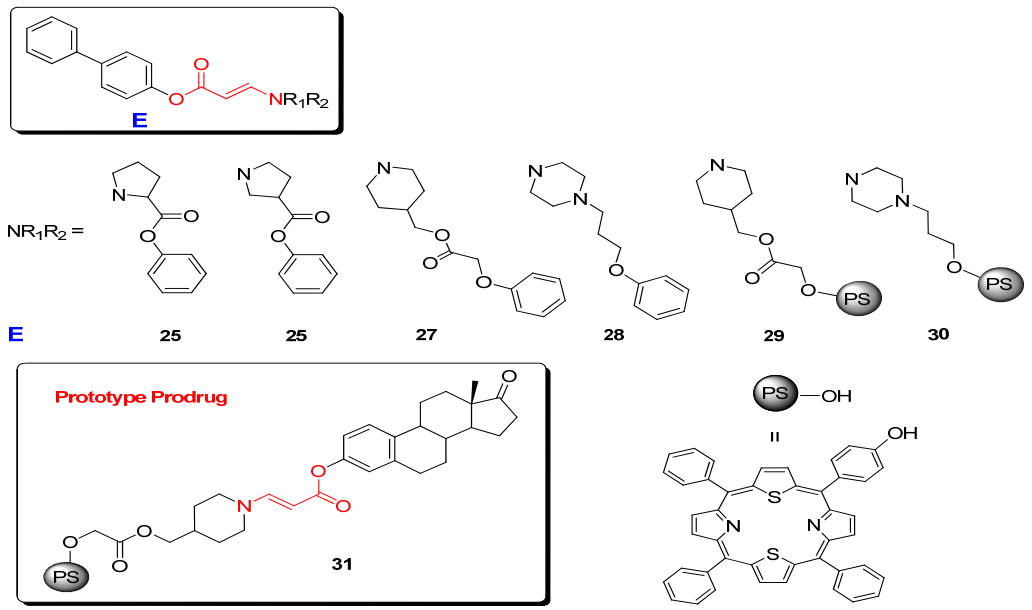

Figure 10. Prepared model substrates and the prototype prodrug.

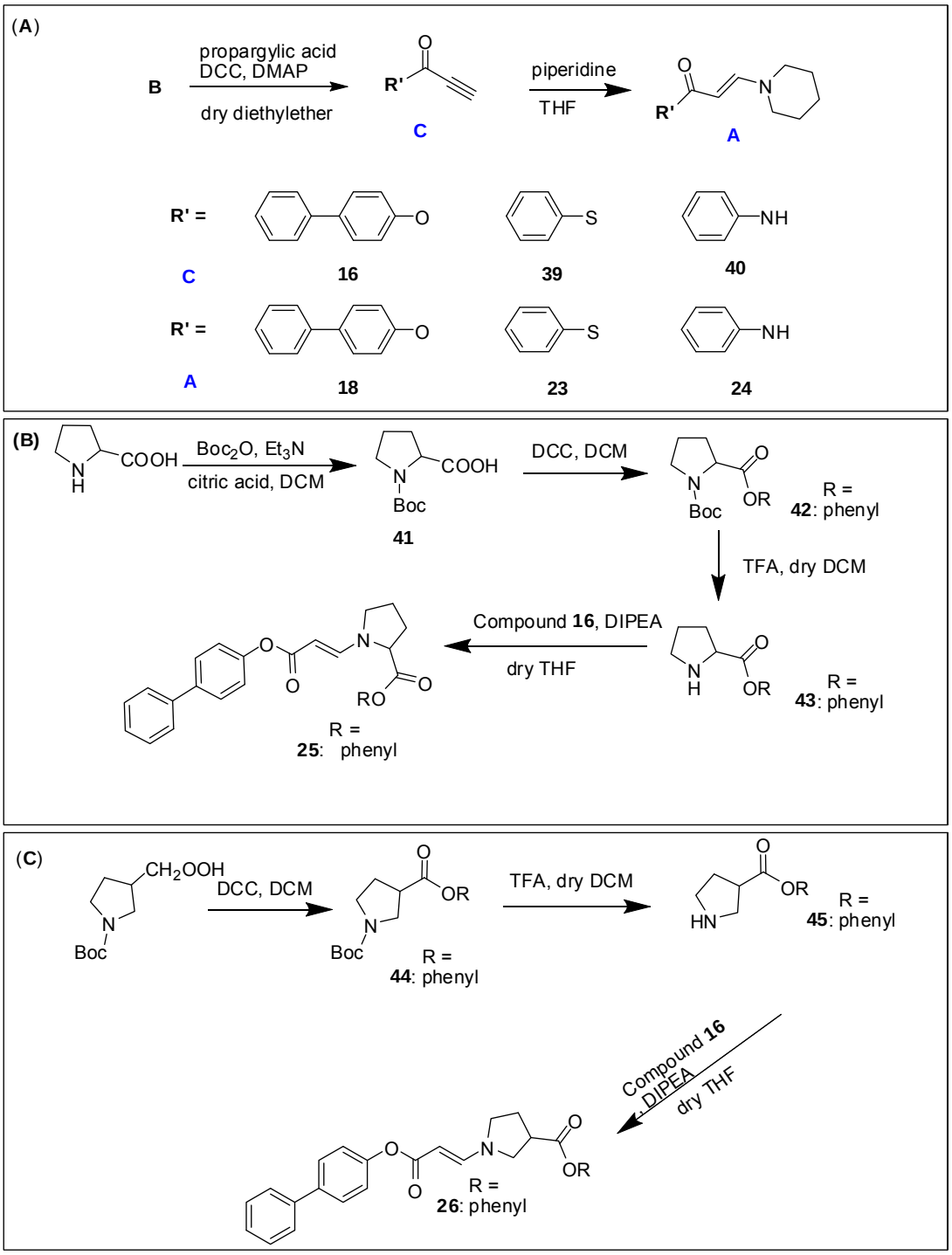

Scheme 2. Prepared substrates for heteroatomacrylate, aminoacylthioate and aminoacrylamide.

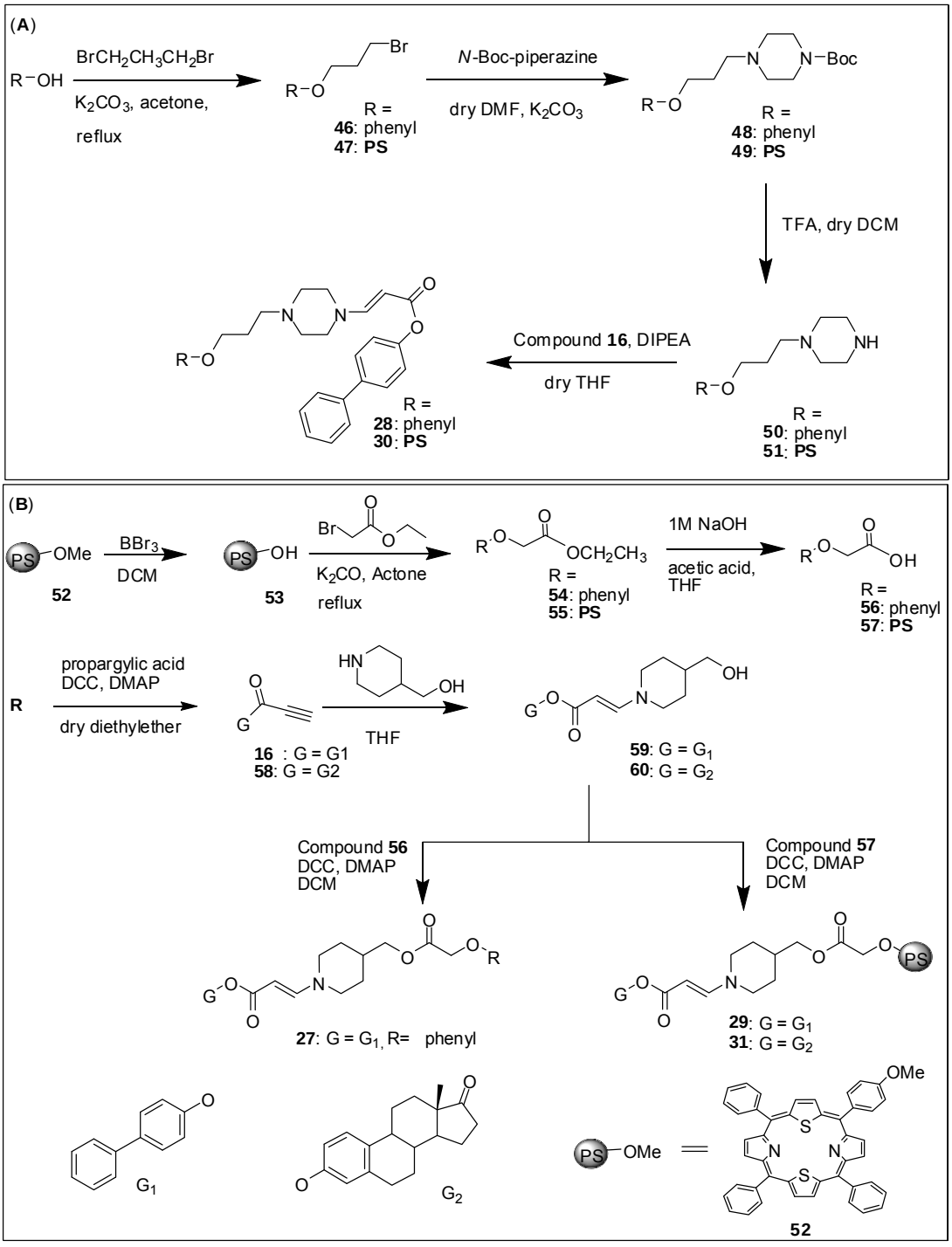

Scheme 3. Prepared model substrates and the prototype prodrug.

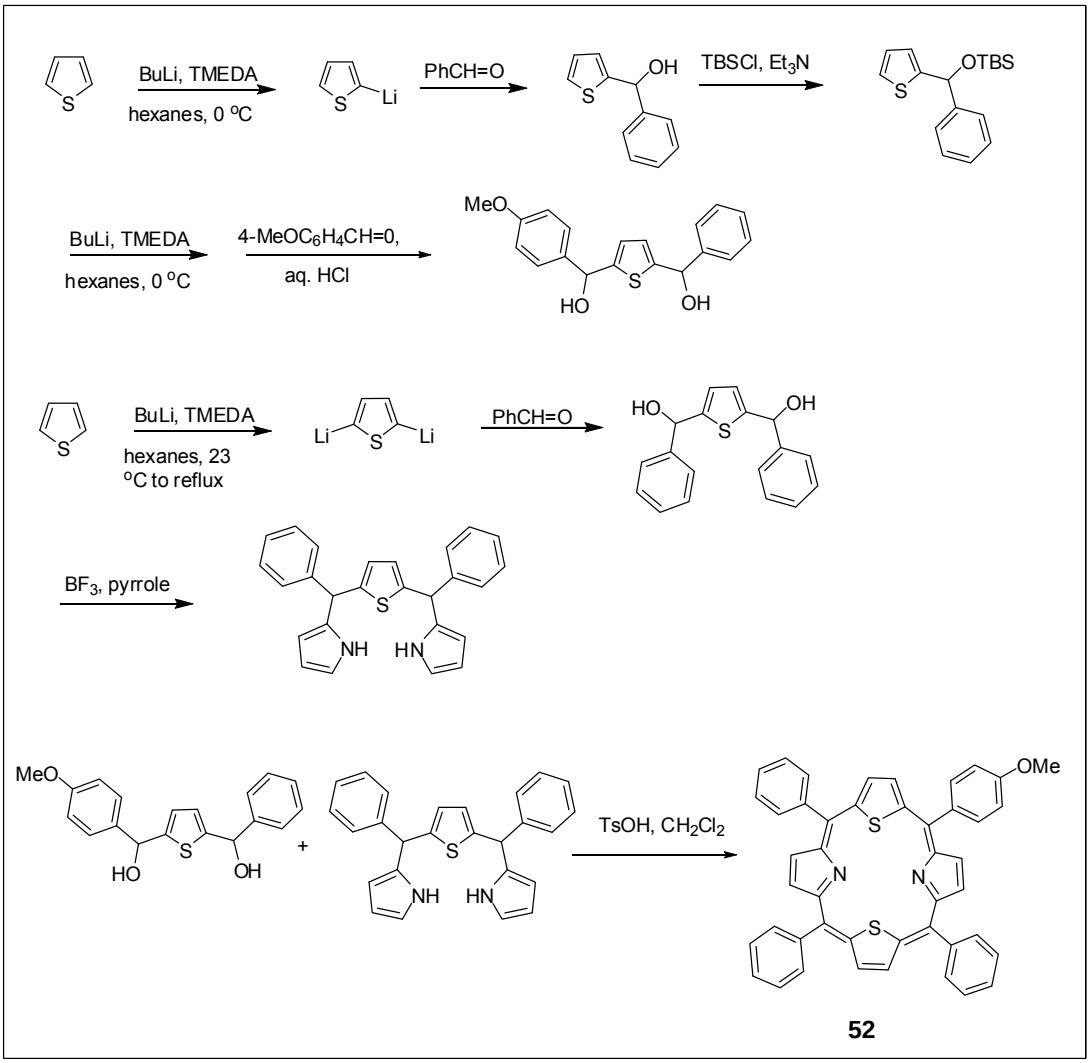

Scheme 4. Synthesis of compound **52**[92]**.**

3.2. Experimental section

3.2.1. Synthesis

3.2.1.1. Biphenyl-4-yl propiolate (16). To an ice cooled and stirred solution of propargylic acid (285 mg, 4.01 mmol) and 4-phenylphenol (693 mg, 4.07 mmol) in dry diethyl ether was added dropwise a solution of *N,N*'-dicyclohexylcarbodiimide (DCC, 840 mg, 4.07 mmol) and 4-dimethylaminopyridine (DMAP, 3.2 mg, 0.03 mmol) in dry diethyl ether (10 mL) during 2 h under nitrogen atmosphere. Reaction mixture was then stirred at room temperature for 10 h, filtered and the solid was washed with diethyl ether. Then, the combined filtrate was washed with 1 N HCl solution followed by washing with brine and dried with anhydrous Na_2SO_4. The solvent was removed under reduced pressure to give the crude product that was then purified by column chromatography using ethyl acetate: hexane (1:9) as an eluant to give compound **16** (0.81 mg, 90 %). ^{1}H NMR (400 MHz, $CDCl_3$): δ 3.12 (s, 1H), 7.24 (s, 1H), 7.26 (s, 1H), 7.38 (s, 1H), 7.47 (t, *J* = 7.8 Hz, 2H), 7.57 (s, 1H), 7.59 (s, 1H), 7.62 (s, 1H), 7.64 (s, 1H). HRMS ESI (*m/z*): Calculated for $C_{15}H_2O_2$ ($[M+H]^+$): 223.0681; found: 223.0734.

3.2.1.2. Biphenyl-4-yl 3-(diethylamino)acrylate (17). Diethylamine (66 mg, 0.89 mmol) and compound **16** (200 mg, 0.89 mmol) were dissolved in dry THF (20 mL), and the solution was stirred at RT for 15 min. The solvent was removed under reduced pressure to give the crude product which was then

purified by column chromatography using ethyl acetate:hexane (7:3) to give compound **17** (237 mg, 89 %). ^{1}H NMR (400 MHz, $CDCl_3$) δ 1.24 (t, J = 7.0 Hz, 6H), 3.28 (br. s , 4H), 4.79 (d, J = 13.0 Hz, 1H), 7.20 (d, J = 8.6 Hz, 2H), 7.36 (t, J = 7.4 Hz, 1H), 7.44 (t, J = 7.8 Hz, 2H), 7.62 (m, 4H), 7.63 (d, J = 13.0 Hz, 1H). HRMS ESI (*m/z*): Calculated for $C_{19}H_{22}NO_2$ ($[M+H]^+$): 296.1572; found: 296.1647.

3.2.1.3. Biphenyl-4-yl 3-(piperidin-1-yl)acrylate (18). The compound **18** was prepared according to the method described for compound **17** employing piperidine (77 mg, 0.89 mmol) and compound **16** (200 mg, 0.89 mmol) to give white solid compound **18** (221 mg, 80%). ^{1}H NMR (400 MHz, $CDCl_3$) δ 1.67 (br s, 6H), 3.30 (s (b), 4H), 4.83 (d, J = 13.1 Hz, 1H), 7.19 (d, J = 8.6 Hz, 2H), 7.34 (t, J = 7.2 Hz, 1H), 7.44 (t, J = 7.8 Hz, 2H), 7.59 (m, 5H). HRMS ESI (*m/z*): Calculated for $C_{20}H_{22}NO_2$ ($[M+H]^+$): 308.1572; found: 308.1646.

3.2.1.4. Biphenyl-4-yl 3-(phenylthio)acrylate (19). To a stirred solution of 1,4-diazabicyclo[2.2.2]octane (DABCO, 10 mg, 0.89 mmol) and thiophenol (99 mg, 0.89 mmol) in dry THF (20 mL) at RT was added compound **16** (200 mg, 0.89) dissolved in dry THF (2 mL) through a syringe over 12 min. The reaction mixture was further stirred for 20 min. 10% $NaOH_{(aq)}$ was added. The combined organic layer was washed with brine, dried over anhydrous

Na_2SO_4, filtered and the solvent was removed by evaporation. The crude product was purified by column chromatography using ethyl acetate:hexane (2:8) as an eluent to give compound **19** (254 mg, 85 %). ^{1}H NMR (400 MHz, $CDCl_3$) *δ* 5.84 (d, *J* = 15.0 Hz, 1H), 7.18 (d, *J* = 8.6 Hz, 2H), 7.46 (m, 6H), 7.58 (m, 6H), 8.05 (d, *J* = 15.0 Hz, 1H). HRMS ESI (*m/z*): Calculated for $C_{21}H_{17}O_2S$ ($[M+H]^+$): 333.0871; found: 333.0852.

3.2.1.5. Biphenyl-4-yl 3-(benzylthio)acrylate (20). The compound **20** was prepared according to the method described for compound **19** employing compound **16** (200 mg, 0.89 mmol) and benzylthiol (112 mg, 0.89 mmol) to give white solid compound **20** (284 mg, 91%). ^{1}H NMR (300 MHz, $CDCl_3$) δ 4.10 (s, 2H), 6.02 (d, *J* = 15.1 Hz, 1H), 7.18 (d, *J* = 8.3 Hz, 2H), 7.39 (m, 8H), 7.57 (t, *J* = 5.9 Hz, 4H), 7.94 (d, *J* = 15.1 Hz, 1H). HRMS ESI (*m/z*): Calculated for $C_{22}H_{19}O_2S$ ($[M+H]^+$): 347.1028; found: 347.1101.

3.2.1.6. Biphenyl-4-yl 3-phenoxyacrylate (21). The compound **21** was prepared according to the method described for compound **19** employing compound **16** (435 mg, 2.15 mmol) and phenol (223 mg, 2.36 mmol) to give white solid compound **21** (510 mg, 80%). ^{1}H NMR (300 MHz, $CDCl_3$) *δ* 5.67 (d, *J* = 12.2 Hz, 1H), 7.40 (d, *J* = 8.9 Hz, 2H), 7.11 (d, *J* = 8.5 Hz, 2H), 7.33 (q, *J* = 7.9 Hz, 5H), 7.49 (t, *J* = 7.0 Hz, 5H), 7.92 (d, *J* = 12.2 Hz, 1H). HRMS ESI (*m/z*): Calculated for $C_{21}H_{I7}O_3$ ($[M+H]^+$): 317.1099; found: 317.1175.

3.2.1.7. Biphenyl-4-yl 3-(benzyloxy)acrylate (22). The compound **22** was prepared according to the method described for compound **19** employing compound **16** (300 mg, 1.34 mmol) and benzylalcohol (161 mg, 1.48 mmol) to give white solid compound **22** (419 mg, 94%). ^{1}H NMR (400 MHz, $CDCl_3$) δ 5.00 (s, 2H), 5.53 (d, *J* = 12.5 Hz, 1H), 7.18 (d, *J* = 8.2 Hz, 2H), 7.39 (m, 8H), 7.57 (t, *J* = 4.8 Hz, 4H), 7.88 (d, *J* = 12.5 Hz, 1H). HRMS ESI (*m/z*): Calculated for $C_{22}H_{19}O_3$ ($[M+H]^+$): 331.1256; found: 331.1332

3.2.1.8. (*E*)-*S*-Phenyl 3-(piperidin-1-yl)prop-2-enethioate (23). The compound **23** was prepared according to the method described for compound **18** employing piperidine (184 mg, 2.18 mmol) and compound **39** (350 mg, 2.18 mmol) to give pale red solid compound **23** (507 mg, 95%). ^{1}H NMR (300 MHz, CD_2Cl_2) δ 1.64 (s, 6H), 3.27 (s, 4H), 5.11 (d, *J* = 12.6 Hz, 1H), 7.38 (s, 3H), 7.45 (d, *J* = 5.2 Hz, 1H), 7.48 (d, *J* = 12.6 Hz, 1H). HRMS ESI (*m/z*): Calculated for $C_{14}H_{18}NOS$ ($[M+H]^+$): 248.1031; found: 248.1125.

3.2.1.9. (*E*)-*N*-Phenyl-3-(piperidin-1-yl)acrylamide (24). The compound **24** was prepared according to the method described for compound **18** employing piperidine (211 mg, 2.48 mmol) and compound **40** (360 mg, 2.48 mmol) to give brown solid compound **24** (497 mg, 87 %). ^{1}H NMR (300 MHz, CD_2Cl_2) δ 1.62 (s, 6H), 3.20 (s, 4H), 4.73 (d, *J* = 12.6 Hz, 1H), 6.89 (s, 1H), 7.00 (t, *J* = 6.2 Hz, 1H), 7.27 (t, *J* = 6.9 Hz, 2H), 7.43 (d, *J* = 12.6 Hz, 1H),

7.51 (d, *J* = 6.9 Hz, 2H). HRMS ESI (*m/z*): Calculated for $C_{14}H_{19}N_2O$ ($[M+H]^+$): 231.1419; found: 231.1512.

3.2.1.10. Phenyl 1-(3-(biphenyl-4-yloxy)-3-oxoprop-1-enyl)pyrrolidine-2-carboxylate (25). The compound **25** was prepared according to the method described for compound **28** employing compound **43** (112 mg, 0.36 mmol), compound **16** (82 mg, 0.36 mmol) and 0.06 ml of *N*,*N*–diisopropylethylamine to give solid compound **25 (**129 mg, 85 %). ^{1}H NMR (400 MHz, $CDCl_3$) *δ* 2.17 (m, 2H, pro), 2.38 (br. s, 2H, pro), 3.28-3.83 (m, 2H, pro) 4.49 (br. s, 1H, pro), 4.87 (d, *J* = 12.0 Hz, 1H), 7.12 (d, *J* = 7.8 Hz, 2H), 7.18 (d, *J* = 8.5 Hz, 2H), 7.31 (m, 2H), 7.41 (q, *J* = 7.5 Hz, 4H), 7.58 (s, 2H), 7.64 (s, 2H), 7.86 (d, *J* = 12.0 Hz, 1H). HRMS ESI (*m/z*): Calculated for $C_{26}H_{24}NO_4$ ($[M+H]^+$): 414.1627; found: 414.1697.

3.2.1.11. Phenyl 1-(3-(biphenyl-4-yloxy)-3-oxoprop-1-enyl)pyrrolidine-3-carboxylate (26). The compound **26** was prepared following all the steps described for compound **25** (137 mg, 90 %**).** ^{1}H NMR (400 MHz, $CDCl_3$) *δ* 1.51-1.71 (m, 1H, pro), 2.45 (br. s, 2H, pro), 3.40-3.95 (m, 4H, pro), 4.78 (d, *J* = 13.0 Hz, 1H), 7.11 (d, *J* = 7.7 Hz, 2H), 7.20 (d, *J* = 8.6 Hz, 2H), 7.35 (s, 1H), 7.44 (q, *J* = 7.6 Hz, 4H), 7.58 (s, 2H), 7.60 (s, 2H), 7.83 (d, *J* = 13.0 Hz, 1H). HRMS ESI (*m/z*): Calculated for $C_{26}H_{24}NO_4$ ($[M+H]^+$): 414.1627; found: 414.1700.

3.2.1.12. (*E*)-Biphenyl-4-yl 3-(4-((2-phenoxyacetoxy)methyl)piperidin-1-yl)acrylate (27). To a stirred solution of compound **56** (75 mg, 0.49 mmol) and compound **59** (250 mg, 0.74 mmol) in dry dichloromethane (DCM) was added dropwise a solution of DCC (407 mg, 1.98 mmol) and DMAP (60 mg, 0.49 mmol) in dry DCM (15 mL). Reaction mixture was then stirred at room temperature for 24 h. The solvent was removed under reduced pressure to give the crude product that was then purified by column chromatography using ethyl acetate: hexane (6:4) as an eluant to give a white solid compound **27** (279 mg, 80 %). ^{1}H NMR (300 MHz, CD_2Cl_2) δ 1.11 (m, 1H), 1.33 (m, 2H), 1.72 (t, *J* = 12.9 Hz, 2H), 1.90 (d, *J* = 9.9 Hz, 1H), 3.05 (br s, 1H), 3.58 (m, 2H), 4.09 (d, *J* = 5.9, 2H), 4.68 (s, 2H), 4.83 (d, *J* = 13.0 Hz, 1H), 6.91 (d, *J* = 7.9 Hz, 2H), 7.02 (t, *J* = 7.2, 1H), 7.15 (d, *J* = 8.3, 2H), 7.33 (m, 2H), 7.45 (t, *J* = 7.50, 2H), 7.59 (br s, 5H). HRMS ESI (*m/z*): Calculated for $C_{29}H_{30}NO_5$ ($[M+H]^+$):472.2046 ; found: 472.2118.

3.2.1.13. Biphenyl-4-yl 3-(4-(3-phenoxypropyl)piperazin-1-yl)acrylate (28). Compound **50** (150 mg, 0.45 mmol) was dissolved in dry THF (20 mL) with stirring under nitrogen. *N*,*N*-diisopropylethylamine (0.08 mL) was added drop wise and then compound **16** (100 mg, 0.45 mmol) dissolved in dry THF (5 mL) was added. The reaction mixture was stirred at RT for 15 min. After the reaction was completed, solvent was removed under reduced pressure to give the crude product which was then purified by column chromatography

using ethyl acetate:hexane (4:6) to give product **28** (173 mg, 87 %). ^{1}H NMR (300 MHz, CD_2Cl_2) δ 1.94 (m, 2H), 2.51 (m, 6H), 3.31 (s, 4H), 4.01 (t, *J* = 6.1 Hz, 2H), 4.80 (d, *J* = 13.0 Hz, 1H), 6.89 (m, 3), 7.12 (d, *J* = 8.2 Hz, 2H), 7.26 (t, *J* = 7.7 Hz, 2H) 7.32 (d, *J* = 6.2 Hz, 1H), 7.42 (t, *J* = 7.5 Hz, 2H), 7.51 (s, 1H), 7.56 (m, 4H). HRMS ESI (*m/z*): Calculated for $C_{28}H_{31}N_2O_3$ ($[M+H]^+$): 443.2256; found: 443.2333.

3.2.1.14. (*E*)-Biphenyl-4-yl3-(4-((2-phenoxy-10,15,20-triphenyl-21,23-dithiaporphyrin acetoxy)methyl)piperidin-1-yl)acrylate (**29).** The compound **29** was prepared according to the method described for compound **27** employing compound **57** (80 mg, 0.11 mmol), compound **59** (56 mg, 0.17 mmol), DCC (45 mg, 0.22 mmol) and DMAP (13 mg, 0.11 mmol) to give a solid red purple compound **29** (128 mg, 74%).^{1}H NMR (300 MHz, CD_2Cl_2) δ 1.01 (m, 2H), 1.24 (m, 2H), 1.60 (m, 2H), 1.80 (d, *J* = 12.2 Hz, 2H), 3.34 (m, 1H), 3.97 (br s, 1H), 4.14 (d, *J* = 5.9, 2H), 4.72 (d, *J* = 12.9 Hz, 1H), 4.88 (s, 2H), 6.97 (d, *J* = 8.6 Hz, 2H), 7.32 (m, 3H), 7.45 (m, 5H), 7.74 (br s, 9H), 8.16 (m, 8H), 8.62 (m, 4H), 9.64 (m, 4H). HRMS ESI (*m/z*): Calculated for $C_{67}H_{52}N_3O_5S_2$ ($[M+H]^+$): 1042.3270; found:1042.3343 .

3.2.1.15. Biphenyl-4-yl3-(4-(3-(5-(4-phenoxy-10,15,20-triphenyl-21,23-dithiaporphyrin propyl)piperazin-1-yl)acrylate (30). The compound **30** was prepared following all the steps described for compound **28** (39 mg, 65

%). ^{1}H NMR (300 MHz, $CDCl_3$) δ 2.08 (br. s, 2H), 2.52 (br. s, 4H), 2.66 (br. s, 2H), 3.33 (br. s, 2H), 4.15 (br. s, 4H), 4.80 (d, *J* = 13.3 Hz, 1H), 7.11 (d, *J* = 8.4 Hz, 2H), 7.17 (s, 1H), 7.26 (m, 1H), 7.35 (t, *J* = 7.6 Hz, 2H), 7.49 (s, 2H), 7.52 (s, 2H), 7.72 (s, 11H) 8.08 (d, *J* = 8.6 Hz, 2H), 8.17 (s, 6H), 8.61 (s, 4H), 9.61 (s, 4H). HRMS ESI (*m/z*): Calculated for $C_{66}H_{53}N_4O_3S_2$ ($[M+H]^+$): 1013.35; found: 1013.3565.

3.2.1.16. (*E*)-((13*S*)-13-Methyl-17-oxo-7,8,9,11,12,13,14,15,16,17-decahydro-6H-cyclopenta[a]phenanthren-3-yl)3-(4-((2-phenoxy-10,15,20-triphenyl-21,23-dithiaporphyrin acetoxy)methyl)piperidin-1-yl)acrylate (31). The compound **31** was prepared according to the method described for compound **27** employing compound **57** (120 mg, 0.17 mmol), compound **60** (108 mg, 0.25 mmol), DCC (68 mg, 0.33 mmol) and DMAP (20 mg, 0.17 mmol) to give a solid red purple compound **31** (211 mg, 75%). ^{1}H NMR (300 MHz, CD_2Cl_2) δ 0.77 (s, 3H), 1.95-1.08 (m, 3H), 1.18-1.39 (m, 7H), 1.55-1.64 (m, 2H), 1.75-1.80 (m, 2H) 1.88-2.08 (m, 2H), 2.18-2.41 (m, 1H), 2.72 (m, 2H), 3.00 (br s, 1H), 3.33 (m, 1H), 3.53 (m, 2H), 3.96 (m, 1H), 4.13 (d, *J* = 6.1 Hz, 2H), 4.69 (d, *J* = 13.3 Hz, 1H), 4.87 (s, 2H), 6.62 (s, 2H), 7.07 (d, *J* = 8.6, 1H), 7.29 (d, *J* = 8.6 Hz, 2H), 7.43 (d, *J* = 13.3 Hz, 1H), 7.74 (br s, 9H), 8.12 (d, *J* = 8.6, 2H), 8.16 (m, 6H), 8.63 (m, 4H), 9.64 (m, 4H). HRMS ESI (*m/z*): Calculated for $C_{73}H_{64}N_3O_6S_2$ ($[M+H]^+$): 1142.4158; found:1142.4233.

3.2.1.17. *S*-Phenyl prop-2-ynethioate (39). The compound **39** was prepared according to the method described for compound **16** employing thiophenol (1g, 9.07 mmol), propargylic acid (0.64 g, 9.07 mmol), DCC (1.87g, 9.07 mmol) and DMAP (7.3 mg, 0.06 mmol) to give brownish liquid compound **39** (1.24 g, 84%). ^{1}H NMR (300 MHz, CD_2Cl_2) δ 3.40 (s, 1H), 7.46 (s, 5H).

3.2.1.18. *N*-Phenylpropiolamide (40). The compound **40** was prepared according to the method described for compound **16** employing aniline (1g, 0.01mol), propargylic acid (0.76g, 0.01 mol), DCC (2.2g, 0.01) and DMAP (8.6 mg, 0.07 mmol) to give brown solid compound **40** (1.35 g, 87 %). ^{1}H NMR (300 MHz, CD_2Cl_2) δ 2.93 (s, 1H), 7.15 (t, J = 6.9 Hz, 1H), 7.33 (t, J = 7.5 Hz, 2H), 7.52 (t, J = 7.4 Hz, 2H), 7.79 (br s, 1H).

3.2.1.19. 1-(*tert*-Butoxycarbonyl)pyrrolidine-2-carboxylic acid (41). (*S*)-Proline (2.3 g, 20 mmol) was dissolved in 40 mL of DCM. To the solution, triethylamine (3.73 mL, 26 mmol) and di-tert-butyl dicarbonate (6.3 g, 28.9 mmol) dissolved in DCM (5 mL) were added. The mixture was stirred at RT for 2.5 h. Then, the reaction was quenched with saturated aqueous citric acid solution (15 mL), washed with brine (30 mL) and water (20 mL). The organic layer was dried over anhydrous Na_2SO_4, filtered and the solvent removed by evaporation. The white crystallized solid formed was washed with hexane to

obtain compound **41** (3.85 g, 90 %). ^{1}H NMR (400 MHz, $CDCl_3$) δ 1.42 (s, 2H), 1.75 – 2.39 (m, 4H), 3.22 – 3.54 (m, 2H), 4.21 – 4.39 (m, 1H).

3.2.1.20. 1-*tert*-Butyl 2-phenyl pyrrolidine-1,2-dicarboxylate (42). Compound **41** (500 mg, 2.32 mmol) and DCC (523 mg, 2.53 mmol) in DCM (12 mL) were stirred at 0 ^{o}C for 30 min under argon atmosphere. To the solution, phenol (199 mg, 2.12 mmol) was added and stirred at RT for 24 h. The reaction mixture was diluted with ethyl acetate (30 mL) and filtered. The combined organic layer was dried over anhydrous sodium sulfate, filtered and the solvent removed by evaporation. The crude product was purified by column chromatography using ethyl acetate–hexane (4:6) to give compound **42** as a white solid (492 mg, 80 %). ^{1}H NMR (400 MHz, $CDCl_3$) δ 1.46 (s, 9H), 1.89 – 2.43 (m, 4H), 3.40 – 3.66 (m, 2H), 4.41 – 4.55 (m, 1H), 7.09 (m, 2H), 7.22 (m, 1H), 7.37 (m, 2H).

3.2.1.21. Phenyl pyrrolidine-2-carboxylate (43). Compound **42** (500 mg, 1.71 mmol) was dissolved in dry DCM (6 mL). Trifluoroacetic acid (0.66 mL, 8.58 mmol) was then added to the solution at 0 ^{0}C and stirred under nitrogen for 1 h. The reaction mixture was then concentrated under vacuum and used directly in the next step without further purification.

3.2.1.22. 1-*tert*-Butyl 3-phenyl pyrrolidine-1,3-dicarboxylate (44). The compound **44** was prepared according to the method described for compound **42** employing 1-(tert-butoxycarbonyl)pyrrolidine-3-carboxylic acid (500 mg, 2.32 mmol), phenol (198 mg, 2.12 mmol) and DCC (522 mg, 2.53) to give pale white solid compound **44** (510 mg, 83 %).^{1}H NMR (400 MHz, $CDCl_3$) δ 1.40 (s, 9H), 1.84 – 1.57 (m, 1H), 2.21(m, 2H), 3.17-3.70 (m, 4H), 7.00 (s, 1H), 7.02 (s, 1H), 7.17 (t, *J* = 7.8 Hz, 1H), 7.32 (t, *J* = 7.8 Hz, 2H).

3.2.1.23. Phenyl pyrrolidine-3-carboxylate (45). The compound **45** was prepared according to the method described for compound **43** employing TFA (0.66 mL, 8.58 mmol) and compound **44**(500 mg, 1.71 mmol) to give white solid compound. Compound was used without further purification after solvent removal.

3.2.1.24. (3-Bromopropoxy)benzene (46). Phenol (1.0 g, 10.6 mmol) was dissolved in acetone (20 mL). Anhydrous potassium carbonate (7.34 g, 53.1 mmol) and 1,3-dibromopropane (8.58 g, 42.5 mmol) was added to the solution. The reaction mixture was refluxed in an oil bath for 12 h. After the reaction, the potassium carbonate was removed by suction filtration and solvent was removed under reduced pressure to give the crude product which was then purified by column chromatography using ethyl acetate:hexane (3:7) to give product **46** (2.05 g, 90 %). ^{1}H NMR (400 MHz,

$CDCl_3$) δ 2.24 (m, 2H), 3.54 (t, J = 6.4 Hz, 2H), 4.03 (t, J = 5.8 Hz, 2H), 6.86 (m, 3H), 7.21 (m, 2H).

3.2.1.25. 5-(3-Bromopropoxy)phenyl-10,15,20-triphenyl-21,13-dithiaporphyrin (47). Compound **47** was prepared according to the method described for compound **46** employing 5-(4-hydroxyphenyl)-10,15,20-triphenyl-21,23dithiaporphyrin (300 mg, 0.45 mmol), 1,3-dibromopropane (364 mg, 1.81 mmol) and potassium carbonate (311 mg, 2.26) to give pale red solid compound **47** (301 mg, 85 %).^{1}H NMR (300 MHz, $CDCl_3$) δ 2.52 (m, 2H), 3.79 (t, J = 6.3 Hz, 2H), 4.41 (t, J = 5.6 Hz, 2H), 7.36 (d, J = 8.3 Hz, 2H), 7.81 (s, 9H), 8.19 (d, J = 8.3 Hz, 2H), 8.26 (d, J = 3.6 Hz, 6H), 8.68 (s, 3H), 8.70 (s, 1H), 9.70 (s, 3H), 9.73 (s, 1H).

3.2.1.26. *tert*-Butyl 4-(3-phenoxypropyl)piperazine-1-carboxylate (48). To a solution of *n*-Boc-piperazine (1.08 g, 5.80 mmol) in dry DMF (10 mL) were added anhydrous potassium carbonate (4.01 g, 29.04 mmol) and compound **46** (1.5 g, 6.97 mmol). The reaction mixture was stirred at RT for 8 h. The potassium carbonate was removed by suction filtration and the solvent was removed under reduced pressure. The residue was dissolved with water and extracted with ethyl acetate. The combined organic layers were dried over anhydrous sodium sulfate and the solvent was removed by evaporation. The crude product was purified by column chromatography using ethyl

acetate:hexane (8:2) to give compound **48** (1.58 g, 85 %). ^{1}H NMR (400 MHz, $CDCl_3$) δ 1.39 (s, 9H), 1.92 (s, 2H), 2.36 (s, 4H), 2.48 (s, 2H), 3.39 (s, 4), 3.95 (m, 2), 6.83 (m, 2H), 7.19 (m, 3H).

3.2.1.27. *tert*-Butyl 4-(5-(3-phenyl-10,15,20-triphenyl-21,13-dithiaporphyrinoxypropyl)piperazine-1-carboxylate (49). The compound **49** was prepared according to the method described for compound **48** employing compound **47** (150 mg, 0.19 mmol), n-Boc-piperazine (29 mg, 0.16 mmol) and potassium carbonate (110 mg, 0.80) to give pale red solid compound **49** (128 mg, 75 %). ^{1}H NMR (300 MHz, $CDCl_3$) δ 1.50 (s, 9H), 2.25 (br s, 2H), 2.60 (br s, 4H), 2.77 (br s, 2H), 3.59 (br s, 4H), 4.33(br s, 2H), 7.33 (d, J = 8.3 Hz, 2H), 7.80 (s, 9H), 8.16 (d, J = 8.3 Hz, 2H), 8.24 (d, J = 4.0, 6H), 8.68 (s, 4H), 9.68 (s, 4H).

3.2.1.28. 1-(3-Phenoxypropyl)piperazine (50). The compound **50** was prepared according to the method described for compound **43** employing TFA (6 mL) and compound **48** (550 mg, 1.72 mmol) to give white solid compound. Compound was used without further purification after solvent removal.

3.2.1.29. 1-3(-(5-(4-Phenyl)-10,15,20-triphenyl-21,23dithiaporphyrin)oxypropylpiperazine (51). Compound **49** (70 mg,

0.09 mmol) was dissolved in dry DCM (6 mL). After trifluoroacetic acid (0.03 mL) was added to the solution at 0 ^{0}C, it was stirred under nitrogen for 1 h. The reaction mixture was then concentrated under vacuum and then used directly in the next step.

3.2.1.30. 5-(4-Methoxyphenyl)-10,15,20-triphenyl-21-23-dithiaporphyrin (52). Compound **52** was prepared following reference.[92]

^{1}H NMR (400 MHz, $CDCl_3$) δ 4.11 (s, 3H), 7.36 (d, J = 8.4 Hz, 2H), 7.81 (s, 9H), 8.12 (d, J = 8.4 Hz, 2H), 8.16 (m, 6H), 8.63 (m, 4H), 9.64 (m, 4H). HRMS ESI (*m/z*): Calculated for $C_{45}H_{31}N_2OS_2$ ($[M+H]^+$): 679.1878; found: 679.186.

3.2.1.31. 5-(4-Hydroxyphenyl)-10,15,20-triphenyl-21,23dithiaporphyrin (53). Compound **53** was prepared following reference.[92]

^{1}H NMR (400 MHz, $CDCl_3$) δ 7.11 (d, J = 8.4 Hz, 2H), 7.63 (s, 9H), 8.10 (d, J = 8.4 Hz, 2H), 8.16 (m, 6H), 8.63 (m, 4H), 9.64 (m, 4H). HRMS ESI (*m/z*): Calculated for $C_{44}H_{29}N_2OS_2$ ($[M+H]^+$): 665.1721; found: 665.1708.

3.2.1.32. Ethyl 2-phenoxyacetate (54). The compound **54** was prepared according to the method described for compound **46** employing phenol (4.5 g, 0.05 mol), ethyl bromoacetate (31 g, 0.19 mol) and potassium carbonate (33 g, 0.24 mol) to give a colorless oily compound **54** (6.9 g, 81 %). ^{1}H NMR

(300 MHz, CD_2Cl_2) δ 1.30 (t, J = 7.0 Hz, 3H), 4.27 (q, J = 7.0 Hz, 2H), 4.62 (s, 2H), 6.91 (d, J = 7.9 Hz, 2H), 6.99 (t, J = 7.0 Hz, 1H), 7.29 (t, J = 7.6 Hz, 2H).

3.2.1.33. Ethyl 5,10,15-triphenyl-20-(4-carboxylatomethoxy)phenyl-21,23-dithiaporphyrin (55). The compound **55** was prepared according to the method described for compound **46** employing compound **53** (0.25 g, 0.38 mol), ethyl bromoacetate (2.1 mL, 19 mmol) and potassium carbonate (2.6 g, 19 mmol) to give purple solid compound **55** (0.22 g, 78 %). ^{1}H NMR (300 MHz, CD_2Cl_2) δ 1.42 (t, J = 7.0 Hz, 3H), 4.42 (q, J = 7.0 Hz, 2H), 4.92 (s, 2H), 7.37 (d, J = 8.2, 2H), 7.81 (br s, 9H), 8.19 (d, J = 8.2, 2H), 8.26 (m, 6H), 8.69 (m, 4H), 9.70 (m, 4H). HRMS ESI (*m/z*): Calculated for $C_{48}H_{35}N_2O_3S_2$ ($[M+H]^+$): 751.2011; found:751.2065 .

3.2.1.34. 2-Phenoxyacetic acid (56). Compound **54** (2 g, 0.011 mol) was dissolved in 100 mL of THF, and 1 M NaOH (110 mL, 0.11 mol) was added. The reaction mixture was stirred at RT for 24 h. The solution was then acidified by the addition of 40 mL of acetic acid. The reaction mixture was diluted with 150 mL of H_2O and the product was extracted with ethyl acetate. The organic extracts was dried over magnesium sulfate and concentrated. The crude product was washed several times with hexane:ethylacetate (9:1) to give a pale white solid (1.58 g, 94 %). ^{1}H NMR (300 MHz, CD_2Cl_2) δ 4.69

(s, 2H), 6.92 (d, *J* = 8.2 Hz, 2H), 7.03 (t, *J* = 7.0 Hz, 1H), 7.32 (t, *J* = 7.6 Hz, 2H),

3.2.1.35. 5,10,15-Triphenyl-20-(4-carboxylatomethoxy)phenyl-21,23-dithiaporphyrin (57). The compound **57** was prepared according to the method described for compound **56** employing compound **55** (0.18 g, 0.24 mmol), 1 M NaOH (20 mL, 20 mmol) and 8 mL of acetic acid to a purple solid compound **57** (0.16 g, 92 %). ^{1}H NMR (300 MHz, CD_2Cl_2) δ 5.00 (s, 2H), 7.42 (d, *J* = 7.8, 2H), 7.80 (br s, 9H), 8.21 (br s, 8H), 8.67 (s, 4H), 9.70 (s, 4H).

3.2.1.36. (13*S*)-13-Methyl-17-oxo-7,8,9,11,12,13,14,15,16,17-decahydro-6*H*-cyclopenta[a]phenanthren-3-ylpropiolate (58). The compound **58** was prepared according to the method described for compound **16** employing estrone (500 mg, 1.85 mmol), propargylic acid (262 mg, 3.69 mmol), DCC (763 mg, 3.69 mmol) and DMAP (2.98 mg, 0.03 mmol) and dry DMF (10 mL) to give white solid compound **58** (417 mg, 70%). ^{1}H NMR (300 MHz, CD_2Cl_2) δ 0.84 (s, 3H), 1.52 (m, 5H), 1.85-2.51 (m, 8H), 2.84 (s, 2H), 2.99 (s, 1H), 6.81 (s, 1H), 6.84 (d, *J* = 9.0 Hz, 1H), 7.24 (d, *J* = 8.9 Hz, 1H). HRMS ESI (*m/z*): Calculated for $C_{21}H_{23}O_3$ ($[M+H]^+$): 323.1569; found: 323.1660.

3.2.1.37. (*E*)-Biphenyl-4-yl 3-(4-(hydroxymethyl)piperidin-1-yl)acrylate (59). The compound **59** was prepared according to the method described for compound **17** employing piperidin-4-ylmethanol (900 mg, 4.05mmol) and compound **16** (466 mg, 4.05 mmol) to give white solid compound **59** (1.15 g, 84%).^{1}H NMR (300 MHz, CD_2Cl_2) δ 1.29 (m, 1H), 1.80 (m, 2H), 3.08 (br s, 1H), 3.51 (s, 2H), 3.62 (d, *J* = 9.9 Hz, 2H), 4.82 (d, *J* = 13.0 Hz, 1H), 7.15 (d, *J* = 8.2 Hz, 2H), 7.35 (m, 1H), 7.45 (t, *J* = 7.0 Hz, 2H), 7.60 (br s, 5H). HRMS ESI (*m/z*): Calculated for $C_{21}H_{23}NO_3Na$ ($[M+Na]^+$):338.1678 ; found: 338.1751.

3.2.1.38. (*E*)-((13*S*)-13-Methyl-17-oxo-7,8,9,11,12,13,14,15,16,17-decahydro-6H-cyclopenta[a]phenanthren-3-yl) 3-(4-(hydroxymethyl)piperidin-1-yl)acrylate (60). The compound **60** was prepared according to the method described for compound **17** employing piperidin-4-ylmethanol (61 mg, 0.53 mmol) and compound **58** (170 mg, 0.53 mmol) to give white solid compound **60** (212 mg, 92%). ^{1}H NMR (300 MHz, CD_2Cl_2) δ 0.91 (s, 3H), 1.20-1.37 (m, 3H), 1.46 (s, 2H), 1.50 (s, 2H), 1.57-1.74 (m, 4H) 1.79 (s, 1H), 1.83 (s, 1H), 1.91 (d, *J* = 11.4 Hz, 1H), 1.98-2.17 (m, 3H), 2.24-2.54 (m, 3H), 2.90 (m, 2H), 3.01(s, 1H), 3.50(s, 2H), 3.60 (d, *J* = 11.1, 2H), 4.78 (d, *J* = 12.9 Hz, 1H), 6.79 (s, 2H), 7.26 (d, *J* = 8.1 Hz, 1H), 7.53 (d, *J* = 12.9 Hz, 1H). HRMS ESI (*m/z*): Calculated for $C_{27}H_{35}NO_4Na$ ($[M+Na]^+$): 460.2566; found: 460.2452.

3.2.1.39. Sodium benzenethiolate (66). A solution of thiophenol (4.3 g, 39 mmol) in 5mL of dry diethyl ether was added to a stirring suspension of sodium (0.45 g, 19.5 mmol) in 20 mL of diethyl ether. Stirring was continued until sodium could no longer be seen. The white solid product was filtered and washed with hexane to remove thiophenol and air dried in a desiccator to give compound **66** (2.31 g, 90 %).

3.2.2.1. (***Z*)-1,2-Bis(phenylthio) ethene (control).** A solution of (*Z*)-1,2-dichloroethene (0.49 g, 5.04 mmol) and compound **66** (2.0 g, 15.15 mmol) in HMPA (10 mL) was stirred under nitrogen for 1 h. The solvent was removed under reduced pressure to give the crude product that was then purified by column chromatography using 100 % hexane as a solvent to give control (1.04 g, 85 %). ^{1}H NMR (400 MHz, $CDCl_3$) δ 6.55 (s, 2H), 7.29 (m, 2H), 7.35 (t, J = 7.7 Hz, 4H), 7.43 (s, 2H), 7.44 (m, 2H). HRMS ESI (*m/z*): Calculated for $C_{14}H_{12}S_2$ $[M]^+$: 244.0380; found: 244.0377.

3.3. Results and discussion

3.3.1 Synthesis and photo-oxidation

Table 2. Yield of click reaction, rate of oxidation by singlet oxygen, and coupling constant of olefinic protons.

Compd #	yield of click reaction	% of photo-oxidation in 25 min	coupling constant (*J*, Hz)
control	85	87	-
17	89	62	13.0
18	80	72	13.1
18a	-	31	-
19	85	0	15.0
20	91	0	15.1
21	80	0	12.2
22	94	0	12.5
23	95	60	12.6
24	87	100	12.6
25	85	32	12.0
26	90	62	12.3
27	84	74	13.0
28	87	50	13.0

29	84	89[c]	13.0
30	65	79[b]	13.3
31	92	90[c]	12.9

[a] DABCO was added in the reaction solution of **18**, [b] oxidation rate in 15 min, [c] oxidation rate in 10 min

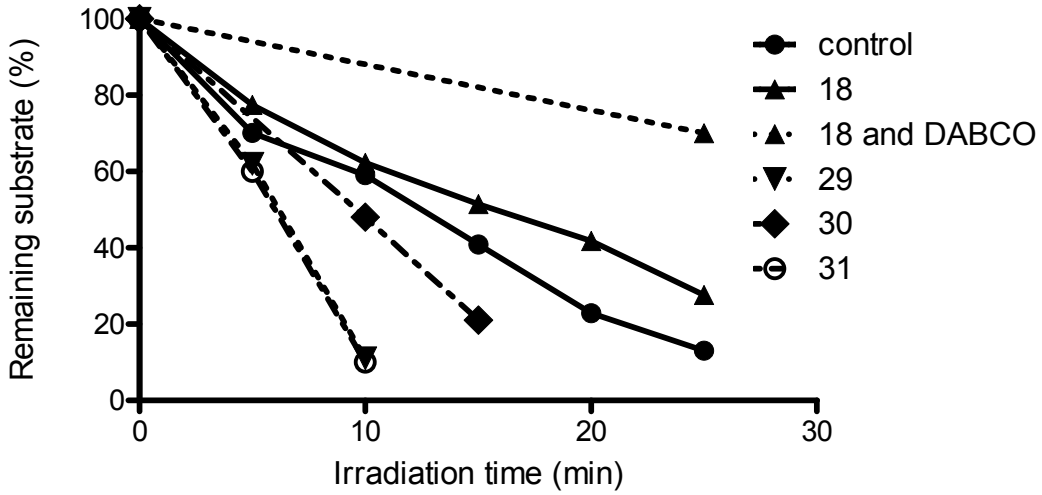

Figure 11. Time-dependent photo-oxidation of model compounds [control = (*Z*)-1,2-bis(phenylthio)ethylene].

Table 3. Percentage of remaining compounds **17**-**31** at different time point during irradiation (690 nm diode laser, 200 mW/cm^2; *: not determined).

	0 min	**5 min**	**10 min**	**15 min**	**20 min**	**25 min**
control	100	70	59	41	23	13
17	100	83	69	58	51	38
18	100	77	62	51	42	28
19	100	-*	-	-	-	100
20	100	-	-	-	-	100
21	100	-	-	-	-	100
22	100	-	-	-	-	100
23	100	-	-	-	-	40
24	100	-	-	-	-	0
25	100	-	-	-	-	60
26	100	-	-	-	-	38
27	100	-	-	-	-	41
28	100	-	-	-	-	50
29	100	62	11	-	-	-
30	100	-	48	21	-	-
31	100	60	10	-	-	-

To evaluate the rate of oxidation by singlet oxygen, the model compounds **17**-**22** were irradiated by a diode laser (690 nm, 200 mW/cm^2, 25 min) in the presence of a photosensitizer 5-(4-methoxyphenyl)-10,15,20-tetraphenyl-21,23-dithiaporphyrin. These compounds were successfully prepared not only under mild and fast reaction conditions (RT, air, 15-20 min) but also gave excellent yields for all substrates (80-95%) with the exception of **30** that gave a lower isolated yield (65%) due to loss in the purification step. All the products from the click reaction step gave *E* isomers based on the coupling constant of two olefinic protons, *J* = 12-15 Hz.The reaction of olefins with singlet oxygen was monitored by the decrease of olefinic proton peaks in ^{1}H-NMR spectra. While **19-22** did not show any reactivity (0 %), compounds **17** and **18** showed significant decrease of the olefinic proton peaks (62 and 72%) in 25 min of the irradiation. Oxidation of only the nitrogen analogues is probably due to electron donation from the nitrogen to the carbonyl group making the olefinic bond electron rich for attack by singlet oxygen.

The aminoarylthioate **23** and aminoacrylamide **24** were evaluated under the same oxidation condition. Interestingly enough, both **23** and **24** also showed fast reaction with singlet oxygen, 60 and 100%, respectively. Among aminoacrylate **18**, aminoarylathioate -**23**-, and aminoacrylamide -**24**-, Compound **24** showed the fastest reaction rate, 100% disappearance of

olefinic protons in 25 min. However, aminoacrylate linker system -**18**- was selected for further investigation because it gave the clean product, 4-phenylphenol. To examine if the cleavage was mediated by singlet oxygen, compound **3** was tested with a singlet oxygen quencher (1,4-diazabicyclo[2.2.2]octane, DABCO) -**18a-** (Fig. A6). It was observed that oxidation of the vinylic bond was greatly reduced (72% → 31%) suggesting the role of singlet oxygen. As an example of aminoacrylate linker with biologically relevant molecule, the model prodrug (compound **31)** was prepared from estrone. It showed a photo-oxidation of 90% in 10 min. similar to compound **29.** The compound **31** successfully released Estrone after irradiation (Fig. A17).[93]

3.3.2. Analysis of cleavage products

The GC-MS analysis of the cleaved mixture of compound **23**, apart from the expected cleavage product, thiophenol, diphenyl disulfide was also detected with a number of minor side products. Diphenyl disulfide seemed to be formed during the GC-MS experimental procedure since it was also observed in GC-MS data of thiophenol standard sample (Fig. A11). It was also supported by the fact that doublet peak at 7.5 ppm from diphenyl disulfide was not observed in the ^{1}H-NMR of the cleaved mixture of **23**. Even though **24** showed the fastest reaction with singlet oxygen, it gave even more number of side products in GC-MS than **23** (Fig. A15).

One key requirement for delivery systems is re-generation of the active form of parent molecules after release. However, in the oxidative cleavage of vinyl diether linkers, two formyl products were produced which did not spontaneously decompose to give alcohol products (Fig. 7).[19, 94] Interestingly, from the model compound **18**, we could recover 4-phenylphenol after the irradiation in addition to one aldehyde product, 1-formyl piperidine (Fig. A9). The two products were confirmed by GC-MS analysis (Fig. A9). The release of the parent phenolic compound was also confirmed from the cleavage of compounds **31** and **32**. The masses of these isolated products were taken and confirmed (Figs. A17, A18, A19)

3.3.3. Possible mechanism of the cleavage of aminoacrylate

The oxidative cleavage of aminoacrylate has not been well studied. Based on our experimental data and mechanism of simple substrate (vinyl diether), we developed two possible mechanisms (Fig. 12). We obtained two products, 3P1 and 3P2. However, there are still issues in both mechanisms. In the first mechanism, although 31A seemed to be stable, it was not detected. Thus, further degradation to the 3P1 is not understandable. On the other hand, in the second mechanism, the degradation of imminium ion (3IB) to the formylamine (3P2) is hard to imagine.[95] Although we are more leaning toward the second mechanism, further detailed studies are necessary to understand the mechanism.

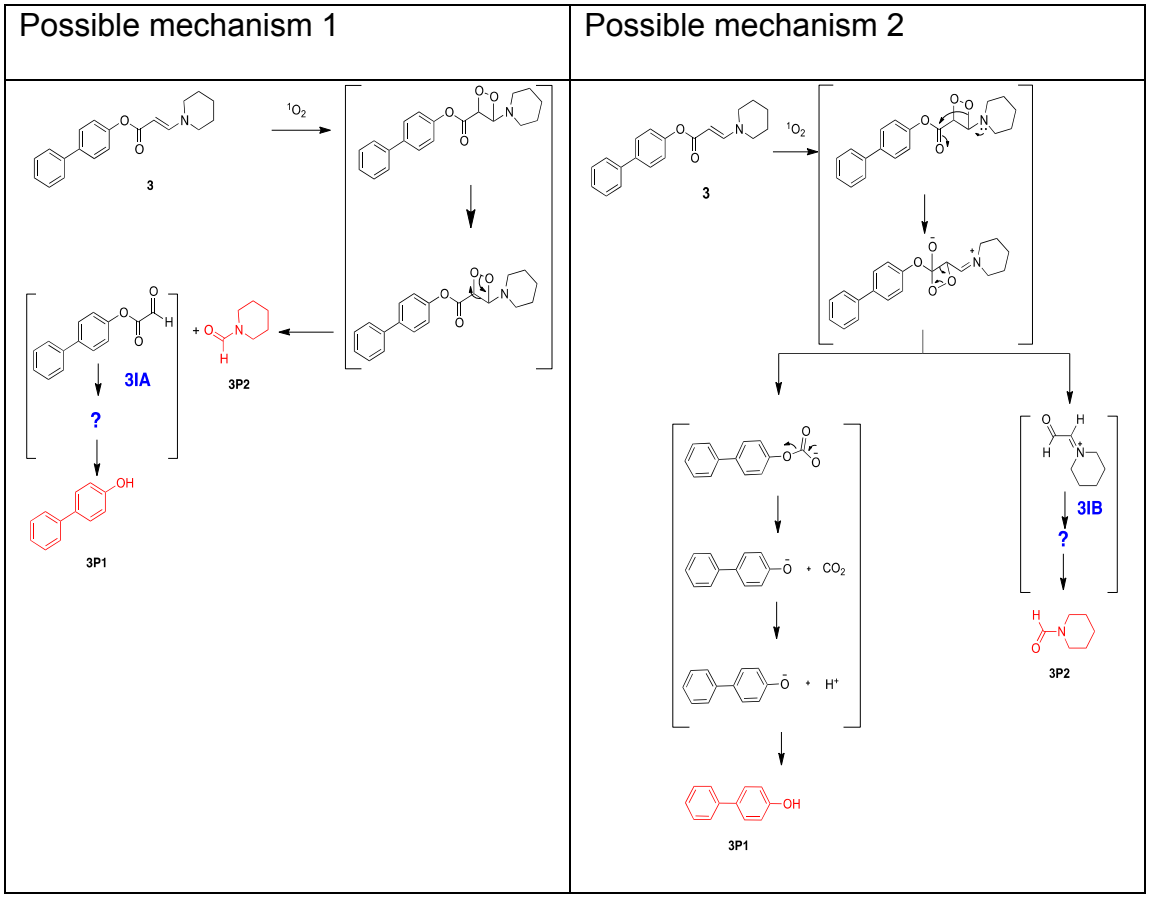

Figure 12. Possible mechanism for the oxidative cleavage of aminoacrylate.

3.4. Conclusion

In conclusion, we proposed and proved a concept of “click and photo-unclick chemistry” using nucleophile-yne type reaction and photo-oxidative cleavage of electron-rich olefins using singlet oxygen. Among aminoacrylate, aminoacrylamide, and amioacrylthiolate, aminoacrylate seemed to be best suited for applications for the release of active compounds due to its fast

photo-oxidation without unnecessary oxidation products. In addition, we proved that the aminoacrylate linker was cleaved fast by the irradiation of long visible light (690 nm) and stable under dark in the biological medium. This combination of click and photo-unclick chemistry would find important applications in the spatio-temporal release of not only drugs but also other bioactive molecules. Since the release can be triggered by tissue penetrable low energy light, this simple but unique chemistry will be applicable in the visible light-controlled release of biologically important molecules at the tissue level.

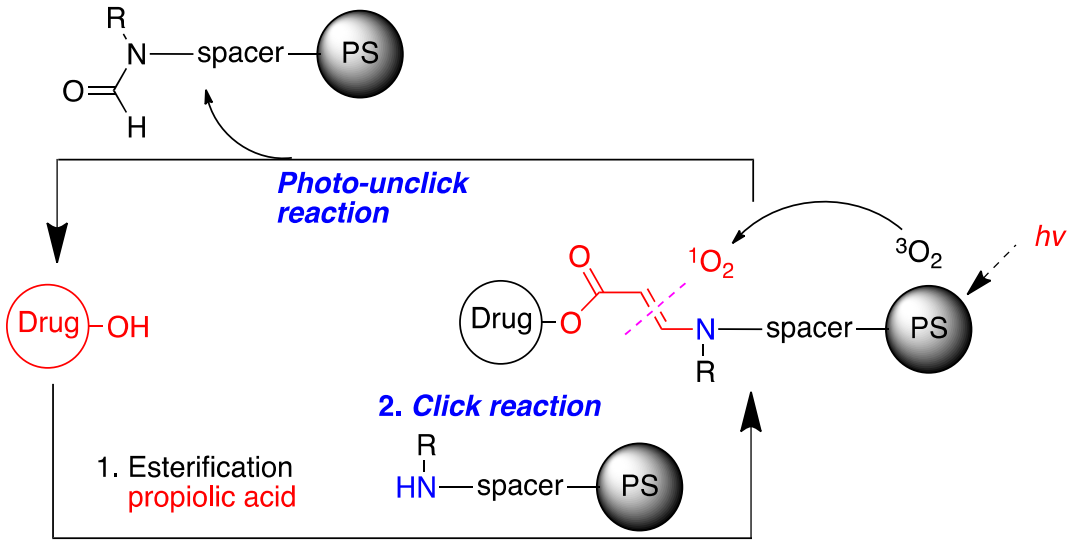

Figure 13. Facile synthesis and cleavage of aminoacrylate and release of a parent drug after its oxidative cleavage.

3.5. Potential for biological application

All the studies so far have been in organic solvent (chloroform, DMSO). However, for this strategy to be practically applicable to the real setting in biology, I needed to demonstrate the cleavage in an aqueous medium. To prove the cleavage in the aqueous medium, I synthesized **PS-L-Rh** and used FRET in monitoring the cleavage by fluorescence in Dulbecco's Modified Eagle Medium with 5% fetal bovine serum commonly used for tissue culture.

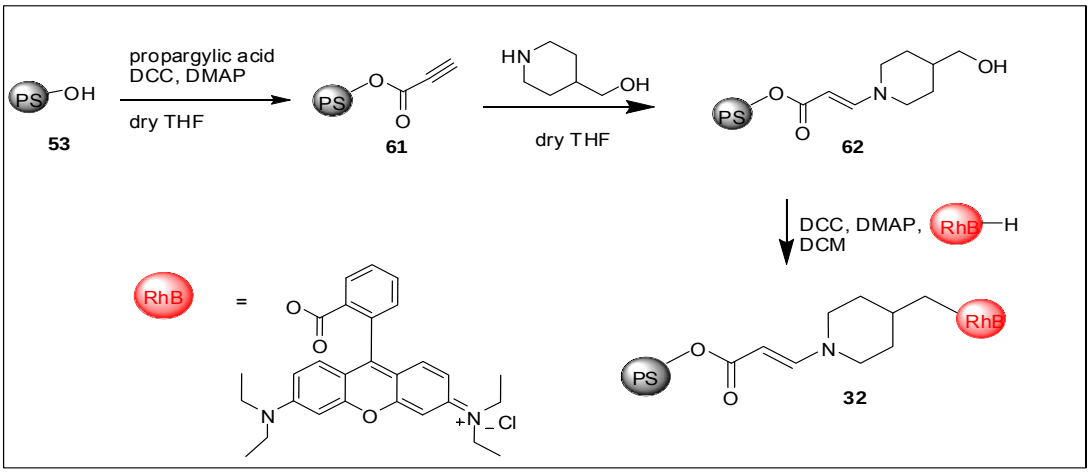

Scheme 5. Prepared **PS-L-Rh** conjugate for FRET studies.

3.6. Experimental section

3.6.1. Synthesis

3.6.1.1. PS-L-Rh (32). The compound **32** was prepared according to the method described for compound **27** employing compound **62** (100 mg, 0.12 mmol), Rhodamine B (58 mg, 0.12 mmol), DCC (99 mg, 0.48 mmol) and DMAP (13 mg, 0.01 mmol) to give a solid red purple compound **32** (101 mg, 65%).^{1}H NMR (300 MHz, CD_2Cl_2) δ 1.14 (m, 6H), 1.36 (m, 3H), 1.65 (m, 3H), 1.89 (m, 2H), 2.13 (s, 1H) 2.83 (s, 2H), 2.91 (s, 2H), 3.18(s, 1H), 3.22 (s, 1H), 3.44 (m, 4H), 3.56 (m, 1H), 3.65 (s, 1H), 4.07 (s, 4H), 4.99 (d, *J* = 13.0 Hz, 1H), 6.65 (s, 4H), 7.13 (d, *J* = 9.1Hz, 1H) , 7.58 (d, *J* = 8.1 Hz, 2H), 7.74 (d, *J* = 13.0 Hz, 1H), 7.84 (s, 10H), 7.97 (s, 1H), 8.13 (d, *J* = 6.6 Hz, 1H), 8.27 (m, 9H), 8.52 (d, *J* = 8.2 Hz, 1H) 8.71 (s, 3H), 8.76 (s, 1H), 9.73 (s, 3H), 9.79 (s, 1H). HRMS ESI (*m/z*): Calculated for $C_{81}H_{71}ClN_5O_5S_2$ ($[M+H]^+$-Cl): 1256.998; found: 1256.4790.

3.6.1.2. Compound 61. The compound **61** was prepared according to the method described for compound **16** employing compound **53** (600 mg, 0.902 mmol), propargylic acid (320 mg, 4.51 mmol), DCC (930 mg, .4.51 mmol) and DMAP (11 mg, 0.09 mmol) and dry THF (10 mL) to give red purple solid compound **61** (400 mg, 70%). **.** ^{1}H NMR (400 MHz, $CDCl_3$) δ 3.1 (s, 1), 4.89 (d, *J* = 12.8 Hz, 1H), 7.49 (d, *J* = 8.4 Hz, 2H) , 7.64 (d, *J* = 12.8 Hz, 1H), 7.75 (m, 9H), 8.17 (m, 8H), 8.61 (m, 3H), 8.67 (d, *J* = 4.5 Hz, 1H) 9.63 (m, 3H) 9.71 (d, *J* = 4.5 Hz, 1H). HRMS ESI (*m/z*): Calculated for $C_{47}H_{29}N_2O_2S_2$ ($[M+H]^+$): 717.1592; found: 717.1591.

3.6.1.3. Compound 62. The compound **62** was prepared according to the method described for compound **17** employing piperidin-4-ylmethanol (64 mg, 0.56mmol) and compound **61** (400 mg, 0.56 mmol) to give red purple solid compound **62** (395 mg, 85%). ^{1}H NMR (300 MHz, CD_2Cl_2) δ1.02 (m, 2H), 1.26 (m, 2H), 1.59 (m, 2H), 1.79 (m, 2H), 3.34 (m, 1H) 3.45 (m, 1H), 3.95 (s, 1), 4.89 (d, *J* = 12.8 Hz, 1H), 7.49 (d, *J* = 8.4 Hz, 2H) , 7.64 (d, *J* = 12.8 Hz, 1H), 7.75 (m, 9H), 8.17 (m, 8H), 8.61 (m, 3H), 8.67 (d, *J* = 4.5 Hz, 1H) 9.63 (m, 3H) 9.71 (d, *J* = 4.5 Hz, 1H). HRMS ESI (*m/z*): Calculated for $C_{53}H_{42}N_3O_3S_2$ ($[M+H]^+$): 832.2589; found: 832.2683.

3.6.2. Procedure for monitoring the cleavage of the aminoacrylate linker by FRET

Stock solutions of compound **32** (2 mM) was prepared in DMSO. 50 µL of stock solutions was then diluted with 950 µL either chloroform or Dulbecco's Modified Eagle Medium with 5% fetal bovine serum to give 100 µM solutions. The resulting solution was irradiated using a diode laser (690 nm, 200 mW/cm^2). 10 µL was taken every 10 min and 990 µL of chloroform was added. The solutions were excited at 525 nm and the fluorescence spectra were recorded from 550 to 750 nm.

3.7. Results and discussion

3.7.1. Synthesis and photo-oxidation

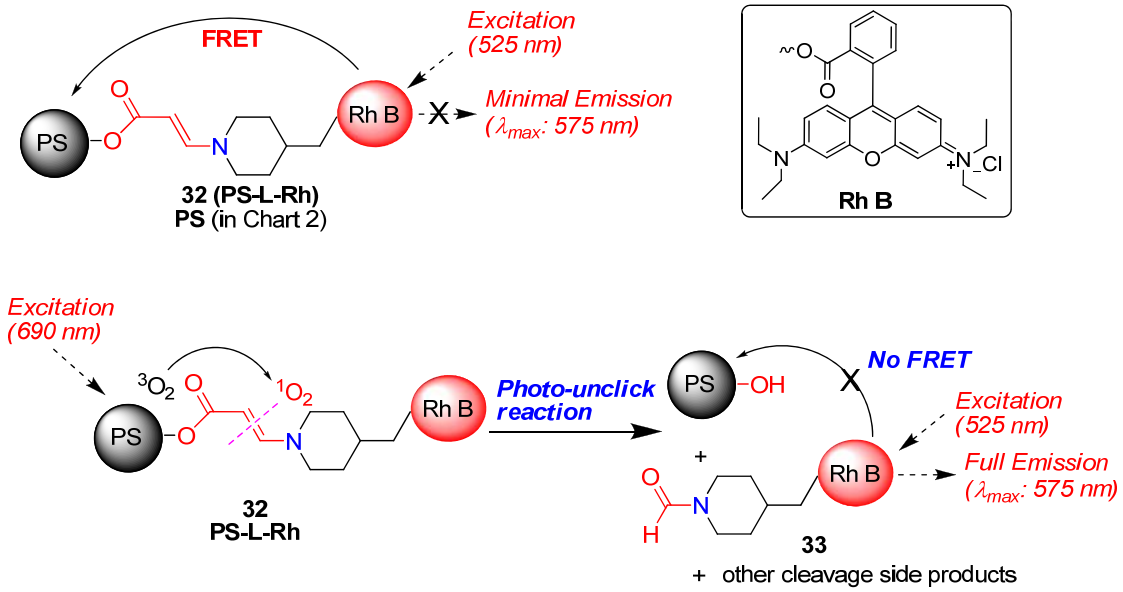

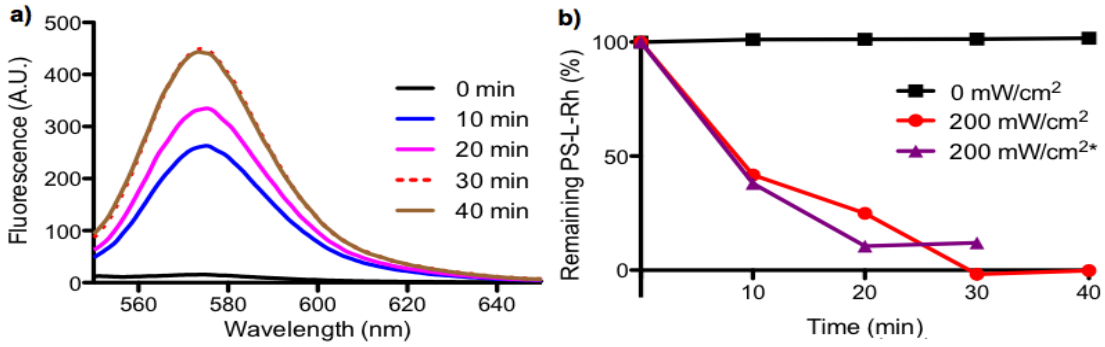

Figure 14. Photocleavage of **32** in a medium: a) fluorescence intensity (excitation at 525 nm) after the irradiation, b) photocleavage of **32** with or

without irradiation in media: *the **32** kept 7 days in the media under dark before the experiment.

To examine photo-cleavage and stability of the linker in an aqueous solution (Dulbecco's Modified Eagle Medium with 5% fetal bovine serum) using FRET (fluorescence energy resonance transfer), compound **32** (**PS-L-Rh**) was designed and prepared by conjugating two dyes [hydroxy-dithiaporphyrin (PS) and rhoadmine B (RhB)] with the aminoacrylate linker (Fig. 14, Scheme 5).[96] (For synthetic convenience the positions of Rh and Rh were switched.) In **PS-L-Rh**, Rh B is a donor and PS (dithiaporphyrin) is an acceptor of the FRET. Fluorescence (λ_{em}: 575 nm, excitation at 525 nm) of Rh is quenched by PS when they are close via the linker. However, once the two dyes are apart after the cleavage of the linker, the fluorescence intensity of Rh increases dramatically since the FRET is not possible. Irradiation time-dependent increase of Rh emission upon irradiation (690 nm diode laser at 200 mW/cm^2) was first confirmed with **PS-L-Rh** in $CHCl_3$. Complete (~100%) cleavage was achieved in 10 min, giving about 8-time increase in Rh fluorescence intensity. This rate is consistent with the cleavage data of **31** (in $CDCl_3$, 90% cleavage in 10 min) monitored by NMR. Then, **PS-L-Rh** in media was irradiated using the same irradiation condition. It showed ~100 % cleavage in 30 min (Fig. 14). The slower cleavage in the medium may be, in part, due to the lower concentration of oxygen (0.27 mM in media vs. 2.4 mM in $CHCl_3$ at the atmospheric pressure)[97] and the shorter lifetime of singlet

oxygen (2 μs in media vs. 60 μs in $CHCl_3$).[58] The similar photocleavage profile of 7-day kept sample with that of fresh sample (Fig. 14) indicates that the aminoacrylate was stable in media at least up to 7 days under dark.

3.8. Conclusion

The observation of the cleavage of **PS-L-Rh** in the aqueous medium is a critical result. This implies this strategy can be translated from the test tube to biological system. The use of FRET for monitoring the cleavage by fluorescence provided a very elegant and convenient method.

Chapter 4. Photocleavable Prodrug of Anticancer Drug Using the Photo-unclick Chemistry

4.1. Introduction

Cancer still remains one of the most challenging health issues of the 21st century. In the U.S., cancer is the second leading cause of death. It is estimated that over half a million people would die of cancer and another 1.6 million would be diagnosed with the disease in 2012 in the U.S. alone.[98] Chemotherapy is one of the three main treatment options for cancers such as chemotherapy, surgery and radiation.[99] It is used for both systemic and local treatments to. To destroy wide-spread cancer cells, chemotherapeutic agents are administered after surgery (adjuvant therapy). It is also used locally to reduce larger tumor before surgery (neo-adjuvant therapy) and to kill residual cancer cells and cancer cells in lymph node after the surgery.[100] It is also used when cancer cells do not respond to hormonal therapy.

Although chemotherapeutic agents are critical components in cancer treatment, their inability to differentiate tumor cells from healthy cells causes damage to healthy cells as well. This eventually leads to undesirable side effects because targets of these agents are critical components during the cellular proliferation such as topoisomerases, DNA, microtubules, etc. Thus, selective damage to cancer cells is the critical goal in anticancer drug development. One of the approaches to achieve the goal is to develop drug

delivery formulations that can specifically deliver the chemotherapeutic agents to tumor and release free drugs in tumor. As described in the introduction sections, some examples include polymers, liposomes, dendrimers, and etc. While the targeted delivery has been made some progress, effective means for the local release of free drugs in tumor are still greatly needed.

I therefore decided to evaluate the photo-unclick chemistry for releasing anticancer drugs from delivery systems. My hypothesis was that the free drugs could be released from inactive/less active form of drug delivery systems upon irradiation if the drug is de-activated using the SO-cleavable linker and the photosensitizer is close to the linker. CMP-L-CA4 was designed as photo-activatable prodrug of anticancer drug, Combretastatin A4 (CA-4).

CA-4 is a cytotoxic and antiangiogenic compound and its water-soluble prodrug (CA-4 phosphate, fosbretabulin) is under clinical study for anticancer therapy. I synthesized a conjugate of CA-4 and hydroxyl-dithiaporphyrin (a photosensitizer) linked through the aminoacrylate linker CA4-L-PS to study the release and cytotoxicity of the anticancer drug CA-4 by NIR light irradiation.

4.2. Experimental section

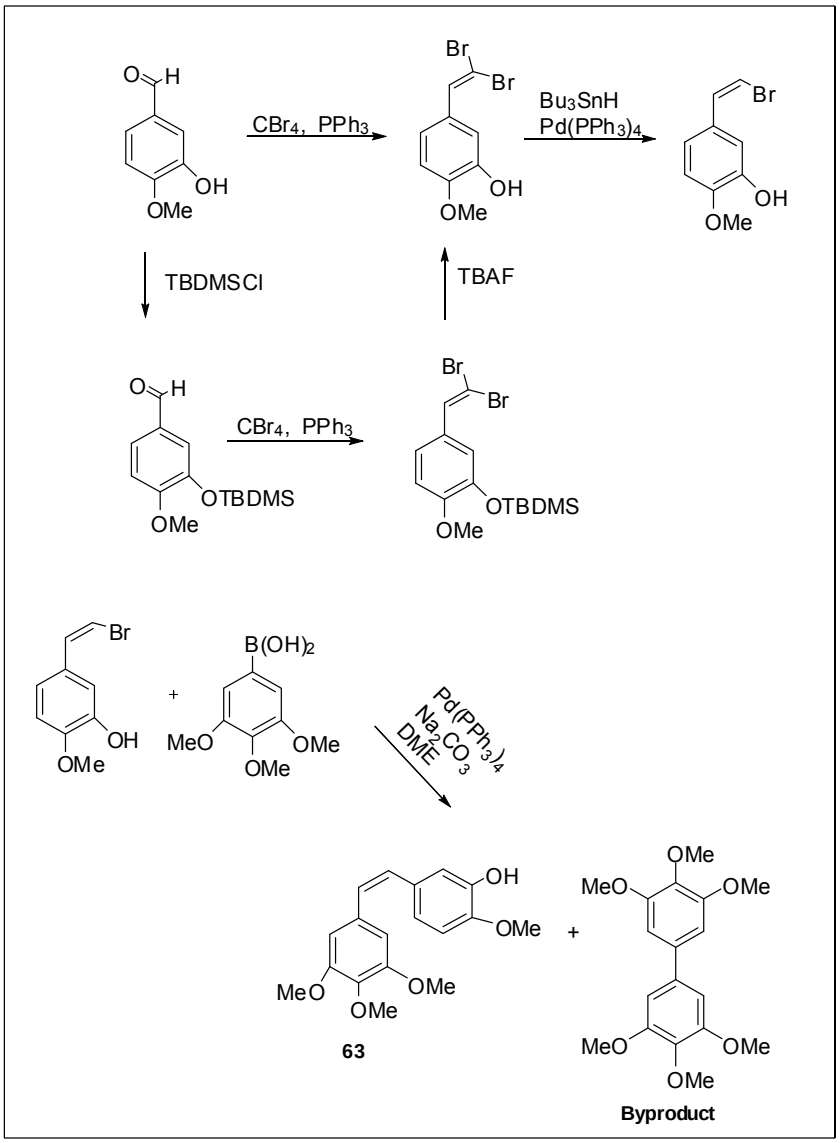

Scheme 6. Synthesis of CA4.[101]

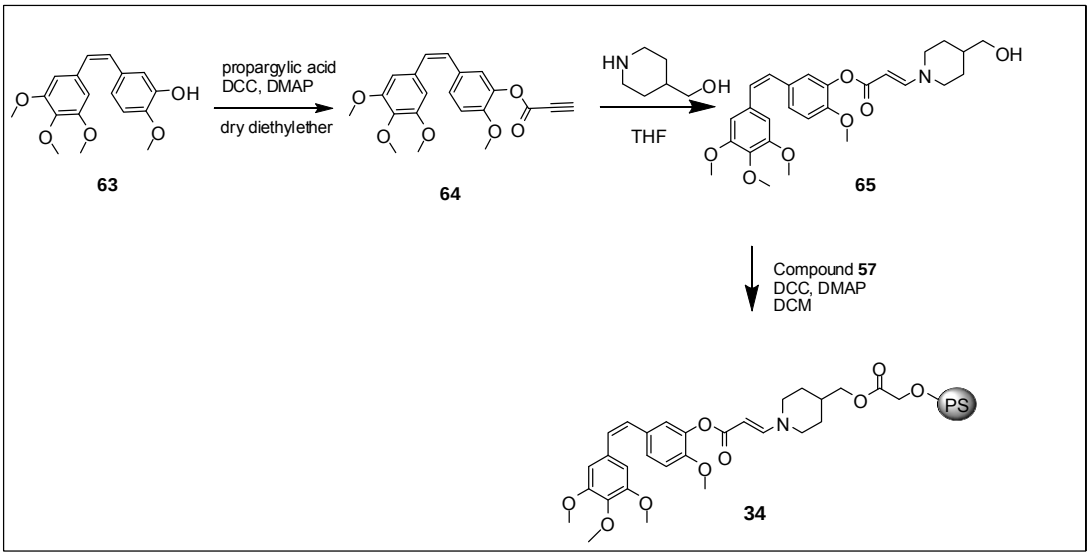

Scheme 7. Synthetic scheme for the preparation of CA4-L-PS.

4.2.1. Synthesis

4.2.1.1. Compound (34). The compound **34** was prepared according to the method described for compound **27** employing compound **57** (200 mg, 0.28 mmol), compound **65** (267 mg, 0.55 mmol), DCC (228 mg, 1.11 mmol) and DMAP (67 mg, 33.7 mmol) to give a solid red purple compound **34** (452 mg, 69%). ^{1}H NMR (300 MHz, CD_2Cl_2) δ 0.90 (m, 2H), 1.28 (m, 2H), 1.41 (m, 2H), 1.87 (m, 1H), 3.09 (s, 1H), 3.66 (s, 6H), 3.75 (d, J = 6.4 Hz, 6H), 4.22 (d, J = 5.2 Hz, 2H), 4.80 (d, J = 12.8 Hz, 1H), 4.96 (s, 2H), 6.44 (s, 2H), 6.52 (s, 2H), 6.84 (d, J = 8.4 Hz, 1H), 6.97 (s, 1H), 7.09 (d, J = 6.2 Hz, 1H), 7.40 (d, J = 7.7 Hz, 2H), 7.50 (d, J = 12.8 Hz, 1H), 7.54 (br s, 9H), 8.27 (m, 8),

8.72 (m, 4H), 9.74 (m, 4H). HRMS ESI (*m/z*): Calculated for $C_{73}H_{62}N_3O_9S_2$ ($[M+H]^+$): 1188.38; found:1188.3875.

4.2.1.2. Compound 63. Combretastatin A4 (CA-4). Compound 63 was synthesized following reported reference.[101,] ^{1}H NMR (300 MHz, CD_2Cl_2) δ 3.70 (s, 6H), 3.84 (s, 3H), 3.87 (s, 3H), 5.53 (s, 1H), 6.41 (d, *J* = 12.3 Hz, 1H), 6.47 (d, *J* = 12.3 Hz, 1H) 6.53 (s, 2H), 6.73 (d, *J* = 8.5 Hz, 1H), 6.80 (dd, *J* = 2.0, 2.0 Hz, 1H) 6.92 (d, *J* = 2.0 Hz, 1H). HRMS ESI (*m/z*): Calculated for $C_{18}H_{20}O_5Na$ ($[M+Na]^+$): 339.13; found: 339.1206.

The compound **64** was prepared according to the method described for compound **16** employing combretastatin A4 (CA-4) (1.00 g, 3.16 mmol), propargylic acid (1.12 g, 15.80 mmol), DCC (3.26 g, 15.80 mmol) and DMAP (0.04 g, 0.32 mmol) and dry diethyl ether (25 mL) to give white solid compound **64** (0.86 g, 74%). ^{1}H NMR (300 MHz, CD_2Cl_2) δ 3.03 (s, 1H), 3.70 (s, 6H), 3.83 (d, *J* = 4.2 Hz, 6H), 6.47 (d, *J* = 3.8 Hz, 4H), 6.87 (d, *J* = 8.7 Hz, 1H), 7.05 (s, 1H), 7.15 (d, *J* = 7.8 Hz, 1H). HRMS ESI (*m/z*): Calculated for $C_{21}H_{20}O_6Na$ ($[M+Na]^+$): 391.13; found: 391.1147.

4.2.1.3. Compound (65). The compound **65** was prepared according to the method described for compound **17** employing piperidin-4-ylmethanol (187 mg, 1.63 mmol) and compound **64** (600 mg, 1.63 mmol) to give brown solid

compound **65** (740.32 mg, 94%).^{1}H NMR (300 MHz, CD_2Cl_2) δ 1.29 (m, 2H), 1.46 (m, 1H), 1.78 (m, 3H), 3.05 (s, 1H), 3.50 (m, 2H), 3.59 (m, 2H), 3.69 (s, 6H), 3.76 (s, 3H), 3.79 (s, 3H), 4.77 (d, *J* = 13.6 Hz, 1H), 6.47 (d, *J* = 4.6 Hz, 2H), 6.54 (s, 2H), 6.86 (d, *J* = 8.5 Hz, 1H), 7.00 (s, 1H), 7.10 (d, *J* = 8.2 Hz, 1H), 7.50 (d, *J* = 13.6 Hz, 1H). HRMS ESI (*m/z*): Calculated for $C_{27}H_{33}NO_7$ Na ($[M+Na]^+$):506.23 ; found: 506.2148.

4.2.2. Intensity dependent cleavage of PS-L-Rh in an aqueous solution

The cleavage at the tissue level could be a difficult task although we were using a tissue penetrable light. It is difficult to make high power density (e.g., > 5 mW/cm^2) in tissue (not at the tip of a fiber but in the larger area/volume) due to the light reflection, scattering and absorption by tissue. We therefore decided to investigate the cleavage of aminoacrylate linker using PS-L-Rh in the medium at different light intensities (200, 50, 5, 1 mW/cm^2). To our surprise the rate of cleavage was not dependant on the light intensity and the linker was cleaved fast with a light intensity as low as 1 mW/cm^2 (Fig. 15). The observation of cleavage at 1 mW/cm^2 in the medium was very exciting because it is a practically achievable intensity in tissue. This gives a strong basis for investigating the cleavage at the tissue level. We used PS-L-Rh and nude mice to investigate the cleavage at the tissue level. Interestingly we observed the cleavage of PS-L-Rh at the tissue level.

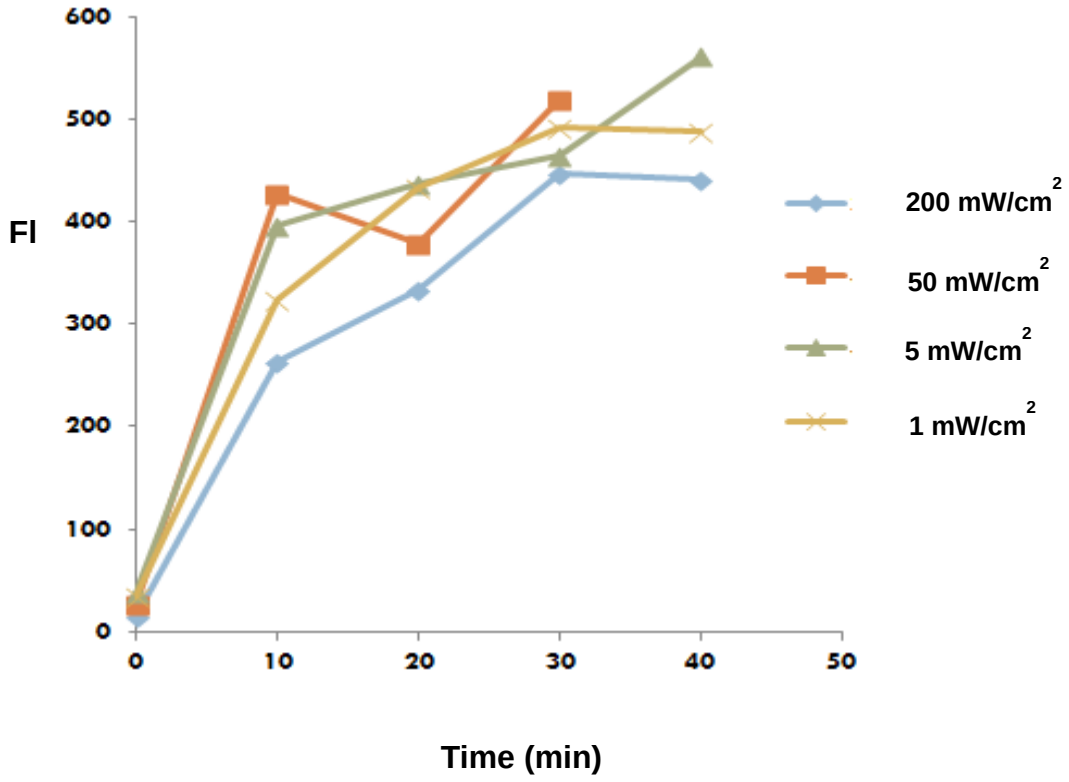

Figure 15. Intensity dependent cleavage of PS-L-Rh in the medium.

4.2.3. Biological studies

4.2.3.1. Dark-toxicity of CA4-L-PS

The cytotoxicity of CA4-L-PS without irradiation was determined. MCF-7 cells (5000 cells/well) were seeded on 96 well plates in the complete medium and then incubated for 24 h at 37 °C in 5 % CO_2. 2 mM of CA4-L-PS stock was prepared by dissolving 3.108 mg in 1.308 mL of DMSO. The prepared stock was further diluted in the complete medium. 10 µL of the respective diluted solution was then added to 190 µL of the complete

medium in each well to achieve final concentrations of 2 nM, 10 nM, 20 nM, 100 nM and 200 nM. The plates were then incubated for 24 h. On day 1 the plate was removed from the incubator and allowed to sit in a dark cabinet for a duration of 30 mins. Later the well plate was incubated at 37°C in 5 % CO_2. Cell viability was determined after 3 days using MTT assay.

A 10 µL solution of MTT (10 mg in 1mL PBS buffer) was added to the wells and the plate was incubated for 4 h. After then, the MTT solution was removed and the cells were dissolved in 200 µL of DMSO and the absorbance was measured at 570 nm with background subtraction at 650 nm. The cell viability was then quantified by measuring the absorbance of the treated wells, compared to that of the untreated wells (controls) and expressed as a percentage.

4.2.3.2. Photo-toxicity of CA4-L-PS

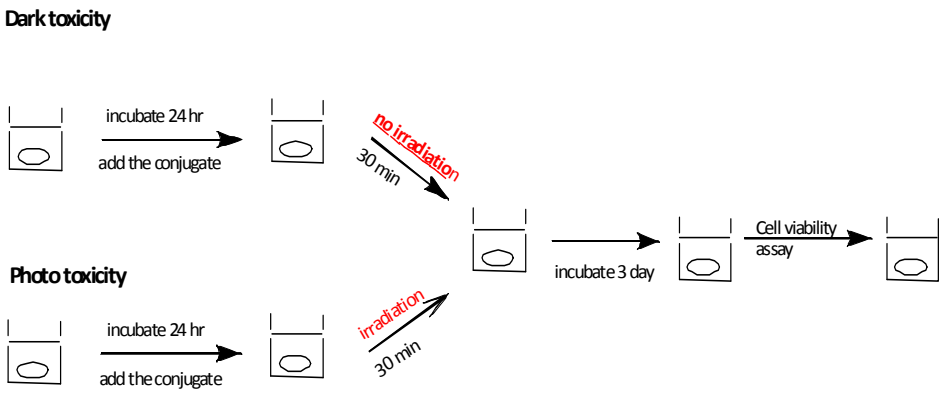

Figure 16. Schematics of photo-toxicity and dark-toxicity experiments.

The cytotoxicity of CA4-L-PS with irradiation with 690 nm diode laser was determined. MCF-7 cells (5000 cells/well) were seeded on 96 well plates in the complete medium and then incubated for 24 h at 37 °C in 5 % CO_2. The same concentrations as used in the dark-toxicity were used. 10 µL of the respective dilute solutions was then added to 190 µL of complete media in each well and the well plate was incubated for 24 h. After the incubation the well plate with the cover removed was placed on an orbital shaker (Lab-line, Barnstead International, IA) and irradiated using a diode laser (690 nm, 5.6 mW/cm^2) for 30 min. To ensure uniformity of the light during the irradiation, the well plate was made to orbit gently on the shaker. After the irradiation, it was incubated 37 °C in 5 % CO2, for 3 days after which the cell viability was determined by MTT assay and expressed as a percent of the controls, cells exposed to light but not treated with CA4-L-PS.[103103, 104]

4.2.3.3. Modified procedure of photo-toxicity of CA-L-PS to eliminate PDT effect

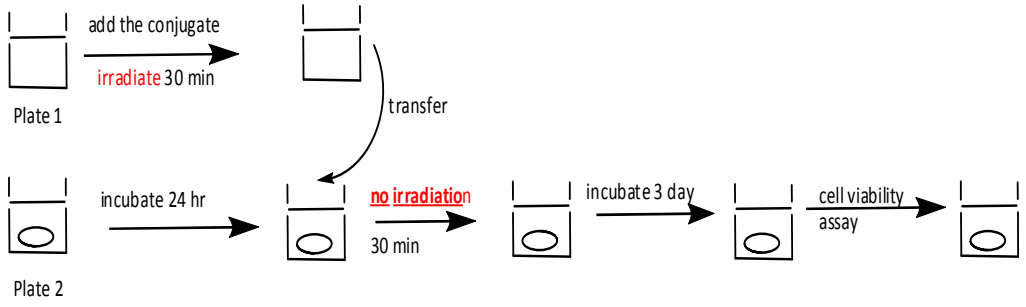

Figure 17. Schematics of photo-toxicity to eliminate PDT effect.

The cytotoxicity of CA4-L-PS with irradiation with 690 nm diode laser was determined. MCF-7 cells (5000 cells/well) were seeded on 96 well plates (plate-1) in the complete medium and then incubated for 24 h at 37 °C in 5 % CO_2. CA4-L-PS of concentrations 4nM, 20nM, 40nM, 200nM, 400nM in 100 µL of the complete medium in plate-2 was irradiated with 690 nm diode laser for 30min at 5.6 mW/cm^2. 100 µL of the medium from plate-1 was removed and the total irradiated medium (100 µL) in each well of plate-2 was added to plate-1 to make a final concentrations of 2nM, 10nM, 20nM, 100nM, 200nM and final volume of 200 µL. It was then incubated 37 °C in 5 % CO^2, for 3 days, after which the cell viability was determined by MTT assay and expressed as a percent of the controls, cells exposed to light and without CA4-L-PS.

4.2.3.4. In vitro toxic studies of CA4-L-PS

The release of drug at the cellular level was investigated by preparing prodrug. MTT colorimetric assay and expression of the inhibitory concentration (IC_{50}) values of the prototype CA4-L-PS without irradiation was compared to the prodrug prototype with irradiation. The results showed IC_{50} values of CA4-L-PS after irradiation very close to IC_{50} of free drug (Fig. 18). A 20 times higher toxicity with irradiation compared to non-irradiation was obtained. While non-irradiated samples did not show any cell kill at 0.1 µM (~30 % cell kill at 0.2 µM), the irradiated samples showed 50% cell kill at

~0.01 μM. These results support the cleavage and release the free drug. From the experiment to avoid PDT effects (4.2.3.3), similar IC_{50} values were obtained for phototoxicity of CA4-L-Rh in consistent with the previous results.

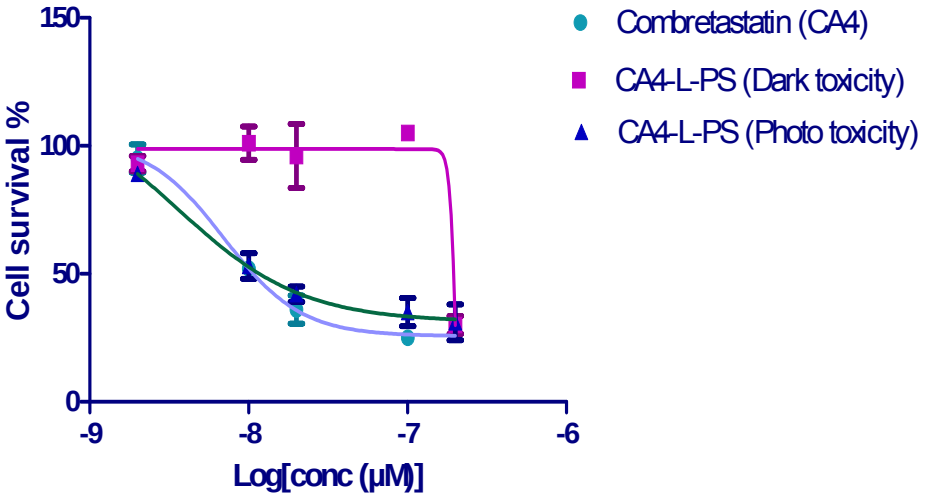

Figure 18. *In vitro* dark and photo toxicities of CA4 and CA4-L-PS.

4.2.3..5 Sub-cellular uptake of PS-L-Rh by fluorescence microsocpy

MCF-7 cells were seeded at 2.0 - 3.0 × 10^4 cells/well in 24 well plates containing 12 mm diameter cover slips and then incubated for 24 h. PS-L-Rh diluted to the appropriate concentrations was then added to the wells . The final concentration in the well plate was 10 μM. The cells were incubated for 8 h. After the incubation, the medium was removed and the cell monolayer was rinsed three times with 1 mL of the complete media. The cover slip was

then mounted and the images were taken using a Leica DMI4000B fluorescence microscope fitted with a QImaging Fast 1394 camera and spot advance version 4.6 processing software. The images were modified for better visualization with Adobe Photoshop Element 5.0. The fluorescence images showed granular fluorescence associated with mitochondrial specificity. L5 filter (excitation filter 480/40, emission filter 527/30) was used to capture signal from Rhodamine. TX2 filter (excitation filter 560/40, emission filter 645/75) over laps with the signal of Soret band of PS and part of the excitation spectrum of Rh.

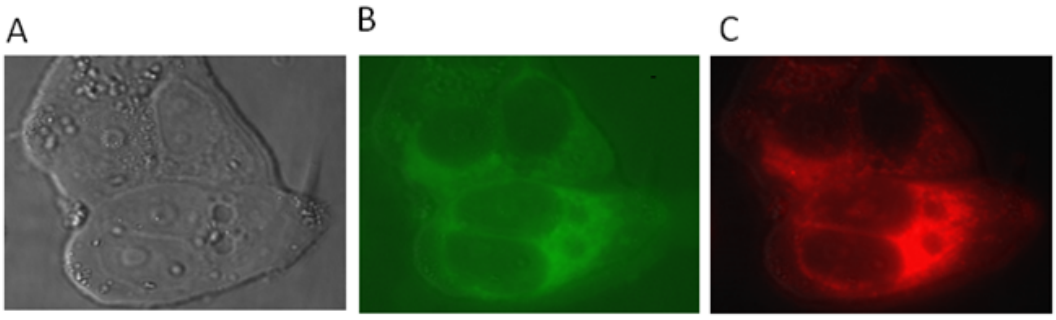

Figure 19. Sub-cellular uptake of PS-L-Rh. A: bright field B: L5-green filter C: TX2-red filter

4.2.4. Cleavage of PS-L-Rh at the tissue level.

4.2.4.1. Material and methods

Female nu/nu mice were purchased from NCI (Federick, MD). Mice were housed and handled in the rodent barrier facility, University of Oklahoma Health Sciences Center, Oklahoma City, OK. All animal

experiments were approved by IACUC, University of Oklahoma Health science Center, Oklahoma City.

4.2.4.2. Preparation of formulation

All the chemicals used were of analytical grade. Power density was measured by thermal sensor (S302C, Thorlabs Inc., Newton NJ) and power meter (PM100D, Thorlabs Inc.). All the procedures beginning from weighing the compound till obtaining the *in vivo* data were done under dark condition. Formulation of PS-L-Rh was prepared by solubilizing PS-L-Rh in Tween 80 (100µL) using a mortar and pestle to get a viscous paste. The paste was left for 4h. Then the viscous paste stirred well and extracted into 5% dextrose solution. The solution was filtered through a 0.2 µm sterile syringe filter. The concentration of the solution was determined by diluting the formulation in DMSO and the absorbance was measured using PerkinElmer UV-Vis Spectrophotometer LAMBDA 25. The concentration was calculated from the extinction coefficient of PS-L-Rh at 438 nm in DMSO (ε = 287,000 $M^{-1}cm^{-1}$) using Beer-lambert law.

4.2.4.3. *In vivo* imaging of the cleavage of PS-L-Rh

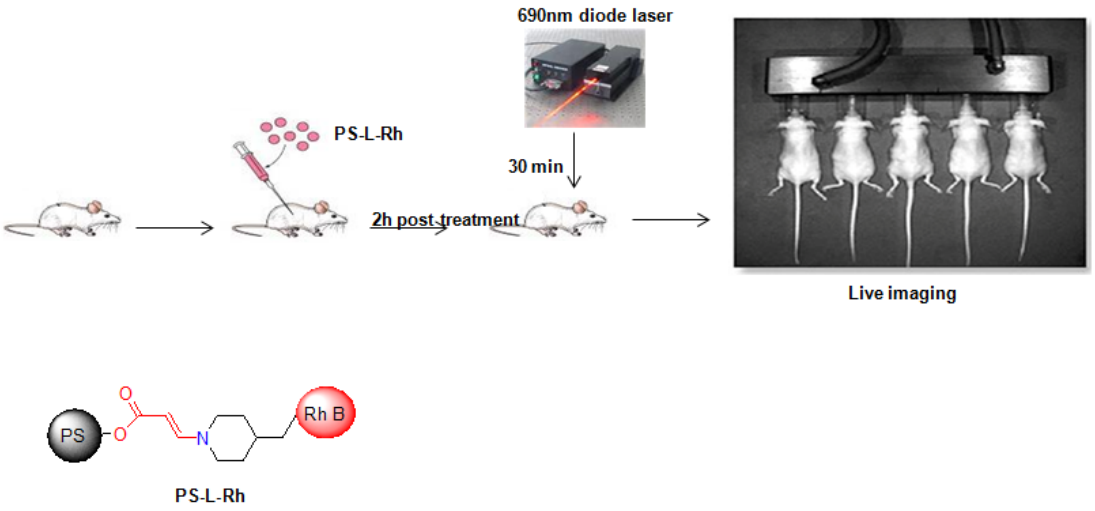

Figure 20. Schematics of *in vivo* imaging.

A four-week old female athymic nu/nu mouse (~20g) was used to investigate the cleavage of PS-L-Rh at the tissue level. Mice were irradiated with a 690 nm diode laser with light intensity 500 mW/cm^2 at the neck region. The mouse was imaged using IVIS Imaging system. IVIS Imaging System (Caliper Life Sciences) consists of a cryogenically cooled imaging system coupled to a data acquisition computer running Living Image® software. Before imaging, the mouse was anesthetized in an acrylic chamber with 2.5% isoflurane/air mixture1 h 30 min after the administration of PS-L-Rh (24 μmol/kg, i.p.), the first image was taken (Fig. 21A). The same mouse was then irradiated for 10 min and another image was taken (Fig. 21B). Additional

two images were taken (Figs. 21C and D). The following parameters were used to acquire images using Living imaging® software : fluorescence mode, exposure time: 5 sec, binning: medium, F/Stop: 2, excitation: 535 nm and emission: 580 nm. During post processing, image counts were adjusted to 3 X 10^4 as minimum and 6.5 X 10^4 as maximum color scale using Living imaging software.

The irradiation time-dependent increase of Rh fluorescence emission was observed (Fig. 21), indicating irradiation time-dependent cleavage of the aminoacrylate linker. There was no increased fluorescence signal from the mice. After irradiating the mice the irradiated region showed signal corresponding to the free Rhodamine release upon cleavage of the PS-L-Rh. The signal intensity increased with irradiation time at different time intervals. Absence of fluorescence signal when the mouse was not irradiated indicates that the PS-L-Rh was stable. Upon irradiation the PS-L-Rh got cleaved due to the cleavable linker and the released Rhodamine showed fluorescence signal.

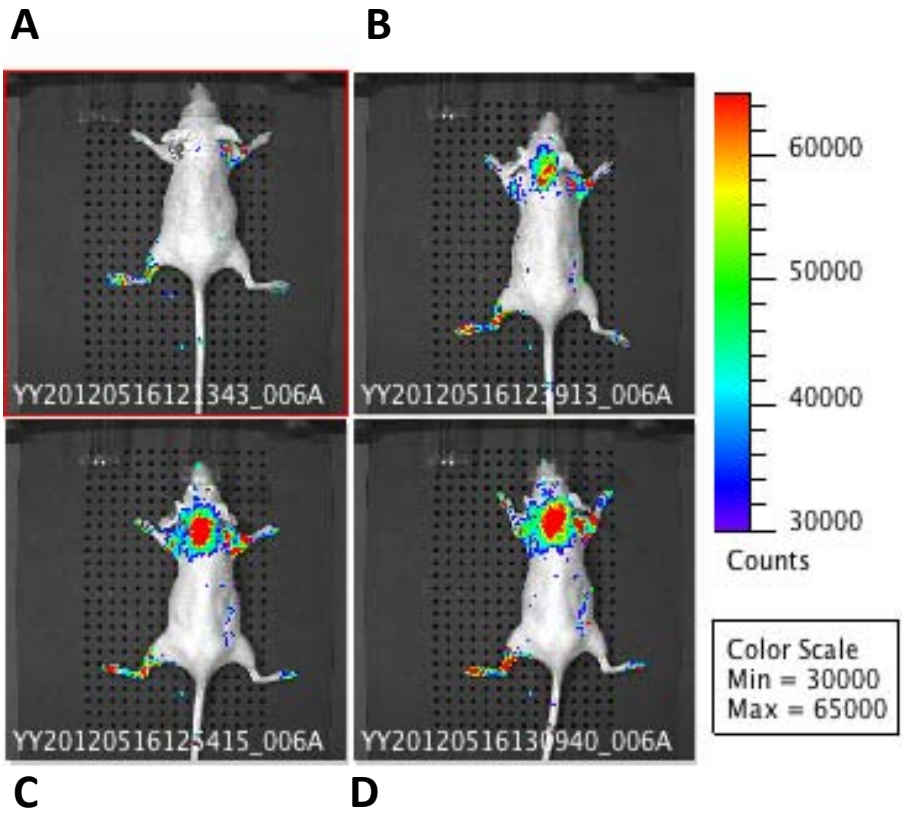

Figure 21. *In vivo* fluorescence images of the mouse after irradiation for 0 (A), end of 30 (B), 40 (C) and 50 (D) min.

4.3. Conclusion

The cleavage of aminoacrylate linker in the cultured cells and tissue was demonstrated using CA4-L-Rh and PS-L-Rh. Based on the close IC50 value of photo-toxicity of CA-L-Rh with IC50 and dark-toxicity of CA4, it was assumed that almost all CA4-L-Rh released CA4. The release could be controlled by the dose of the irradiation. Even though the *in vivo* experimental

conditions should be further optimized, the results clearly prove the cleavage of aminoacrylate linker in mouse.

Chapter 5. Conclusion

The ultimate goal of this study was to develop new bio-orthogonal strategy using near IR for bioactive compound (drug) release from delivery vehicles (prodrugs, nano-drug delivery system: dendrimers, liposomes, polymer). The choice of light for remote-activation is due to highly specific spatial and temporal control of bioactive compound release. This will ultimately lead to address some of the unmet need of drug delivery: reducing the toxicity of drugs and improving their release profile. However, the major hurdle for achieving our aim was identifying potential linker and development of facile synthesis for the linker.

We therefore systemically examined various substituted olefins to find the optimal linker for our strategy and to estimate rates of photo-oxidation. This screening process led to the discovery of vinyl dithioether and vinyl diether as potential singlet oxygen mediated cleavable linker. This finding was very promising because both vinyl dithioether and vinyl diether were cleaved by singlet oxygen more than 80% within 15 min without oxygen saturation. The vinyl diether was our first choice because the photo oxidation did not generate any side product. However, the synthesis of vinyl diether was a big challenge, although, structurally it looks simple. Reported synthetic methods were limited only for symmetric molecules and resulted in low yield or non-stereospecificity. In addition, those required lengthy and multiple steps with some having harsh reaction conditions.

To overcome the above limitation, my colleagues (Dr. Pagula and Mr. Nkepang) and i developed a facile and versatile synthetic method for *E*-1,2-diheteroatom-substituted electron-rich alkene. Even though our new synthetic method for vinyl diether was an improvement compared to previous reported method. There was a limitation that was the use of *n*-butyllithium in one of the steps. This made our developed synthetic method not practically useful for our purpose.

We set out new conditions for the ideal linker, which were fast cleavage by singlet oxygen > 80 %/20 min, facile synthesis (mild reaction conditions, high yield), stability (against hydrolysis in various pH and metabolism), and regeneration of an intact form of drug without formylation, safety (non-toxicity by cleaved byproducts). I started searching for new linkers and my attention was drawn to β-Enamino ketone. Although it showed relatively fast photo-oxidation by singlet oxygen at the first screen, it was not selected for further investigation. β-Enamino group showed important properties as an ideal linker such as fast cleavage (> 80% in 10 min), facile synthesis by a click chemistry, regeneration of parent drugs without formylation, stability in water and medium in dark. Thus, we proposed the concept of click and photo-unclick chemistry for the synthesis and cleavage of the β-enamino ketone.

With these interesting results in test tubes, the prodrug CA4-L-PS was prepared to test our concept of the photo-unclick chemistry in cultured cells.

The results obtained were consistent with our expectation. While the dark-toxicity of CA4-L-PS was about 20 times lower than that of free CA-4 (IC_{50}: 200 vs. 8 uM), photo-toxicity of CA4-L-PS was very close to that free CA-4 (IC_{50}: 6 vs. 8 uM). It makes sense based on other study in our group by Dr. Hossion, where near 100% of drugs were released from similar type of prodrugs by irradiation. We also confirmed that this photo-toxicity by CA4-L-PS came from released CA-4, not from singlet oxygen (PDT effect).

The next key question from the clinical point was whether the photo-cleavage could be made at the tissues level. Attenuation of incident light by tissue is a key-limiting factor. From our previous study, we observed that about 2.6 ± 0.5 mW/cm^2 was made at muscle about 3 mm below skin even when 200 mW/cm^2 light (690 nm) was applied externally. Thus, we first determined light intensity-dependent rate of the cleavage of CMP-L-Rh, from 200 – 1 mW/cm^2 see if the cleavage occur by low intensity light. To our surprise, the cleavage was not much dependent on the light intensity at least within the tested range: We therefore set to investigate the cleavage in mouse. We used PS-L-Rh and a nude mouse to investigate the cleavage at the tissue level. Interestingly we observed sign of the light dose-dependent cleavage of PS-L-Rh.

We envision that this linker and its click and photo-unclick chemistry can find many applications, not limited to anticancer drugs and prodrugs, for spatio-temporally controlled release of active compounds but delivery

vehicles liposomes, polymers, quantum dots, gold nanoparticle, carbon-nanotube etc.

References

1. Majoros, I. J.; Williams, C. R.; Baker, J. R., Jr., Current dendrimer applications in cancer diagnosis and therapy. *Curr Top Med Chem* **2008,** *8*, 1165-79.

2. Lee, R. J.; Low, P. S., Folate-mediated tumor cell targeting of liposome-entrapped doxorubicin in vitro. *Biochim Biophys Acta* **1995,** *1233*, 134-44.

3. Brigger, I.; Dubernet, C.; Couvreur, P., Nanoparticles in cancer therapy and diagnosis. *Adv Drug Deliv Rev* **2002,** *54*, 631-51.

4. Feazell, R. P.; Nakayama-Ratchford, N.; Dai, H.; Lippard, S. J., Soluble single-walled carbon nanotubes as longboat delivery systems for platinum(IV) anticancer drug design. *J Am Chem Soc* **2007,** *129*, 8438-9.

5. Destito, G.; Yeh, R.; Rae, C. S.; Finn, M. G.; Manchester, M., Folic acid-mediated targeting of cowpea mosaic virus particles to tumor cells. *Chem Biol* **2007,** *14*, 1152-62.

6. Lee, E. S.; Oh, K. T.; Kim, D.; Youn, Y. S.; Bae, Y. H., Tumor pH-responsive flower-like micelles of poly(L-lactic acid)-b-poly(ethylene glycol)-b-poly(L-histidine). *J Control Release* **2007,** *123*, 19-26.

7. Perelman, L. A.; Pacholski, C.; Li, Y. Y.; VanNieuwenhze, M. S.; Sailor, M. J., pH-triggered release of vancomycin from protein-capped porous silicon films. *Nanomedicine (Lond)* **2008,** *3*, 31-43.

8. Lai, C. Y.; Trewyn, B. G.; Jeftinija, D. M.; Jeftinija, K.; Xu, S.; Jeftinija, S.; Lin, V. S., A mesoporous silica nanosphere-based carrier system with chemically removable CdS nanoparticle caps for stimuli-responsive controlled release of neurotransmitters and drug molecules. *J Am Chem Soc* **2003,** *125*, 4451-9.

9. Meers, P., Enzyme-activated targeting of liposomes. *Adv Drug Deliv Rev* **2001,** *53*, 265-72.

10. De Geest, B. G.; Skirtach, A. G.; Mamedov, A. A.; Antipov, A. A.; Kotov, N. A.; De Smedt, S. C.; Sukhorukov, G. B., Ultrasound-triggered release from multilayered capsules. *Small* **2007,** *3*, 804-8.

11. Deckers, R.; Rome, C.; Moonen, C. T., The role of ultrasound and magnetic resonance in local drug delivery. *Journal of Magnetic Resonance Imaging* **2008,** *27*, 400-9.

12. Hernot, S.; Klibanov, A. L., Microbubbles in ultrasound-triggered drug and gene delivery. *Adv Drug Deliv Rev* **2008,** *60*, 1153-66.

13. Kim, H. J.; Matsuda, H.; Zhou, H. S.; Honma, I., Ultrasound-triggered smart drug release from a poly(dimethylsiloxane)-mesoporous silica composite. *Adv Mater* **2006,** *18*, 3083-3088.

14. Derfus, A. M.; von Maltzahn, G.; Harris, T. J.; Duza, T.; Vecchio, K. S.; Ruoslahti, E.; Bhatia, S. N., Remotely triggered release from magnetic nanoparticles. *Adv Mater* **2007,** *19*, 3932-3936.

15. Needham, D.; Dewhirst, M. W., The development and testing of a new temperature-sensitive drug delivery system for the treatment of solid tumors. *Adv Drug Deliv Rev* **2001,** *53*, 285-305.

16. Ruebner, A.; Yang, Z. W.; Leung, D.; Breslow, R., A cyclodextrin dimer with a photocleavable linker as a possible carrier for the photosensitizer in photodynamic tumor therapy. *Proc Natl Acad Sci USA* **1999,** *96*, 14692-14693.

17. Jiang, M. Y.; Dolphin, D., Site-specific prodrug release using visible light. *J Am Chem Soc* **2008,** *130*, 4236-7.

18. Greer, A.; Zamadar, M.; Ghosh, G.; Mahendran, A.; Minnis, M.; Kruft, B. I.; Ghogare, A.; Aebisher, D., Photosensitizer Drug Delivery via an Optical Fiber. *J Am Chem Soc* **2011,** *133*, 7882-7891.

19. Mahendran, A.; Kopkalli, Y.; Ghosh, G.; Ghogare, A.; Minnis, M.; Kruft, B. I.; Zamadar, M.; Aebisher, D.; Davenport, L.; Greer, A., A Hand-held

Fiber-optic Implement for the Site-specific Delivery of Photosensitizer and Singlet Oxygen. *Photochem Photobiol* **2011**.

20. Zhang, Z. Y.; Smith, B. D., Synthesis and characterization of NVOC-DOPE, a caged photoactivatable derivative of dioleoylphosphatidylethanolamine. *Bioconjugate Chem* **1999,** *10*, 1150-1152.

21. Wijtmans, M.; Rosenthal, S. J.; Zwanenburg, B.; Porter, N. A., Visible light excitation of CdSe nanocrystals triggers the release of coumarin from cinnamate surface ligands. *Journal of the American Chemical Society* **2006,** *128*, 11720-11726.

22. Alvarez-Lorenzo, C.; Bromberg, L.; Concheiro, A., Light-sensitive Intelligent Drug Delivery Systems. *Photochem Photobiol* **2009,** *85*, 848-860.

23. Lemke, E. A.; Summerer, D.; Geierstanger, B. H.; Brittain, S. M.; Schultz, P. G., Control of protein phosphorylation with a genetically encoded photocaged amino acid. *Nat Chem Biol* **2007,** *3*, 769-72.

24. Furuta, T.; Wang, S. S.; Dantzker, J. L.; Dore, T. M.; Bybee, W. J.; Callaway, E. M.; Denk, W.; Tsien, R. Y., Brominated 7-hydroxycoumarin-4-ylmethyls: photolabile protecting groups with biologically useful cross-sections for two photon photolysis. *Proc Natl Acad Sci U S A* **1999,** *96*, 1193-200.

25. Link, K. H.; Shi, Y.; Koh, J. T., Light activated recombination. *J Am Chem Soc* **2005,** *127*, 13088-9.

26. Mal, N. K.; Fujiwara, M.; Tanaka, Y., Photocontrolled reversible release of guest molecules from coumarin-modified mesoporous silica. *Nature* **2003,** *421*, 350-3.

27. Agasti, S. S.; Chompoosor, A.; You, C. C.; Ghosh, P.; Kim, C. K.; Rotello, V. M., Photoregulated release of caged anticancer drugs from gold nanoparticles. *J Am Chem Soc* **2009,** *131*, 5728-9.

28. Meinhardt, M.; Krebs, R.; Anders, A.; Heinrich, U.; Tronnier, H., Wavelength-dependent penetration depths of ultraviolet radiation in human skin. *J Biomed Opt* **2008,** *13*, -.

29. Juzenas, P.; Juzeniene, A.; Kaalhus, O.; Iani, V.; Moan, J., Noninvasive fluorescence excitation spectroscopy during application of 5-aminolevulinic acid in vivo. *Photoch Photobio Sci* **2002,** *1*, 745-748.

30. Weissleder, R., A clearer vision for in vivo imaging. *Nat Biotechnol* **2001,** *19*, 316-317.

31. Dougherty, T. J.; Gomer, C. J.; Henderson, B. W.; Jori, G.; Kessel, D.; Korbelik, M.; Moan, J.; Peng, Q., Photodynamic therapy. *J Natl Cancer I* **1998,** *90*, 889-905.

32. Dolmans, D. E.; Fukumura, D.; Jain, R. K., Photodynamic therapy for cancer. *Nat Rev Cancer* **2003,** *3*, 380-7.

33. Sharman, W. M.; Allen, C. M.; van Lier, J. E., Photodynamic therapeutics: basic principles and clinical applications. *Drug Discov Today* **1999,** *4*, 507-517.

34. Moan, J.; Peng, Q., An outline of the hundred-year history of PDT. *Anticancer Res* **2003,** *23*, 3591-600.

35. Nyman, E. S.; Hynninen, P. H., Research advances in the use of tetrapyrrolic photosensitizers for photodynamic therapy. *J Photochem Photobiol B* **2004,** *73*, 1-28.

36. Weishaupt, K. R.; Gomer, C. J.; Dougherty, T. J., Identification of singlet oxygen as the cytotoxic agent in photoinactivation of a murine tumor. *Cancer Res* **1976,** *36*, 2326-9.

37. Halliwell, B.; Gutteridge, J. M., Oxygen toxicity, oxygen radicals, transition metals and disease. *Biochem J* **1984,** *219*, 1-14.

38. Huang, Z., A review of progress in clinical photodynamic therapy. *Technol Cancer Res Treat* **2005,** *4*, 283-93.

39. Miller, J. D.; Baron, E. D.; Scull, H.; Hsia, A.; Berlin, J. C.; McCormick, T.; Colussi, V.; Kenney, M. E.; Cooper, K. D.; Oleinick, N. L., Photodynamic therapy with the phthalocyanine photosensitizer Pc 4: the case experience with preclinical mechanistic and early clinical-translational studies. *Toxicol Appl Pharmacol* **2007,** *224*, 290-9.

40. Calzavara-Pinton, P. G.; Venturini, M.; Sala, R., Photodynamic therapy: update 2006. Part 2: Clinical results. *J Eur Acad Dermatol Venereol* **2007,** *21*, 439-51.

41. Hopper, C., Photodynamic therapy: a clinical reality in the treatment of cancer. *Lancet Oncol* **2000,** *1*, 212-9.

42. Triesscheijn, M.; Baas, P.; Schellens, J. H.; Stewart, F. A., Photodynamic therapy in oncology. *Oncologist* **2006,** *11*, 1034-44.

43. van den Bergh, H., On the evolution of some endoscopic light delivery systems for photodynamic therapy. *Endoscopy* **1998,** *30*, 392-407.

44. Panjehpour, M.; Overholt, B. F.; Haydek, J. M., Light sources and delivery devices for photodynamic therapy in the gastrointestinal tract. *Gastrointest Endosc Clin N Am* **2000,** *10*, 513-32.

45. Wilson, B. C.; Patterson, M. S., The physics, biophysics and technology of photodynamic therapy. *Phys Med Biol* **2008,** *53*, R61-109.

46. Tromberg, B. J.; Orenstein, A.; Kimel, S.; Barker, S. J.; Hyatt, J.; Nelson, J. S.; Berns, M. W., In vivo tumor oxygen tension measurements for the evaluation of the efficiency of photodynamic therapy. *Photochem Photobiol* **1990,** *52*, 375-85.

47. Brown, J. M.; Giaccia, A. J., The unique physiology of solid tumors: opportunities (and problems) for cancer therapy. *Cancer Res* **1998,** *58*, 1408-16.

48. Cardenas-Navia, L. I.; Richardson, R. A.; Dewhirst, M. W., Targeting the molecular effects of a hypoxic tumor microenvironment. *Front Biosci* **2007,** *12*, 4061-78.

49. Woodhams, J. H.; Macrobert, A. J.; Bown, S. G., The role of oxygen monitoring during photodynamic therapy and its potential for treatment dosimetry. *Photochem Photobiol Sci* **2007,** *6*, 1246-56.

50. Iinuma, S.; Schomacker, K. T.; Wagnieres, G.; Rajadhyaksha, M.; Bamberg, M.; Momma, T.; Hasan, T., In vivo fluence rate and fractionation effects on tumor response and photobleaching: photodynamic therapy with two photosensitizers in an orthotopic rat tumor model. *Cancer Res* **1999,** *59*, 6164-70.

51. Solban, N.; Rizvi, I.; Hasan, T., Targeted photodynamic therapy. *Lasers Surg Med* **2006,** *38*, 522-31.

52. Verma, S.; Watt, G. M.; Mai, Z.; Hasan, T., Strategies for enhanced photodynamic therapy effects. *Photochem Photobiol* **2007,** *83*, 996-1005.

53. Sharman, W. M.; van Lier, J. E.; Allen, C. M., Targeted photodynamic therapy via receptor mediated delivery systems. *Adv Drug Deliv Rev* **2004,** *56*, 53-76.

54. Schneider, R.; Tirand, L.; Frochot, C.; Vanderesse, R.; Thomas, N.; Gravier, J.; Guillemin, F.; Barberi-Heyob, M., Recent improvements in the use of synthetic peptides for a selective photodynamic therapy. *Anticancer Agents Med Chem* **2006,** *6*, 469-88.

55. Devasagayam, T. P.; Kamat, J. P., Biological significance of singlet oxygen. *Indian J Exp Biol* **2002,** *40*, 680-92.

56. Wasserman, H. H. M. R. W., *Singlet oxygen*. Academic Press: New York, 1979; p xviii, 684 p.

57. Clo, E.; Snyder, J. W.; Ogilby, P. R.; Gothelf, K. V., Control and selectivity of photosensitized singlet oxygen production: Challenges in complex biological systems. *Chembiochem* **2007,** *8*, 475-481.

58. Turro, N. J., *Modern molecular photochemistry*. University Science Books: Mill Valley, Calif., 1991; p 628 p.

59. Kearns, D. R., Physical and Chemical Properties of Singlet Molecular Oxygen. *Chem Rev* **1971,** *71*, 395-&.

60. Frimer, A. A., Reaction of Singlet Oxygen with Olefins - Question of Mechanism. *Chem Rev* **1979,** *79*, 359-387.

61. Foote, C. S.; Denny, R. W., Chemistry of Singlet Oxygen .12. Electronic Effects on Rate and Products of Reaction with Olefins. *J Am Chem Soc* **1971,** *93*, 5162-5167.

62. Clennan, E. L.; Nagraba, K., Additions of Singlet Oxygen to Alkoxy-Substituted Dienes - the Mechanism of the Singlet Oxygen 1,2-Cycloaddition Reaction. *J Am Chem Soc* **1988,** *110*, 4312-4318.

63. Bartlett, P. D., 4-Membered Rings and Reaction-Mechanisms. *Chem Soc Rev* **1976,** *5*, 149-163.

64. Waterhouse, D. N.; Madden, T. D.; Cullis, P. R.; Bally, M. B.; Mayer, L. D.; Webb, M. S., Preparation, characterization, and biological analysis of liposomal formulations of vincristine. *Methods Enzymol* **2005,** *391*, 40-57.

65. Haran, G.; Cohen, R.; Bar, L. K.; Barenholz, Y., Transmembrane ammonium sulfate gradients in liposomes produce efficient and stable entrapment of amphipathic weak bases. *Biochimica Et Biophysica Acta* **1993,** *1151*, 201-15.

66. Goren, D.; Horowitz, A. T.; Tzemach, D.; Tarshish, M.; Zalipsky, S.; Gabizon, A., Nuclear delivery of doxorubicin via folate-targeted

liposomes with bypass of multidrug-resistance efflux pump. *Clin Cancer Res* **2000,** *6*, 1949-57.

67. Allen, T. M.; Cullis, P. R., Drug delivery systems: entering the mainstream. *Science* **2004,** *303*, 1818-22.

68. Shive, M. S.; Anderson, J. M., Biodegradation and biocompatibility of PLA and PLGA microspheres. *Adv Drug Deliv Rev* **1997,** *28*, 5-24.

69. Wiener, E. C.; Brechbiel, M. W.; Brothers, H.; Magin, R. L.; Gansow, O. A.; Tomalia, D. A.; Lauterbur, P. C., Dendrimer-based metal chelates: a new class of magnetic resonance imaging contrast agents. *Magn Reson Med* **1994,** *31*, 1-8.

70. Jansen, J. F. G. A.; Debrabandervandenberg, E. M. M.; Meijer, E. W., Encapsulation of Guest Molecules into a Dendritic Box. *Science* **1994,** *266*, 1226-1229.

71. D'Emanuele, A.; Attwood, D., Dendrimer-drug interactions. *Adv Drug Deliver Rev* **2005,** *57*, 2147-2162.

72. Jansen, J. F. G. A.; Meijer, E. W.; Debrabandervandenberg, E. M. M., The Dendritic Box - Shape-Selective Liberation of Encapsulated Guests. *J Am Chem Soc* **1995,** *117*, 4417-4418.

73. Pan, D.; Turner, J. L.; Wooley, K. L., Folic acid-conjugated nanostructured materials designed for cancer cell targeting. *Chem Commun* **2003**, 2400-2401.

74. Daly, T.; Royal, R. E.; Kershaw, M. H.; Treisman, J.; Wang, G.; Li, W. P.; Herlyn, D.; Eshhar, Z.; Hwu, P., Recognition of human colon cancer by T cells transduced with a chimeric receptor gene. *Cancer Gene Ther* **2000,** *7*, 284-291.

75. Sakharov, D. V.; Jie, A. F. H.; Filippov, D. V.; Bekkers, M. E. A.; van Boom, J. H.; Rijken, D. C., Binding and retention of polycationic peptides and dendrimers in the vascular wall. *Febs Lett* **2003,** *537*, 6-10.

76. Wiwattanapatapee, R.; Lomlim, L.; Saramunee, K., Dendrimers conjugates for colonic delivery of 5-aminosalicylic acid. *J Control Release* **2003,** *88*, 1-9.

77. Faler, G. R., I.A study of the kinetics of the 1,2-cycloaddition of singlet oxygen to vinyl ethers. II. An investigation of the reaction of singlet oxygen with adamantylideneadamantane. In pp vii, 157 leaves.

78. Frimer, A. A.; Bartlett, P. D.; Boschung, A. F.; Jewett, J. G., Reaction of Singlet Oxygen with 4-Methyl-2,3-Dihydro-Gamma-Pyrans. *J Am Chem Soc* **1977,** *99*, 7977-7986.

79. Jefford, C. W.; Kohmoto, S., The Effect of Solvent on Competing Hydroperoxide and Dioxetane Formation on Photosensitized Oxygenation of Olefins. *Helv Chim Acta* **1982,** *65*, 133-136.

80. Gollnick, K.; Knutzenmies, K., Dye-Sensitized Photooxygenation of 2,3-Dihydrofurans - Competing [2+2] Cycloadditions and Ene Reactions of Singlet Oxygen with a Rigid Cyclic Enol Ether System. *J Org Chem* **1991,** *56*, 4017-4027.

81. Sales, F.; Serratosa, F., Diphenoxyethyne - Highly Electrophilic Acetylene Diether. *Tetrahedron Lett* **1979**, 3329-3330.

82. Foote, C. S., Photosensitized Oxygenations and Role of Singlet Oxygen. *Accounts Chem Res* **1968,** *1*, 104-&.

83. Kearns, D. R., Selection Rules for Singlet-Oxygen Reactions . Concerted Addition Reactions. *J Am Chem Soc* **1969,** *91*, 6554-&.

84. Bartlett, P. D.; Mendenha.Gd; Schaap, A. P., Competitive Modes of Reaction of Singlet Oxygen. *Ann Ny Acad Sci* **1970,** *171*, 79-&.

85. Wamser, C. C.; Herring, J. W., Photooxidation of Benzophenone Oxime and Derivatives. *J Org Chem* **1976,** *41*, 1476-1477.

86. Yang, J. K.; Bauld, N. L., Synthesis of cis- and trans-1,2-diphenoxyethenes and p,p '-disubstituted diaryloxyethenes. *J Org Chem* **1999,** *64*, 9251-9253.

87. Nkepang, G.; Pogula, P. K.; Bio, M.; You, Y., Synthesis and singlet oxygen reactivity of 1,2-diaryloxyethenes and selected sulfur and nitrogen analogs. *Photochem Photobiol* **2012,** *88*, 753-9.

88. Murthy, R. S.; Bio, M.; You, Y. J., Low energy light-triggered oxidative cleavage of olefins. *Tetrahedron Lett* **2009,** *50*, 1041-1044.

89. Lowe, A. B.; Hoyle, C. E.; Bowman, C. N., Thiol-yne click chemistry: A powerful and versatile methodology for materials synthesis. *J Mater Chem* **2010,** *20*, 4745-4750.

90. Ichinose, Y.; Wakamatsu, K.; Nozaki, K.; Birbaum, J. L.; Oshima, K.; Utimoto, K., Et3b Induced Radical-Addition of Thiols to Acetylenes. *Chem Lett* **1987**, 1647-1650.

91. Deshmukh, A. R. A. S.; Joshi, G. D.; Gore, K. G.; Kulkarni, G. H., A Simple Short Synthesis of Isotachin-C. *Synthetic Commun* **1990,** *20*, 2259-2265.

92. You, Y.; Gibson, S. L.; Hilf, R.; Davies, S. R.; Oseroff, A. R.; Roy, I.; Ohulchanskyy, T. Y.; Bergey, E. J.; Detty, M. R., Water soluble, core-modified porphyrins. 3. Synthesis, photophysical properties, and in vitro studies of photosensitization, uptake, and localization with carboxylic acid-substituted derivatives. *J Med Chem* **2003,** *46*, 3734-47.

93. Bio, M.; Nkepang, G.; You, Y., Click and photo-unclick chemistry of aminoacrylate for visible light-triggered drug release. *Chem Commun (Camb)* **2012,** *48*, 6517-9.

94. Zamadar, M.; Ghosh, G.; Mahendran, A.; Minnis, M.; Kruft, B. I.; Ghogare, A.; Aebisher, D.; Greer, A., Photosensitizer drug delivery via an optical fiber. *J Am Chem Soc* **2011,** *133*, 7882-91.

95. Orito, K.; Manske, R. H.; Rodrigo, R., Photosensitized Oxidation of an Enaminoketone - Total Synthesis of a Rhoeadine Alkaloid. *J Am Chem Soc* **1974,** *96*, 1944-1945.

96. Ngen, E. J.; Rajaputra, P.; You, Y., Evaluation of delocalized lipophilic cationic dyes as delivery vehicles for photosensitizers to mitochondria. *Bioorgan Med Chem* **2009,** *17*, 6631-6640.

97. Montalti, M.; Murov, S. L.; Handbook of, p., Handbook of photochemistry. In CRC/Taylor & Francis: 2006.

98. Jemal, A.; Siegel, R.; Ward, E.; Hao, Y. P.; Xu, J. Q.; Thun, M. J., Cancer Statistics, 2009. *Ca-Cancer J Clin* **2009,** *59*, 225-249.

99. McArthur, H. L.; Hudis, C. A., Breast cancer chemotherapy. *Cancer J* **2007,** *13*, 141-147.

100. Buzdar, A. U., Preoperative chemotherapy treatment of breast cancer - A review. *Cancer* **2007,** *110*, 2394-2407.

101. Gaukroger, K.; Hadfield, J. A.; Hepworth, L. A.; Lawrence, N. J.; McGown, A. T., Novel syntheses of cis and trans isomers of combretastatin A-4. *J Org Chem* **2001,** *66*, 8135-8.

103. You, Y.; Gibson, S. L.; Detty, M. R., Phototoxicity of a core-modified porphyrin and induction of apoptosis. *J Photochem Photobiol B* **2006,** *85*, 155-62.

104. You, Y.; Gibson, S. L.; Hilf, R.; Ohulchanskyy, T. Y.; Detty, M. R., Core-modified porphyrins. Part 4: Steric effects on photophysical and biological properties in vitro. *Bioorg Med Chem* **2005,** *13*, 2235-51.

Appendix

Figures

A1. ^{1}H NMR spectrum of the photolysis reaction mixture of **3**.

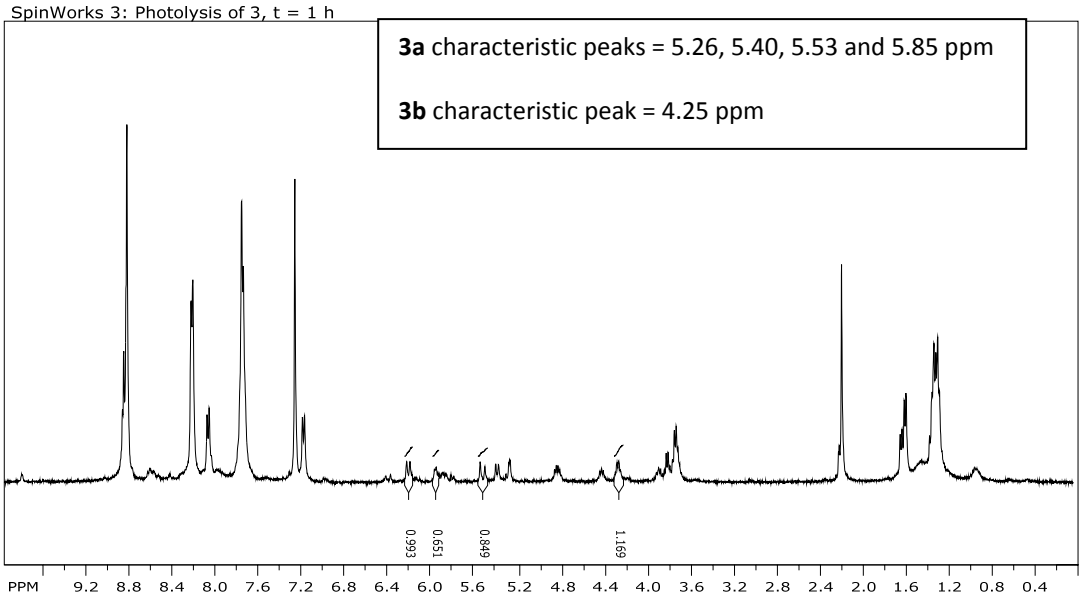

A2. ^{1}H NMR spectrum of the photolysis reaction mixture of **4**.

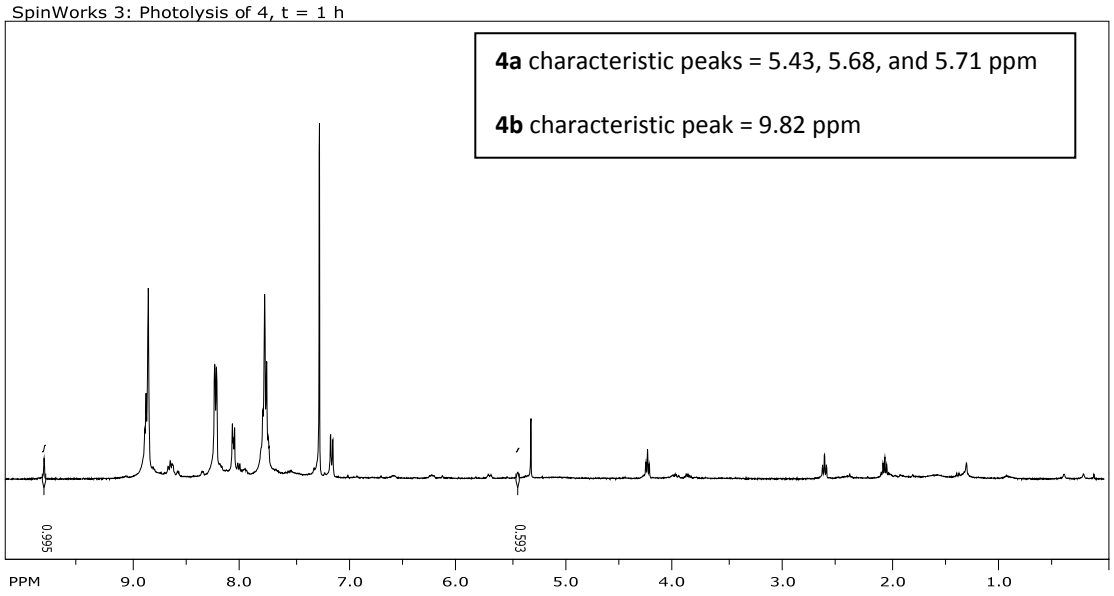

A3. ^{1}H NMR spectrum of the photolysis reaction mixtures of **8**.

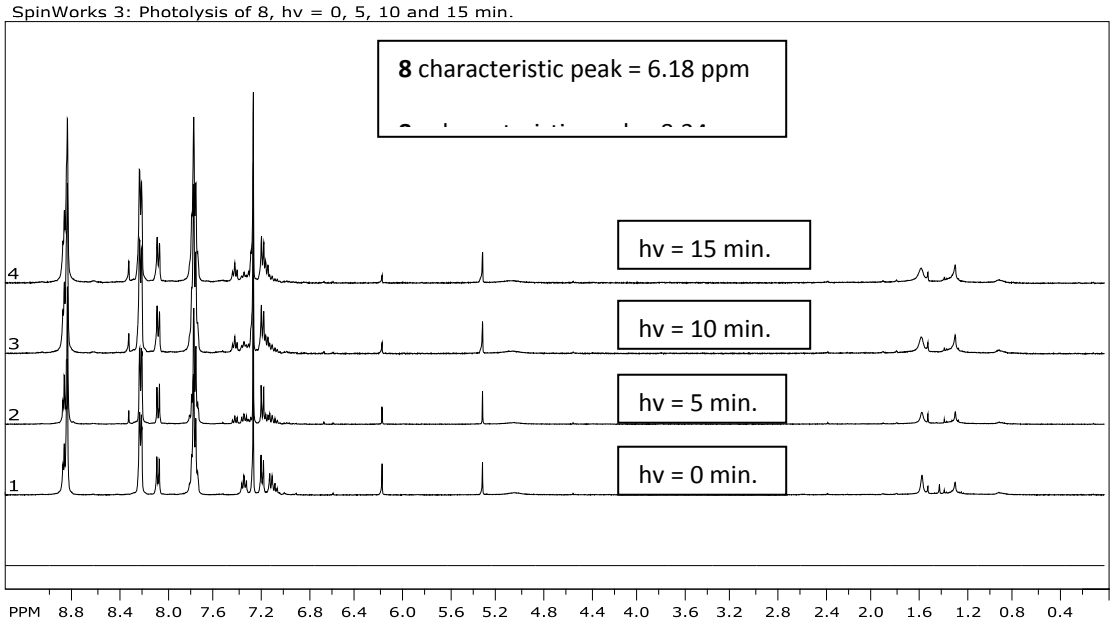

A4. ^{1}H NMR spectrum of the photolysis reaction mixtures of **9**.

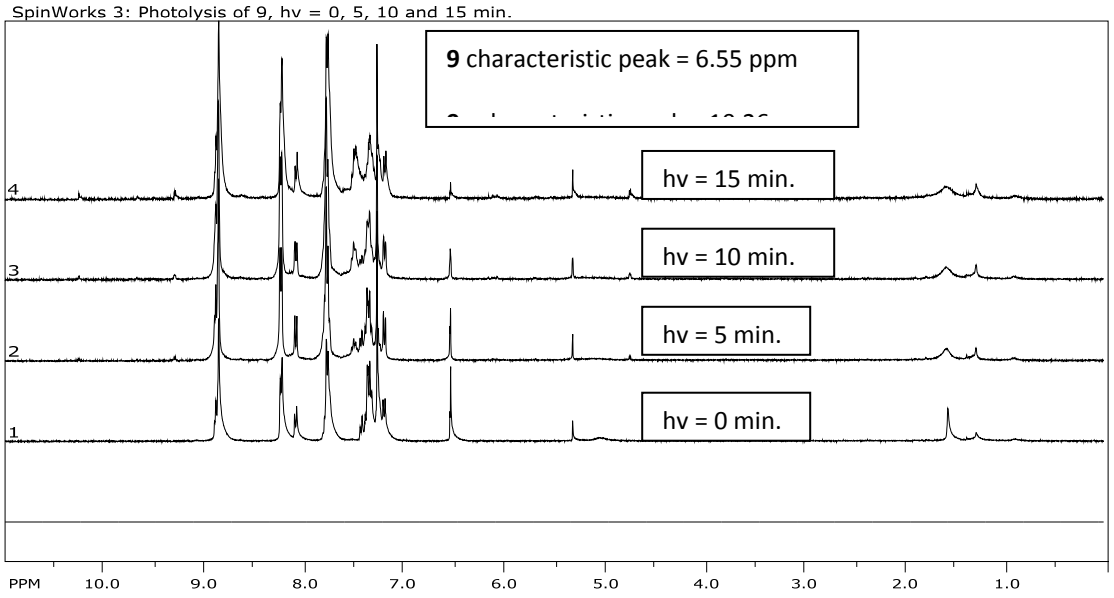

A5. ^{1}H-NMR spectrum of the photo-oxidation of **18**.

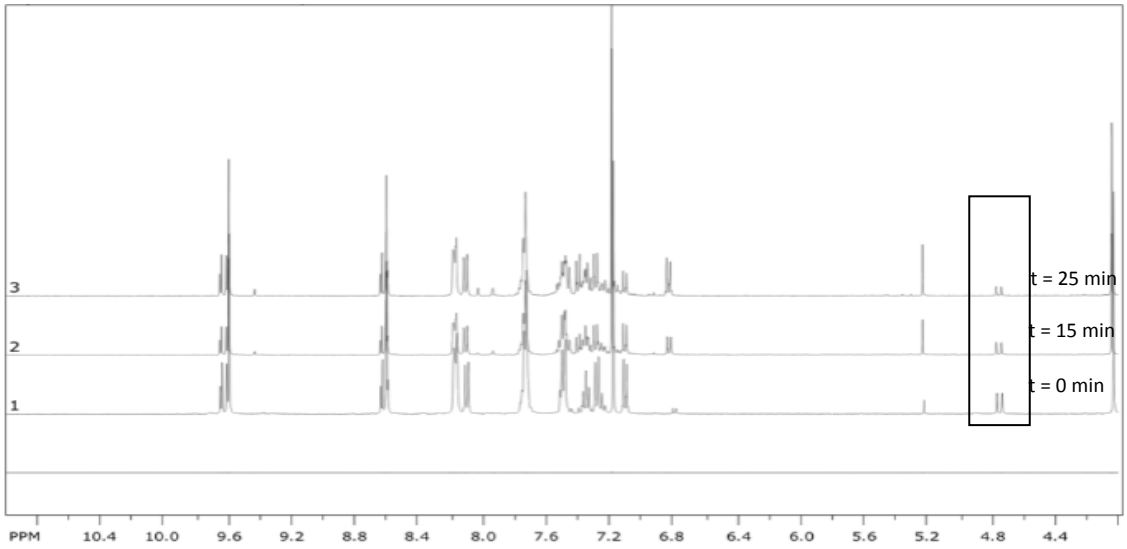

A6. ^{1}H-NMR spectrum of the photo-oxidation of **18** and DABCO.

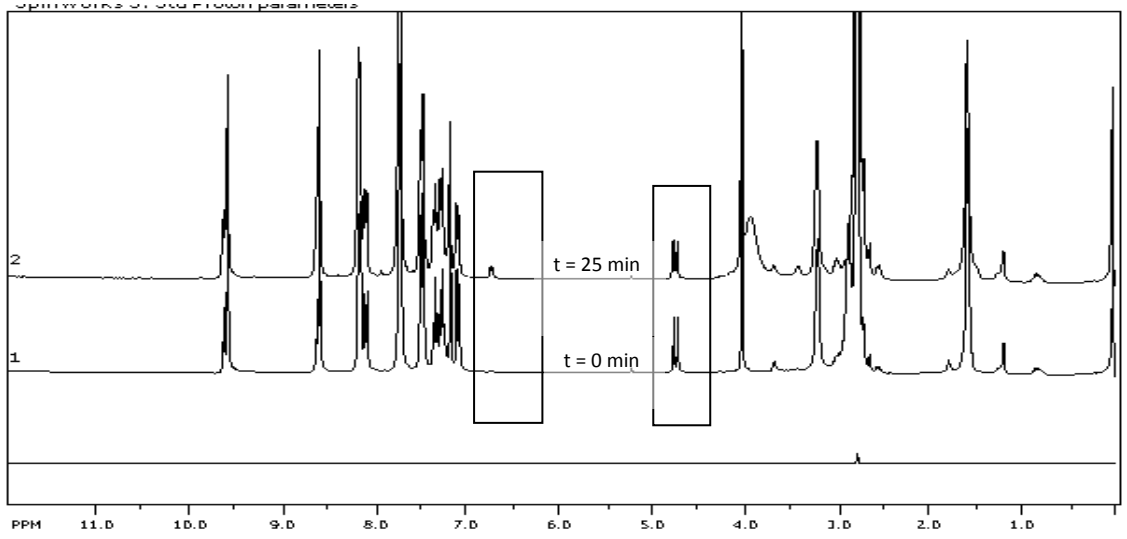

A7. ^{1}H-NMR spectrum of the photo-oxidation of **24**.

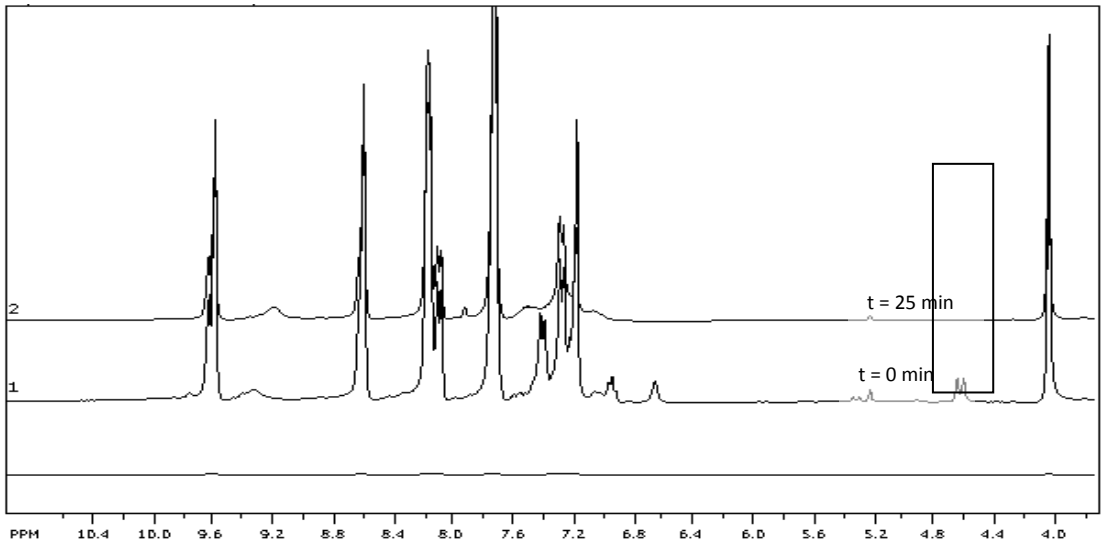

A8. GC-MS spectrum of 4-phenylphenol standard sample (retention time = 13.43 min, MW = 170).

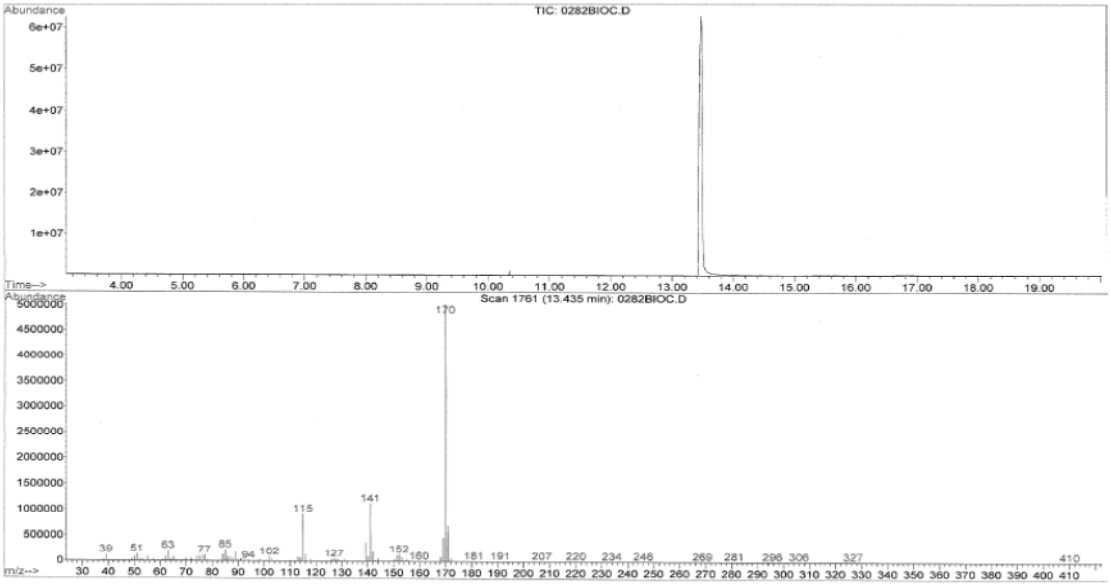

A9. GC-MS spectrum of cleavage mixture of compound 18 (4-phenylphenol peak observed: retention time = 13.43 min, MW = 170).

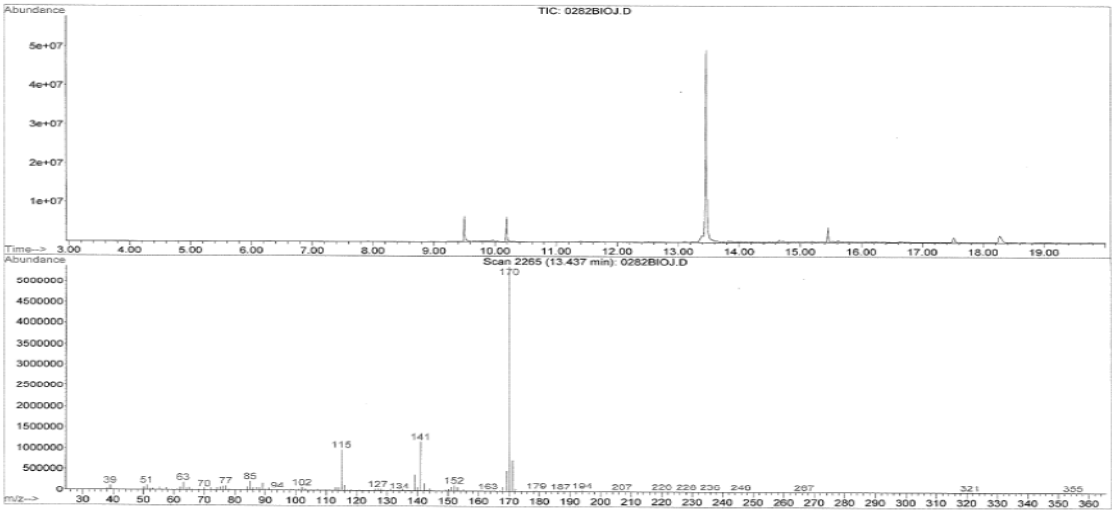

A10. GC-MS spectrum of thiophenol standard sample (retention time = 7.54 min, MW = 110).

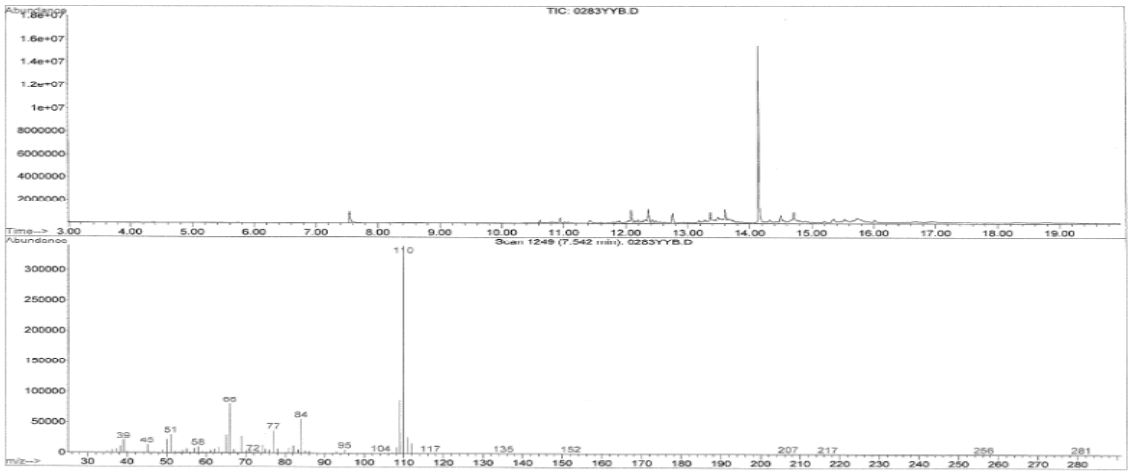

A11. GC-MS spectrum of thiophenol standard sample (diphenyl disulfide observed, retention time = 14.14 min, MW = 218).

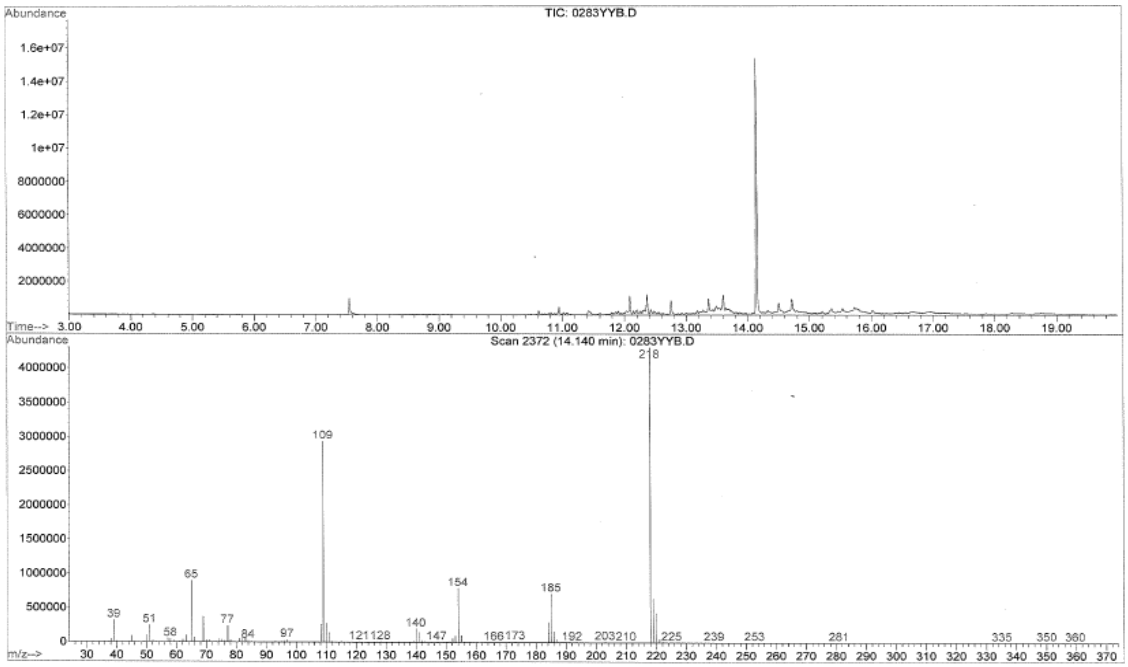

A12. GC-MS spectrum of the cleavage mixture of **23** (thiophenol observed: retention time = 7.55 min, MW = 110).

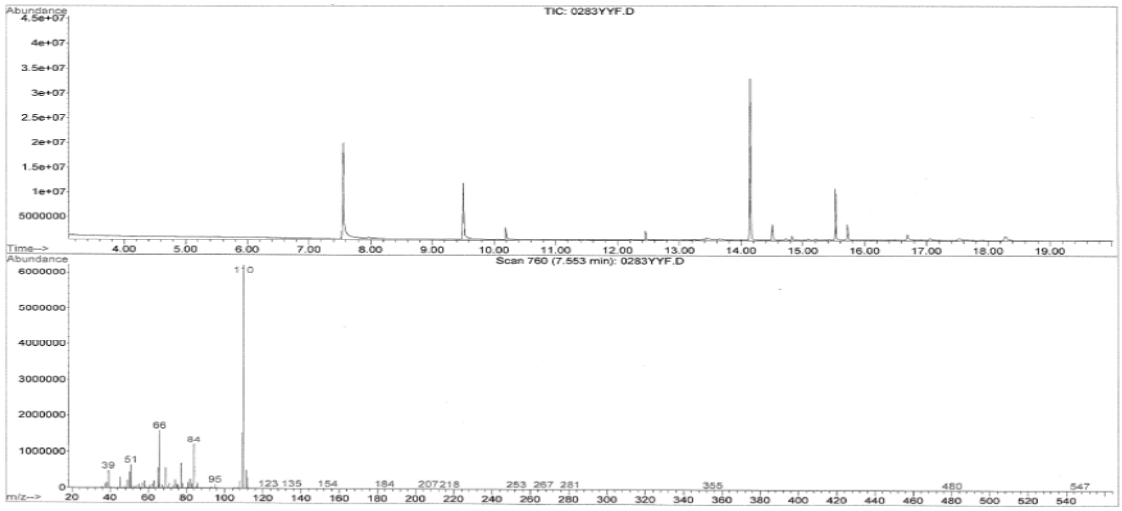

A13. GC-MS spectrum of the cleavage mixture of 23 (diphenyl disulfide observed: retention time = 14.14 min, MW = 218).

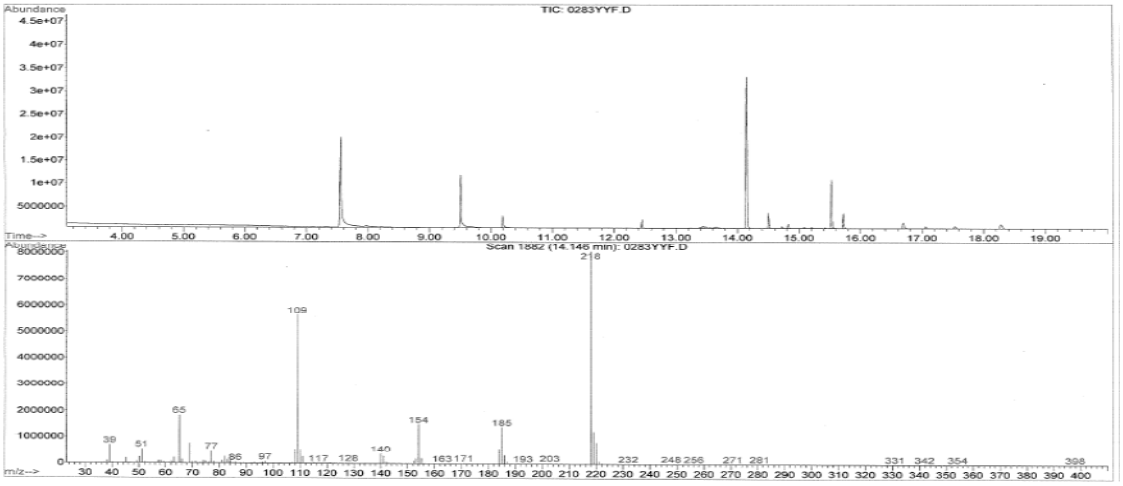

A14. GC-MS spectrum of aniline standard sample (retention time =7.77 min, MW = 93).

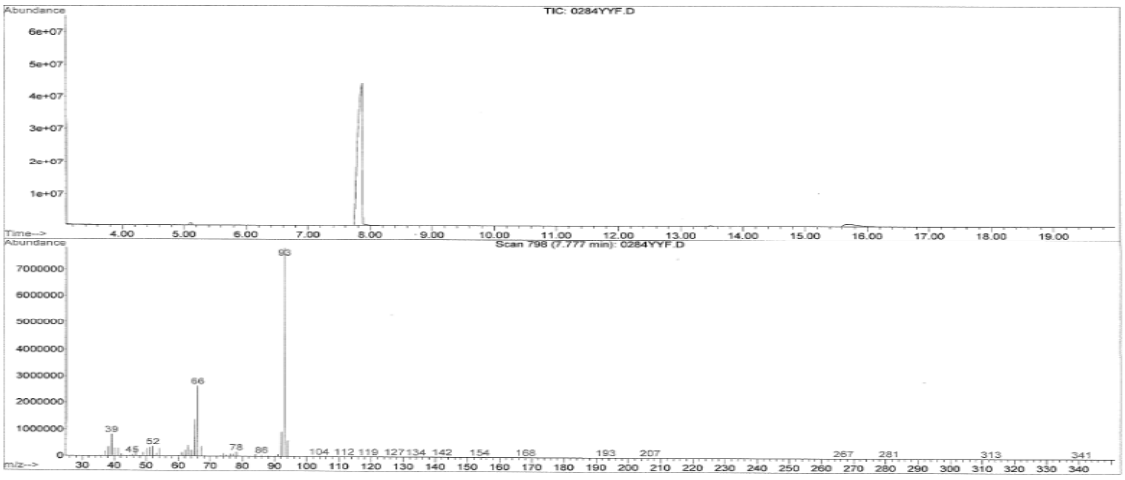

A15. GC-MS spectrum of the cleavage mixture of 24 (aniline observed: retention time = 7.89 min, MW = 93).

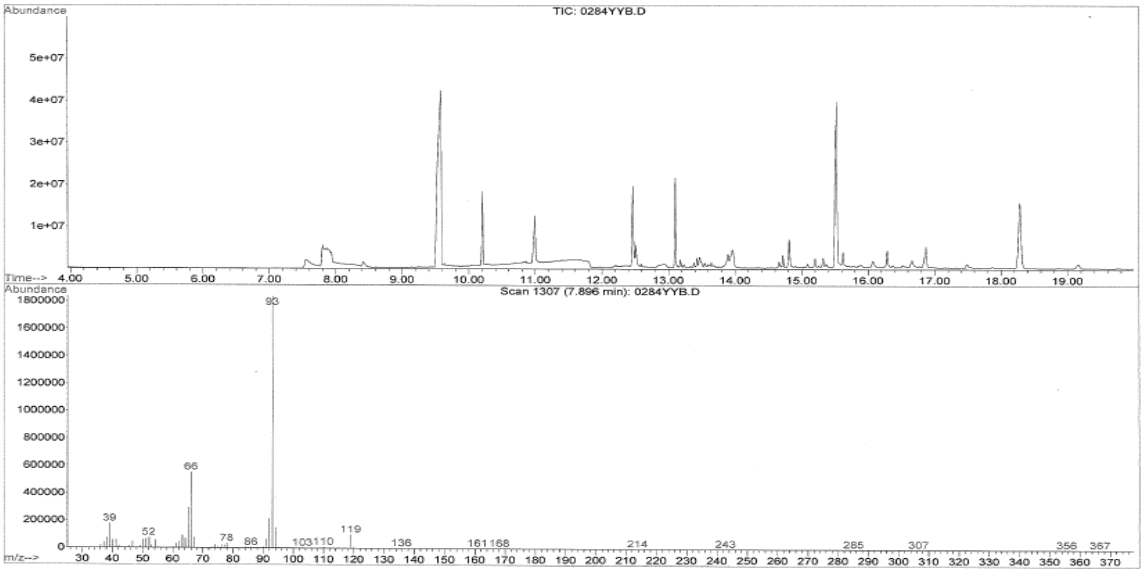

A16. GC-MS spectrum of Estrone standard sample (retention time = 19.51 min, MW = 270).

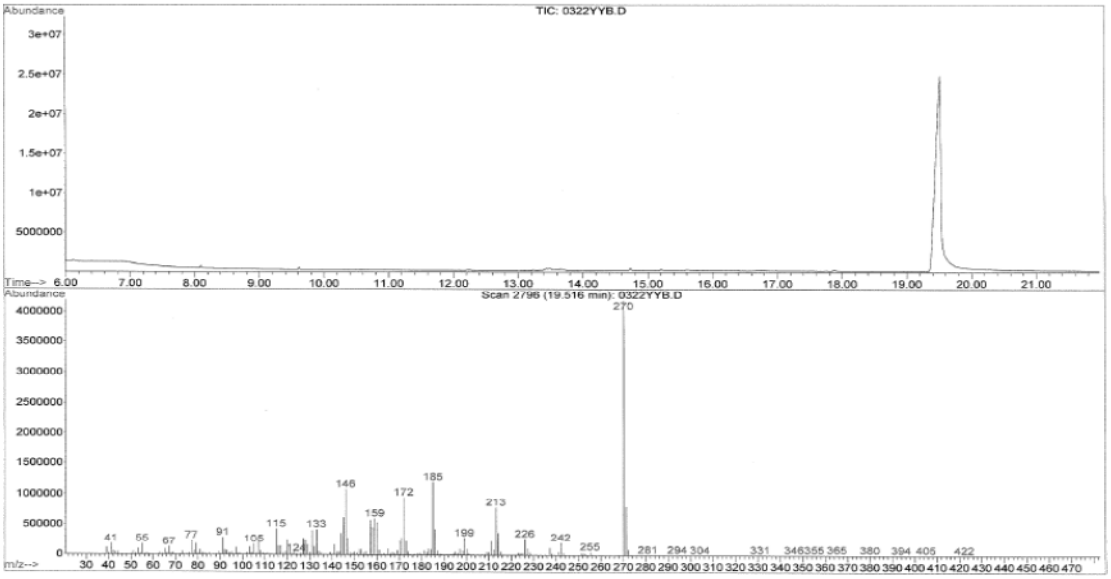

A17. GC-MS spectrum of the cleavage mixture of 31 (Estrone observed: retention time = 19.6 min, MW = 270).

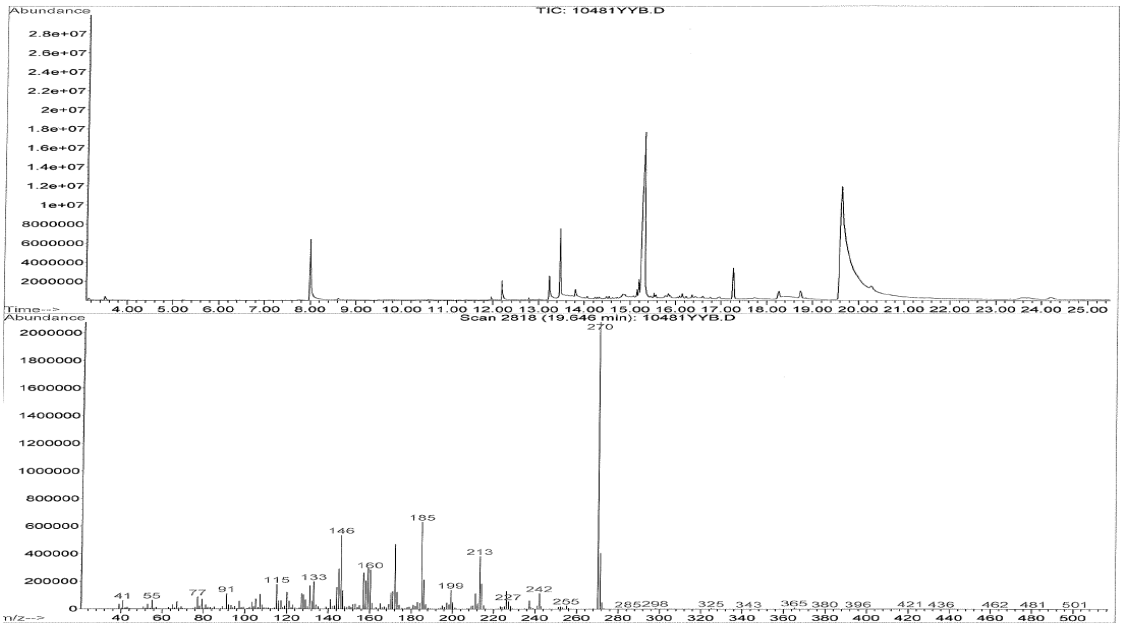

A18. Mass spectrum of isolated cleaved product 5-(4-Hydroxyphenyl)-10,15,20-triphenyl-21,23-dithiaporphyrin form the oxidation of **32**

Calculated for $C_{44}H_{29}N_2OS_2$ ($[M+H]^+$):665.1643 ; found: 665.1717.

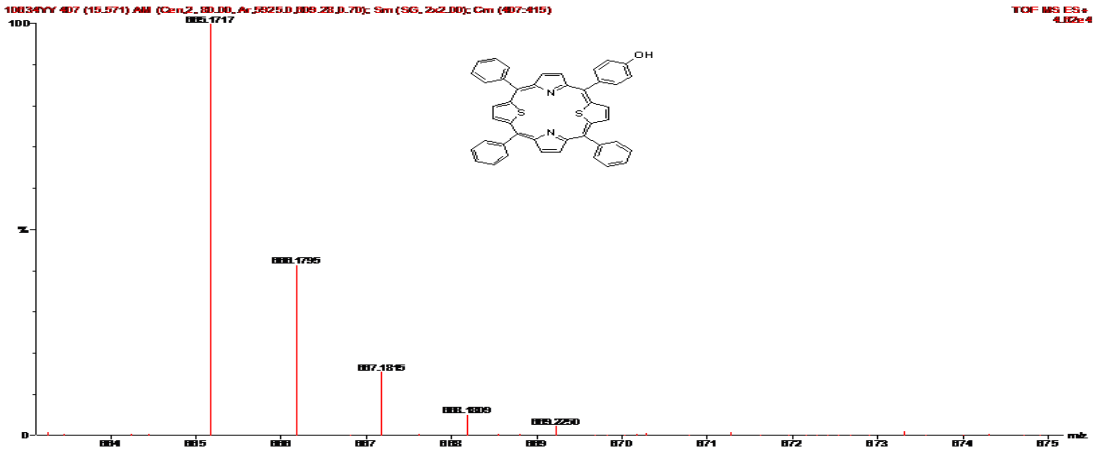

A19. Mass spectrum of isolated cleaved product N-(6-(diethylamino)-9-(2-(((1-formylpiperidin-4-yl)methoxy)carbonyl)phenyl)-3H-xanthem-3-ylidene)-N-ethylethanaminium chloride from the oxidation of **32**.

Calculated for $C_{35}H_{43}ClN_3O_4$ ($[M+H]^+$-Cl):568.833 ; found: 568.3196

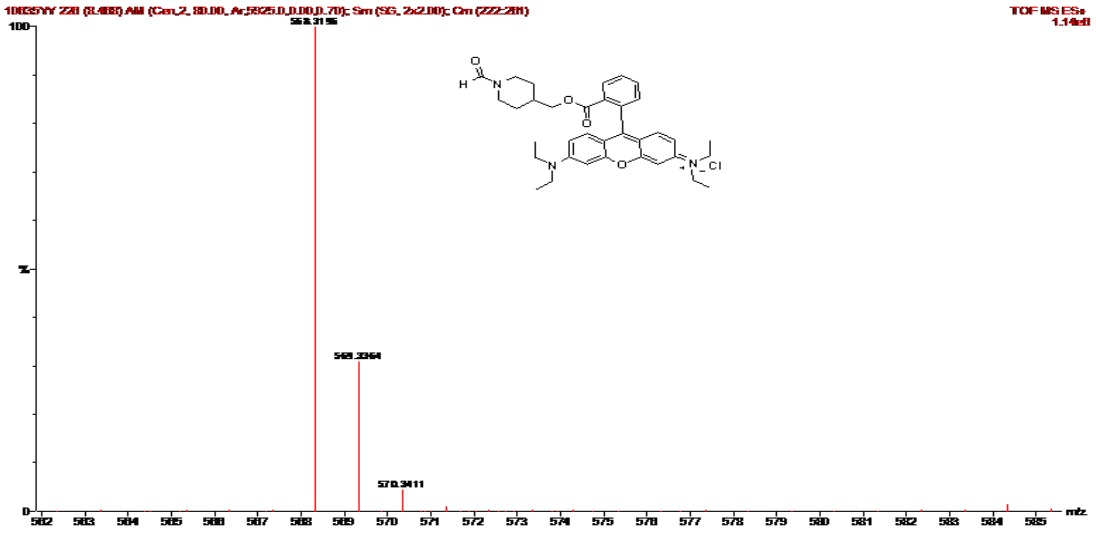

NMR spectra

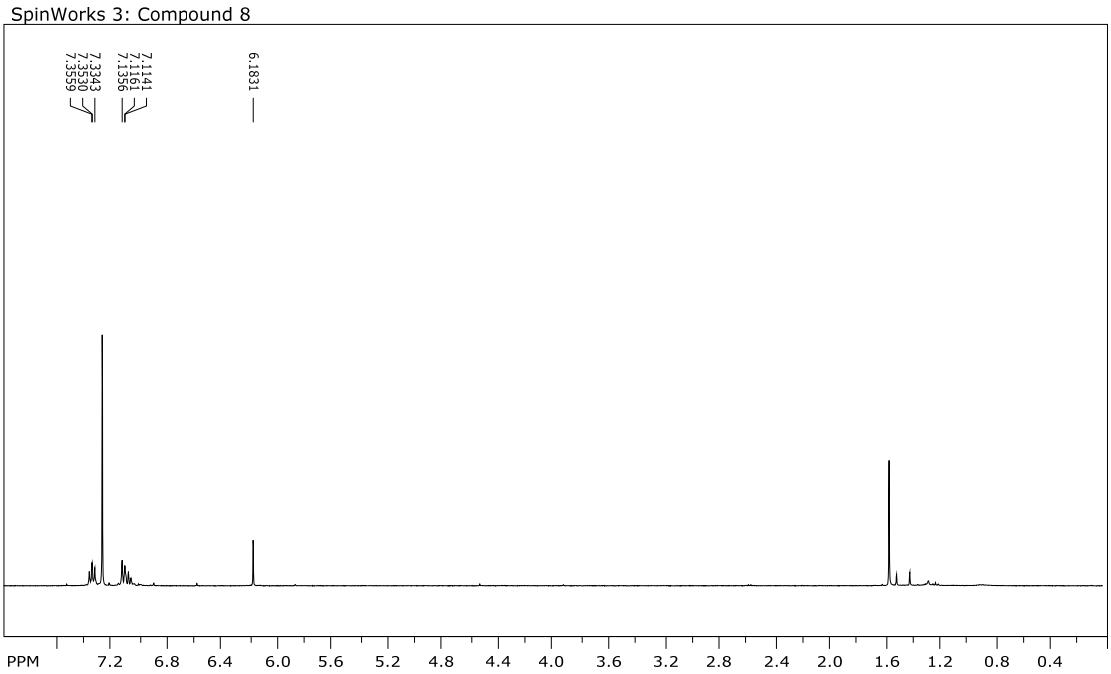

^{1}H NMR spectrum of compound **8**.

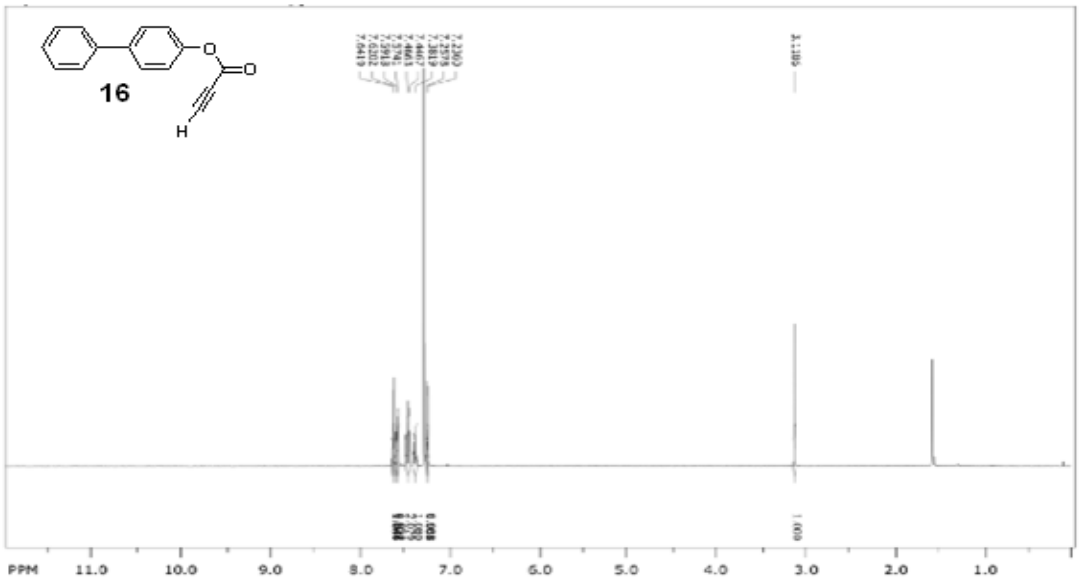
16
PPM
11.0
10.0
9.0
8.0
7.0
6.0
5.0
4.0
3.0
2.0
1.0

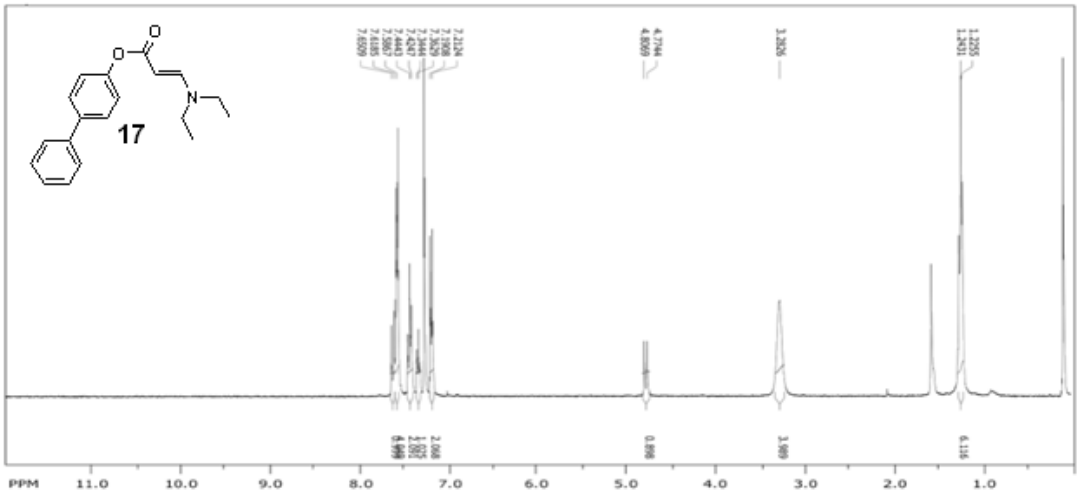
17
PPM
11.0
10.0
9.0
8.0
7.0
6.0
5.0
4.0
3.0
2.0
1.0

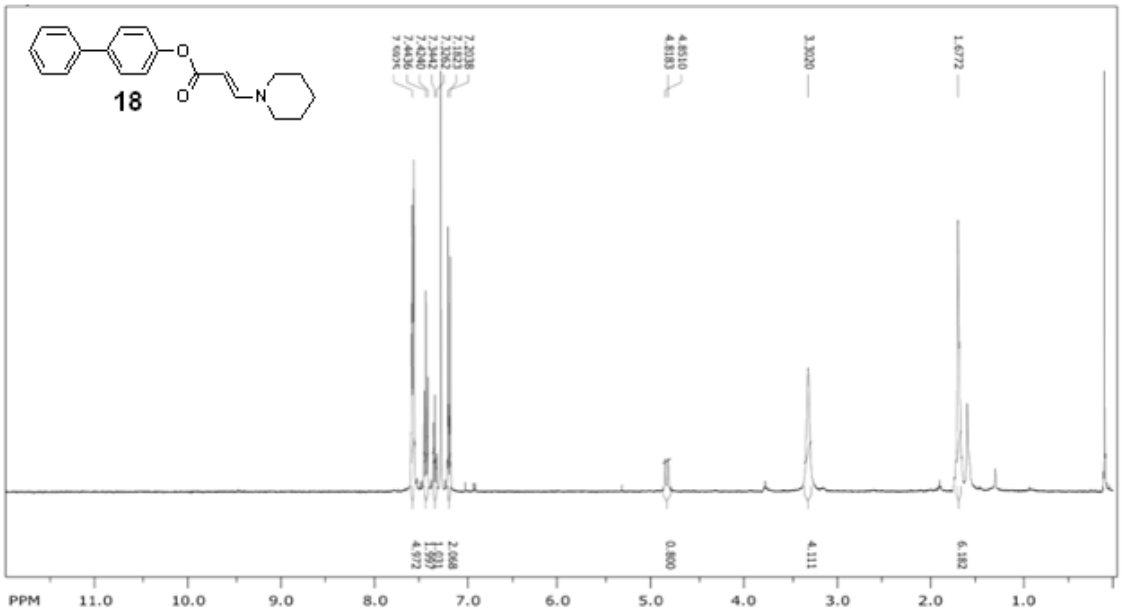
18
PPM 11.0 10.0 9.0 8.0 7.0 6.0 5.0 4.0 3.0 2.0 1.0

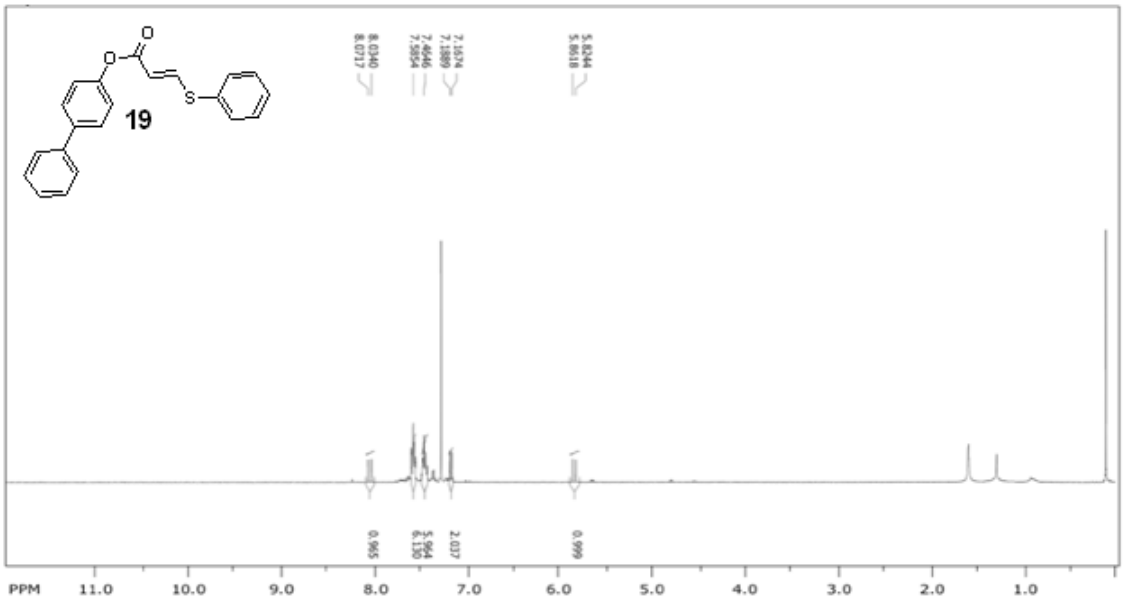
19
PPM 11.0 10.0 9.0 8.0 7.0 6.0 5.0 4.0 3.0 2.0 1.0

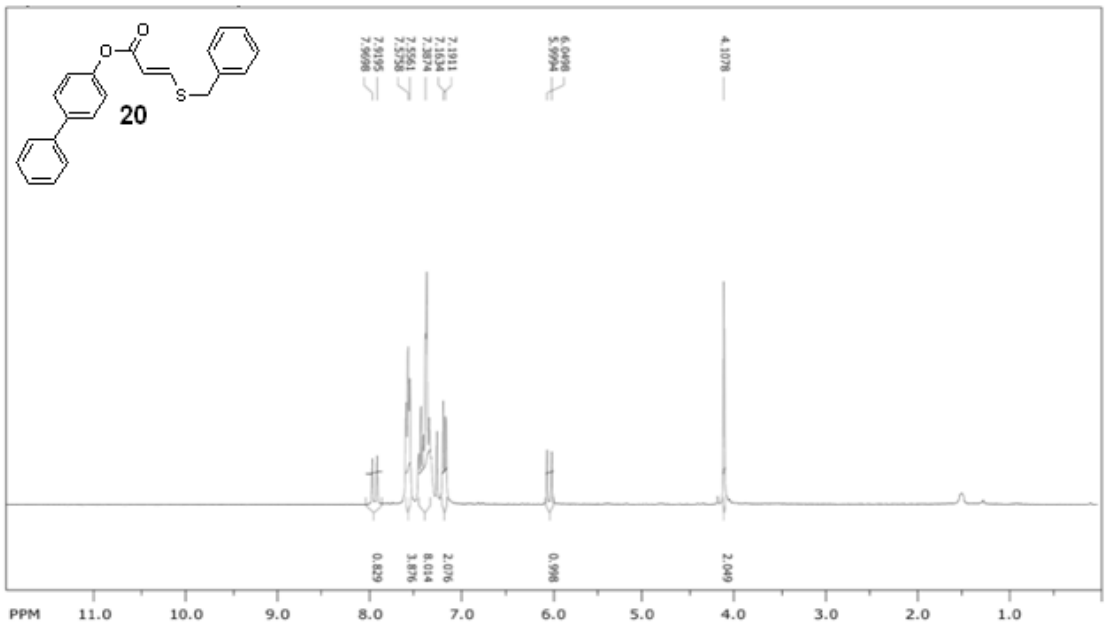
20
PPM
11.0
10.0
9.0
8.0
7.0
6.0
5.0
4.0
3.0
2.0
1.0

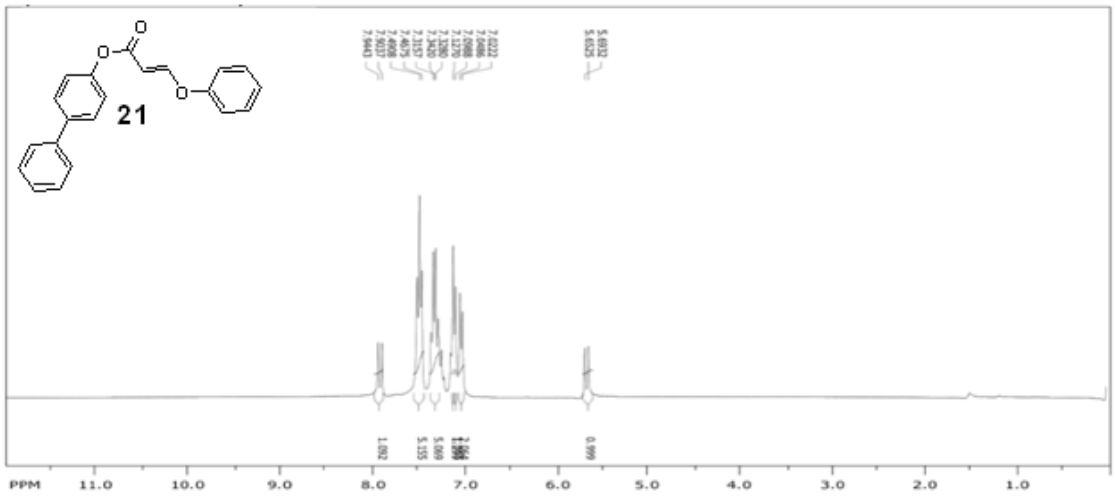
21
PPM
11.0
10.0
9.0
8.0
7.0
6.0
5.0
4.0
3.0
2.0
1.0

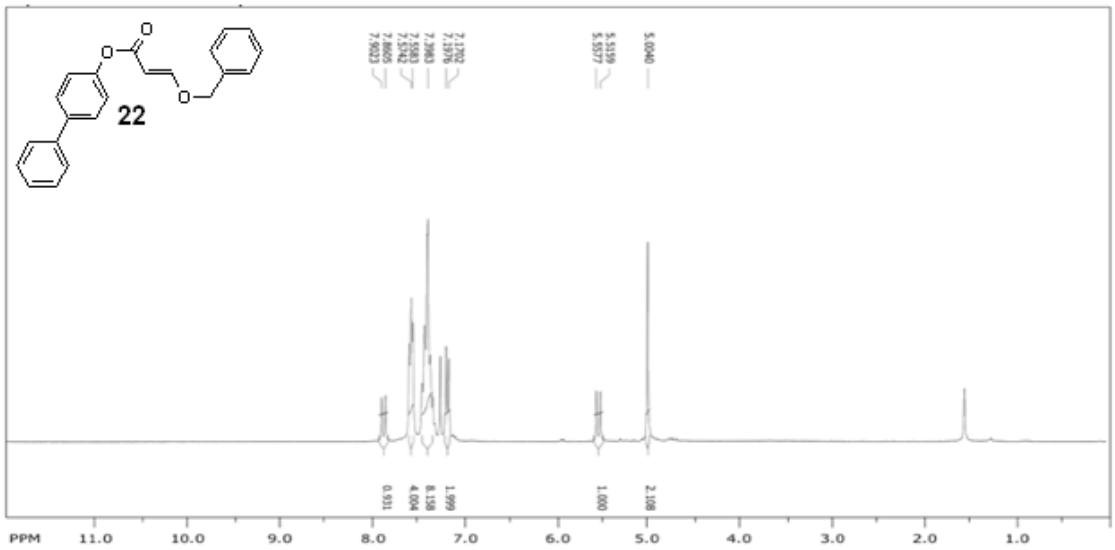
22
PPM
11.0
10.0
9.0
8.0
7.0
6.0
5.0
4.0
3.0
2.0
1.0

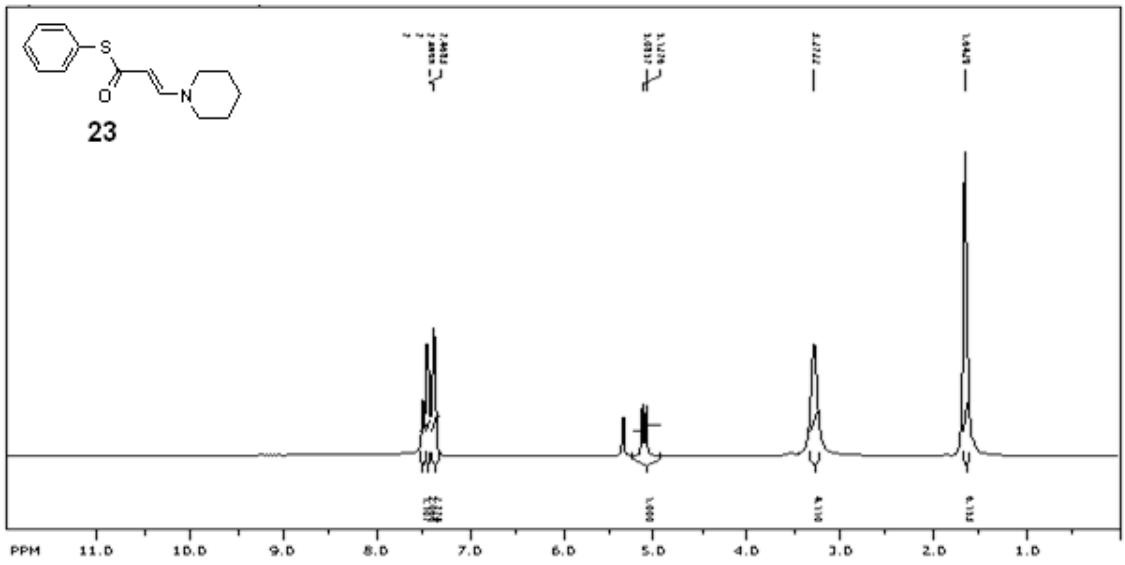
23
PPM
11.0
10.0
9.0
8.0
7.0
6.0
5.0
4.0
3.0
2.0
1.0

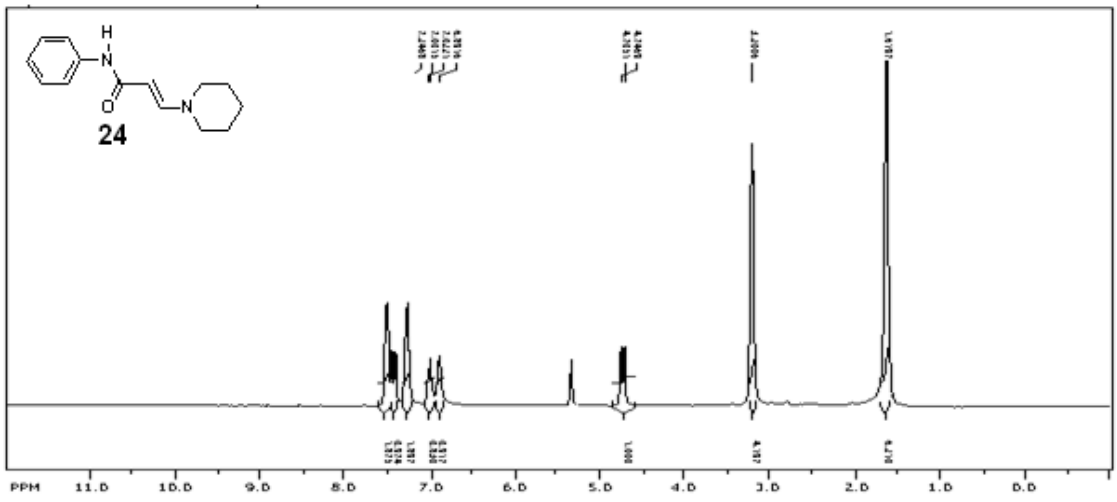
24
PPM
11.0
10.0
9.0
8.0
7.0
6.0
5.0
4.0
3.0
2.0
1.0
0.0

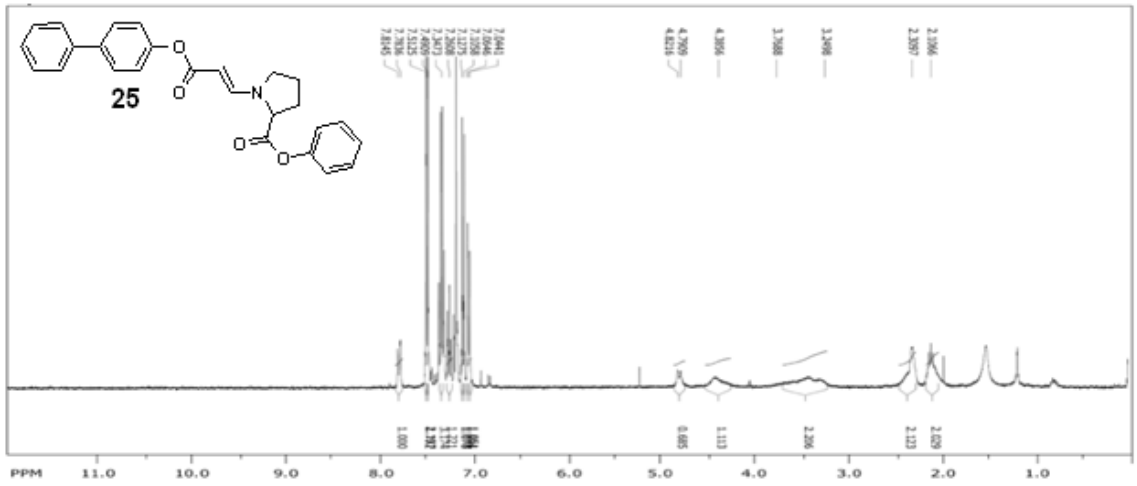
25
PPM
11.0
10.0
9.0
8.0
7.0
6.0
5.0
4.0
3.0
2.0
1.0

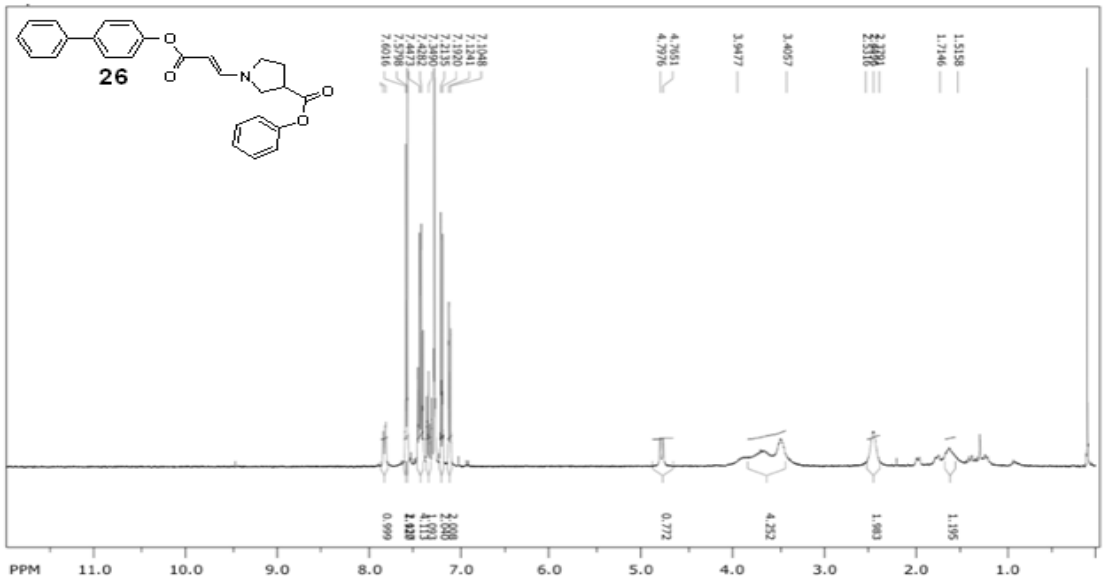
26
PPM
11.0
10.0
9.0
8.0
7.0
6.0
5.0
4.0
3.0
2.0
1.0

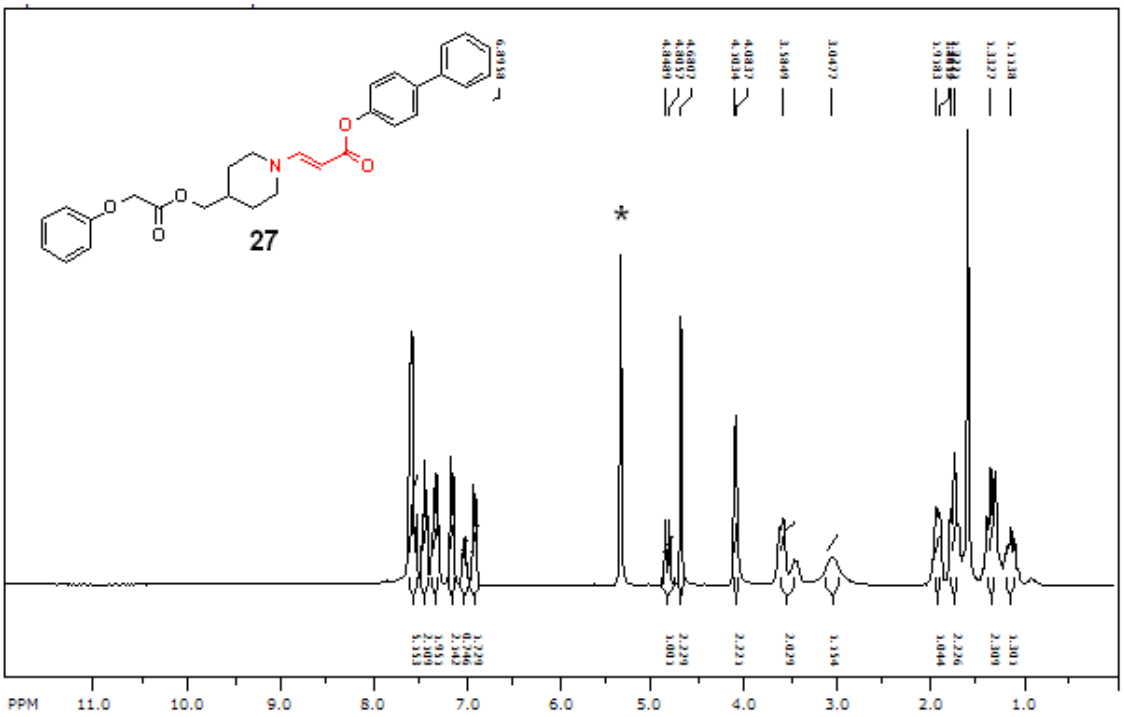
27
*
PPM
11.0
10.0
9.0
8.0
7.0
6.0
5.0
4.0
3.0
2.0
1.0

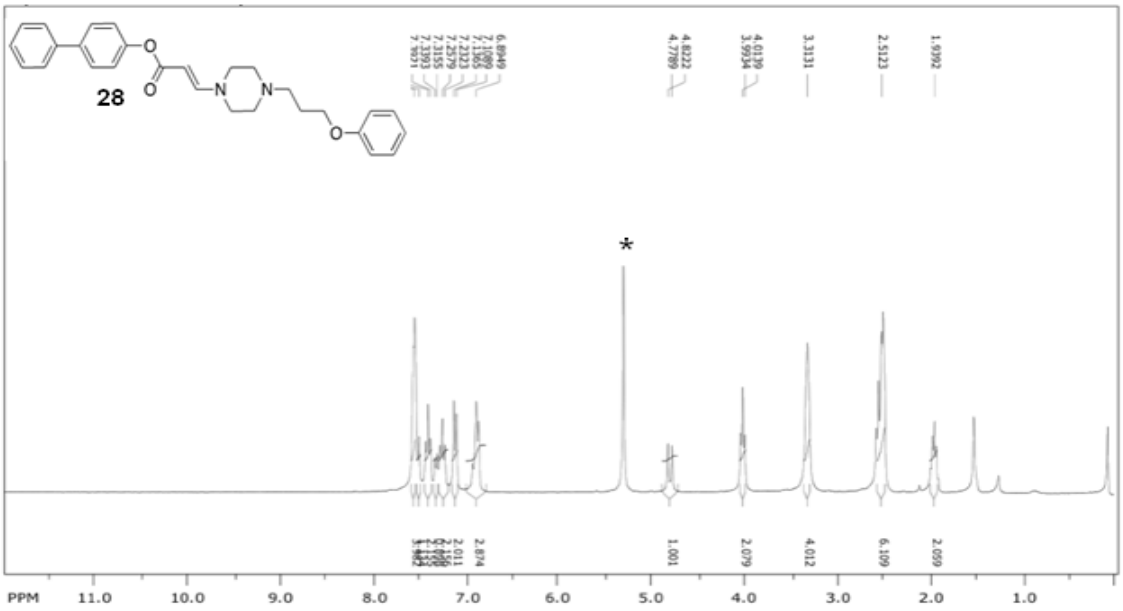
28
*
PPM
11.0
10.0
9.0
8.0
7.0
6.0
5.0
4.0
3.0
2.0
1.0

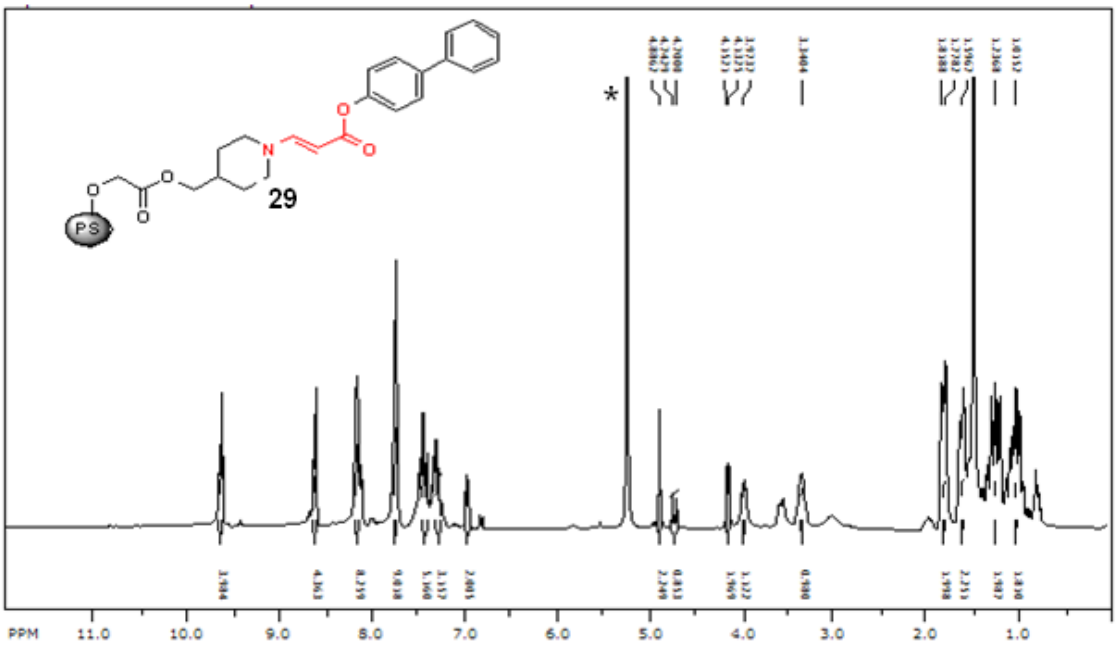
29
PS
*
PPM
11.0
10.0
9.0
8.0
7.0
6.0
5.0
4.0
3.0
2.0
1.0

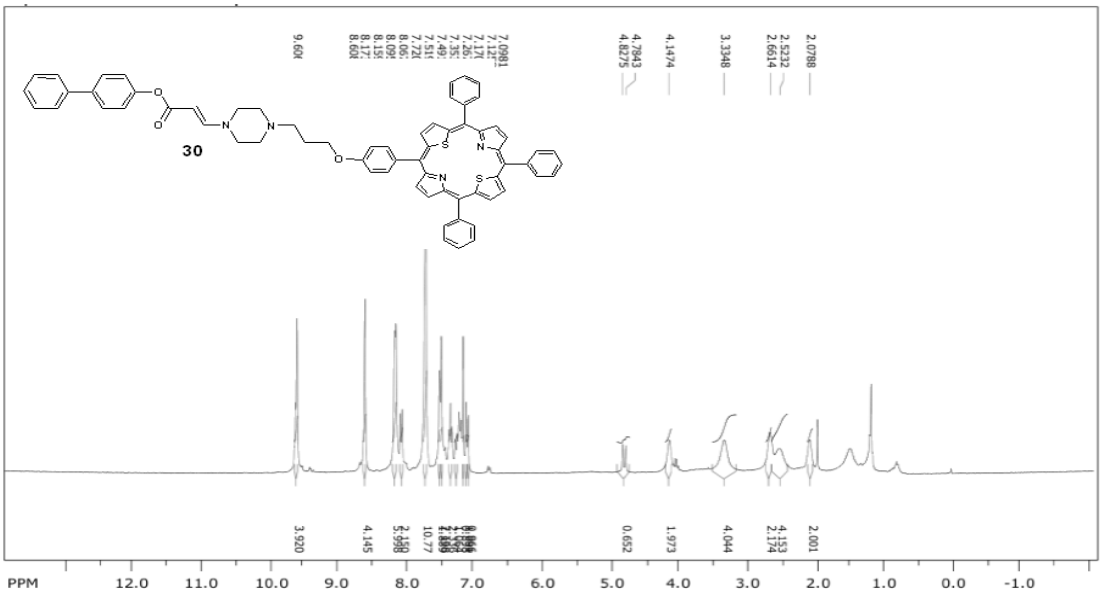
30
PPM
12.0
11.0
10.0
9.0
8.0
7.0
6.0
5.0
4.0
3.0
2.0
1.0
0.0
-1.0

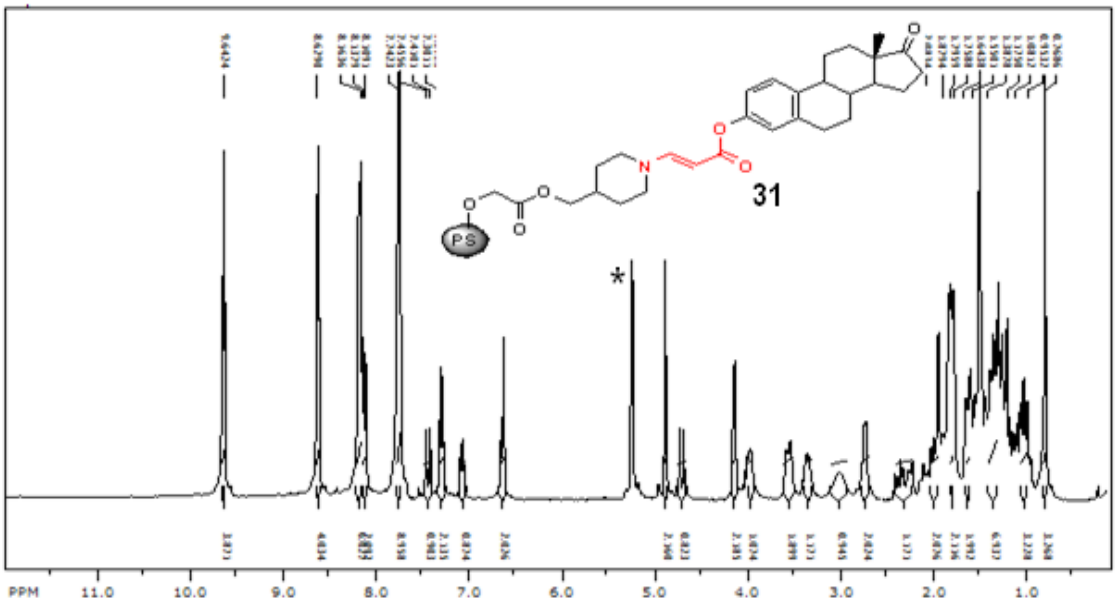
31
PS
*
PPM
11.0
10.0
9.0
8.0
7.0
6.0
5.0
4.0
3.0
2.0
1.0

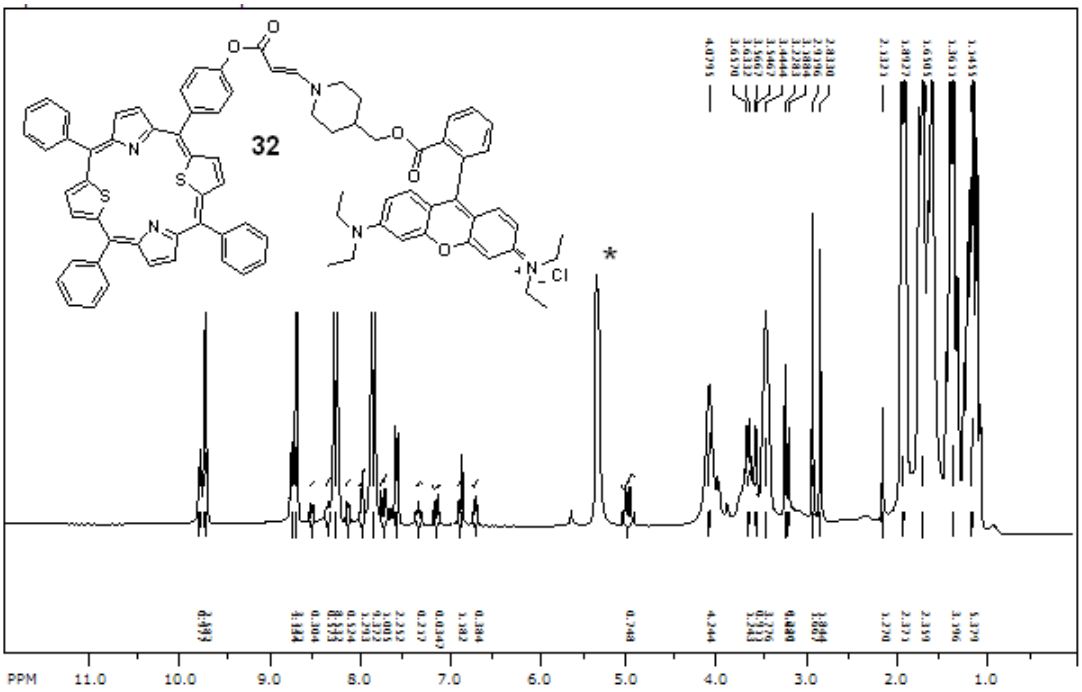

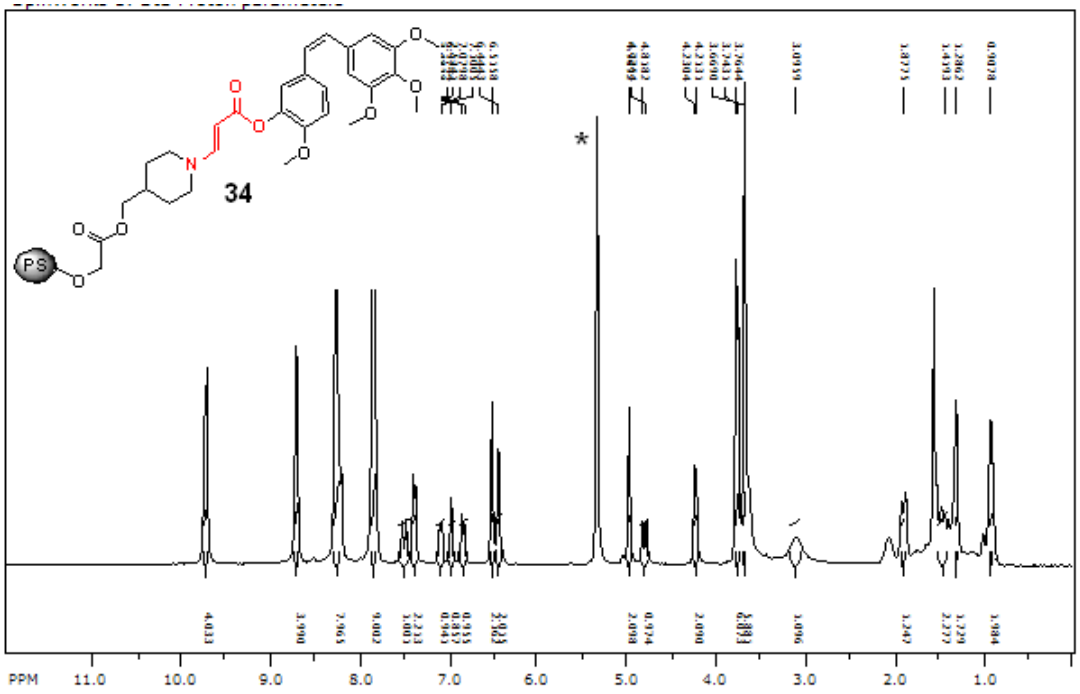

* The peaks at 5.4 ppm were from a solvent: dichloromethane.